1996

Synthesis, characterization, and structure of reduced tungsten chalcogenide cluster complexes

Xiaobing Xie
Iowa State University

INFORMATION TO USERS

This manuscript has been reproduced from the microfilm master. UMI films the text directly from the original or copy submitted. Thus, some thesis and dissertation copies are in typewriter face, while others may be from any type of computer printer.

The quality of this reproduction is dependent upon the quality of the copy submitted. Broken or indistinct print, colored or poor quality illustrations and photographs, print bleedthrough, substandard margins, and improper alignment can adversely affect reproduction.

In the unlikely event that the author did not send UMI a complete manuscript and there are missing pages, these will be noted. Also, if unauthorized copyright material had to be removed, a note will indicate the deletion.

Oversize materials (e.g., maps, drawings, charts) are reproduced by sectioning the original, beginning at the upper left-hand corner and continuing from left to right in equal sections with small overlaps. Each original is also photographed in one exposure and is included in reduced form at the back of the book.

Photographs included in the original manuscript have been reproduced xerographically in this copy. Higher quality 6" x 9" black and white photographic prints are available for any photographs or illustrations appearing in this copy for an additional charge. Contact UMI directly to order.

UMI

A Bell & Howell Information Company
300 North Zeeb Road, Ann Arbor MI 48106-1346 USA
313/761-4700 800/521-0600

Synthesis, characterization, and structure of reduced tungsten chalcogenide cluster complexes

by

Xiaobing Xie

A dissertation submitted to the graduate faculty

in partial fulfillment of the requirements for the degree of

DOCTOR OF PHILOSOPHY

Major: Inorganic Chemistry

Major Professor: Robert E. McCarley

Iowa State University

Ames, Iowa

1996

Graduate College
Iowa State University

This is to certify that the Doctoral dissertation of

Xiaobing Xie

has met the dissertation requirements of Iowa State University

Signature was redacted for privacy.

Major Professor

Signature was redacted for privacy.

For the Major Program

Signature was redacted for privacy.

For the Graduate College

TABLE OF CONTENTS

LIST OF FIGURES

GENERAL INTRODUCTION

CHAPTER 1.

CHAPTER 2.

CHAPTER 3.

CHAPTER 4

LIST OF TABLES

CHAPTER 1

CHAPTER 2

CHAPTER 3

CHAPTER 4

GENERAL INTRODUCTION

Statement of Problem

Over the previous twenty years, ternary molybdenum chalcogenides of the general formula $M_xMo_6Y_8$ (M = ternary metal cation; Y = chalcogenide), known as Chevrel phases, have been extensively studied. Many of these compounds have been found to have superconductivity,[1,2] catalytic activity[3-7] and ionic conductivity.[8,9]

The rich chemistry of the Chevrel phases raises considerable interest in finding the tungsten analogues of these phases. However, no such analogue has ever been synthesized, although the Chevrel phases are usually prepared directly from elements at high temperatures above 1000°C. The absence of the tungsten analogues may be caused by their thermodynamic instability at such high temperatures. Thus it might be necessary to avoid high-temperature synthetic procedures in order to establish the ternary and binary tungsten chalcogenides. A major focus of the McCarley research group has been on the preparation of $M_6Y_8L_6$ (M = Mo, W; Y = S, Se, Te) cluster complexes as low temperature pathways to the Chevrel phases.

A similarity was noted that both molybdenum(II) / tungsten(II) halides and the Chevrel phases contain hexanuclear cluster units, although the overall structures are quite different. The structure of the Mo_6Y_8 unit is shown in Figure 1. This cluster consists of an octahedron of molybdenum atoms with eight triply bridging

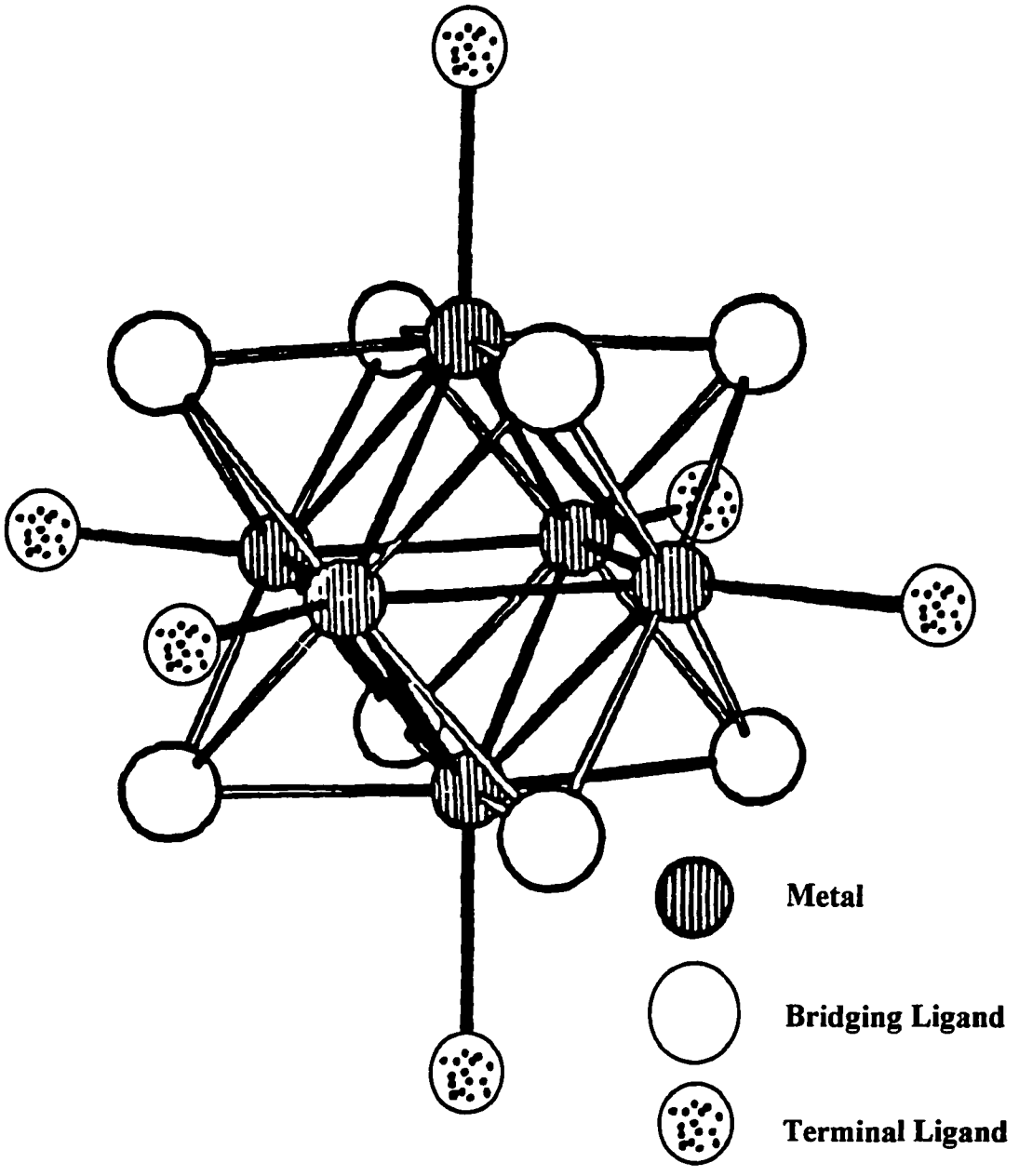

Figure 1. Structure of the $M_6X^i_8L^a_6$ cluster

ligands (chalcogenide or halogen) capping each cube face. These bridging ligands are noted by Schäfer as *"i"* for *"inner"*. The six terminal positions located at the vertices of the octahedron are noted as "*a*" for "*ausser*". The hexanuclear molybdenum clusters can combine in various ways as evidenced in Figure 2. The *a-i* designation, which is evidenced in the Chevrel phases, signifies a ligand in the terminal position of one cluster that is shared through a bridging position of another cluster. The ligands are shared as *a-a* in the α-molybdenum / tungsten (II) halides.

The similarity and difference in the structures of these two classes of compounds has led to the investigation of many mixed halide-chalcogenide hexamolybdenum clusters with structures related to the Chevrel phases.[10-13] The first molecular chalcohalide, $[(pyH)_3(Mo_6Cl_7S)Cl_6]$, was reported by Michel and McCarley.[14] This $Mo_6SCl_7^{3+}$ cluster was prepared by the sulfidation of molybdenum (II) chloride (Mo_6Cl_{12}). Additional substitution of sulfur for chlorine into Mo_6Cl_{12} has resulted in a series of molecular complexes, $Mo_6S_xCl_{8-x}L_y$, where x varies from 3 to 8.[15-20] Reactions which produce incomplete replacement of the chlorine have shown mixtures of cluster products that possess a wide range of x values. The fully sulfided cluster complexes are better characterized as evidenced by the single crystal structure solutions for the triethylphosphine, tetrahydrothiophene, pyridine, piperidine, and pyrrolidine adducts.[17-20] Concurrently, the triethylphosphine adduct has been reported by an unrelated synthetic procedure.[21,22]

The success in preparing hexamolybdenum sulfide cluster complexes through the sulfidation of molybdenum (II) chloride also led to the exploration of the tungsten

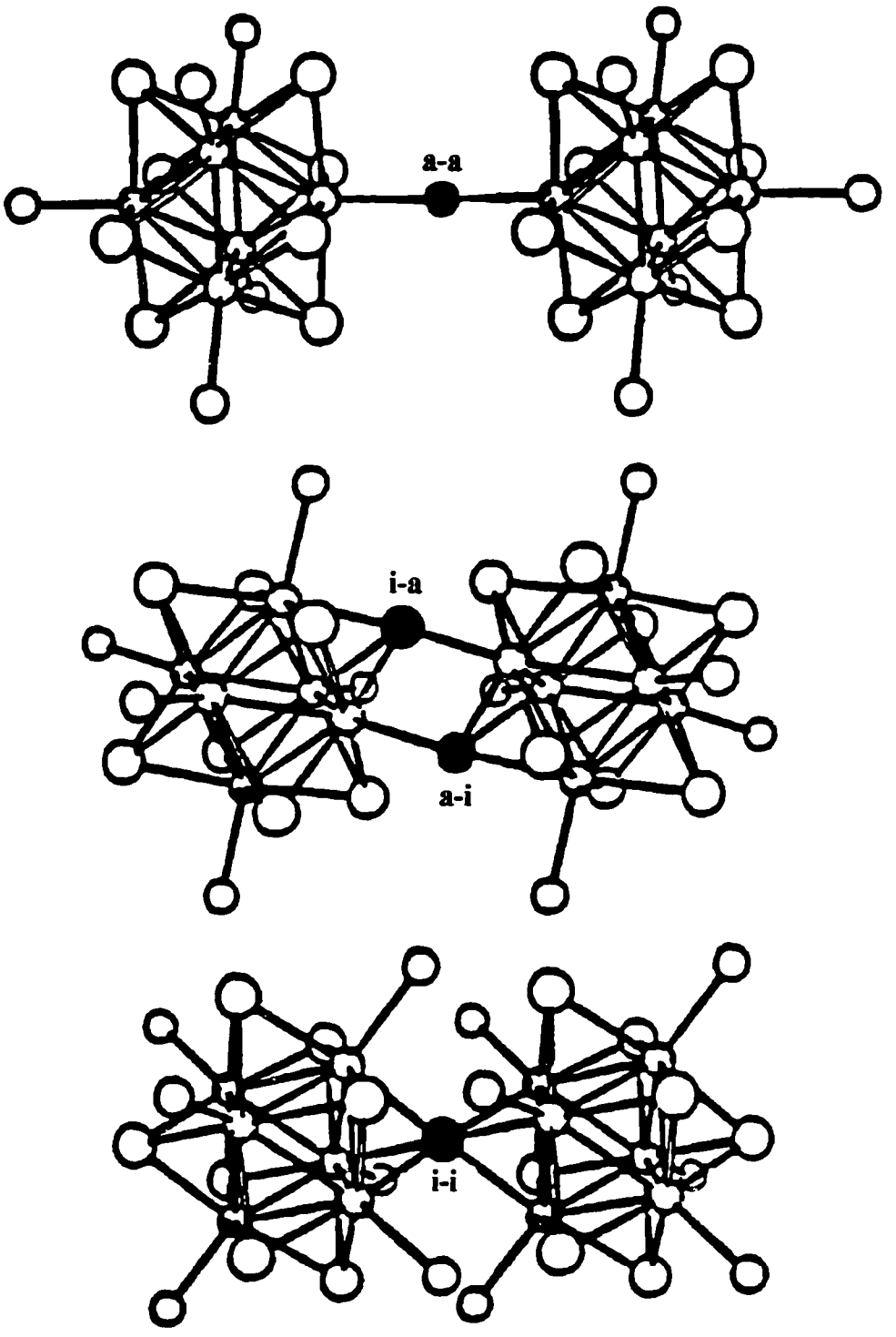

Figure 2. Possible ways that ligands can be shared between two $M_6X^i_8L^a_6$ clusters

analogues. This research has resulted in the preparation of structurally characterized adducts of the $W_6S_8L_6$ cluster unit where L is pyridine,[23,24] triethylphosphine,[24] and tetrahydrothiophene.[24] Such progress not only has established the new chemistry of molecular W_6S_8 clusters, but also will provide opportunities to approach the still unknown "tungsten Chevrel phases" via use of molecular precursors.

The focus of this project has been to further develop the understanding of these hexatungsten chalcogenide cluster complexes and move towards the overall goal of finding low temperature routes to the ideal "tungsten Chevrel phases". Areas of investigation have included the preparation and characterization of new sulfide, selenide, and telluride complexes, and the subsequent deligation of these cluster complexes in attempts to form tungsten analogues of Chevrel phases.

Dissertation Organization

This dissertation consists of four papers. Each paper is formatted for publication in a technical journal and the cited references are found at the end of each paper. A General Summary follows the four papers. The references cited in the General Introduction are found at the end of the dissertation.

Review of Previous Work

Chevrel Phases

In 1971, Chevrel *et al.* reported the existence of a new series of ternary molybdenum sulfides.[25] These materials, with the general formula $M_xMo_6Y_8$ (M= ternary metal, Y= chalcogen, $0 \leq x \leq 4$), have been found in about 160 different compounds and solid solutions with over 45 different ternary metal cations.[26] Chevrel phases have also been produced with both molybdenum and chalcogen substitution, where the metals (Nb, Ta, Re, Ru, Rh) replaced molybdenum ($Mo_{6-x}M_xY_8$) and Cl, Br, I, O were substituted for the chalcogen ($Mo_6Y_{8-x}X_x$).[2] Almost all of these compounds were synthesized directly from the ternary metal, chalcogen, and molybdenum (or binary chalcogenides) at 1000-1300°C with several annealings at 1000-1200°C. An exception is the metastable Mo_6S_8, which can only be prepared by indirect routes.[27,28]

There are generally two classes of compounds among the Chevrel phases. The first class corresponds to M being a small cation (Cu, Co, Fe, Ni) where the cation concentration is variable ($Cu_xMo_6S_8$, $1.8 \leq x \leq 4.0$). The large M cations (Pb, Sn, RE), where the cation concentrations are equal to 1.0 or have a very narrow domain ($Sn_xMo_6S_8$, $0.9 \leq x \leq 1.1$), make up the second class. Substitution of a second metal cation for the large cation can occur and results in a wide range of solid solutions.

The first ternary molybdenum sulfide crystal structure was determined for $Ni_2Mo_6S_8$[29] and the observation was made that nearly all of these compounds crystallize in a hexagonal-rhombohedral structure ($R\bar{3}$) with α_R~90° and a_R~6.5Å. However, when the ternary metal is small and the metal concentration increases, several phases do undergo a triclinic distortion ($P\bar{1}$).[25] All of these structures are closely related to the Mo_6Y_8 unit and can be described as a three dimensional network of interlinked Mo_6Y_8 clusters. As shown in Figure 2, the cluster unit is a molybdenum octahedron with each face capped by one chalcogen. The actual structure shows an elongation along the ternary axis which results in a distortion of the molybdenum octahedron. Alternatively described, the molybdenum atoms are slightly outside the face centers of the sulfur cube. The clusters are linked together such that each of the six bridging chalcogens not located on the ternary axis (three-fold axis in $R\bar{3}$) serves as a terminal ligand for one of the six neighboring clusters, as shown in Figure 3. The connectivity can be described as $(Mo_6Y_2^{i}Y_{6/2}^{i-a})Y_{6/2}^{a-i}$. This strong linkage can be evidenced by the short, covalent Mo-Y intercluster distances of 2.4-2.6 Å which are nearly as short as the intracluster Mo-Y distances and make possible the direct, though weak, intercluster Mo-Mo interactions (3.1-3.4 Å).

This arrangement of the Mo_6Y_8 units leaves cavities in the chalcogen network as indicated by "1" and "2" in Figure 4. The largest cavity (site 1), with approximately cubic shape, lies at the origin of the rhombohedral cell. Much smaller holes (site 2) are found on either side of the large cavity (site 1). These cavities are

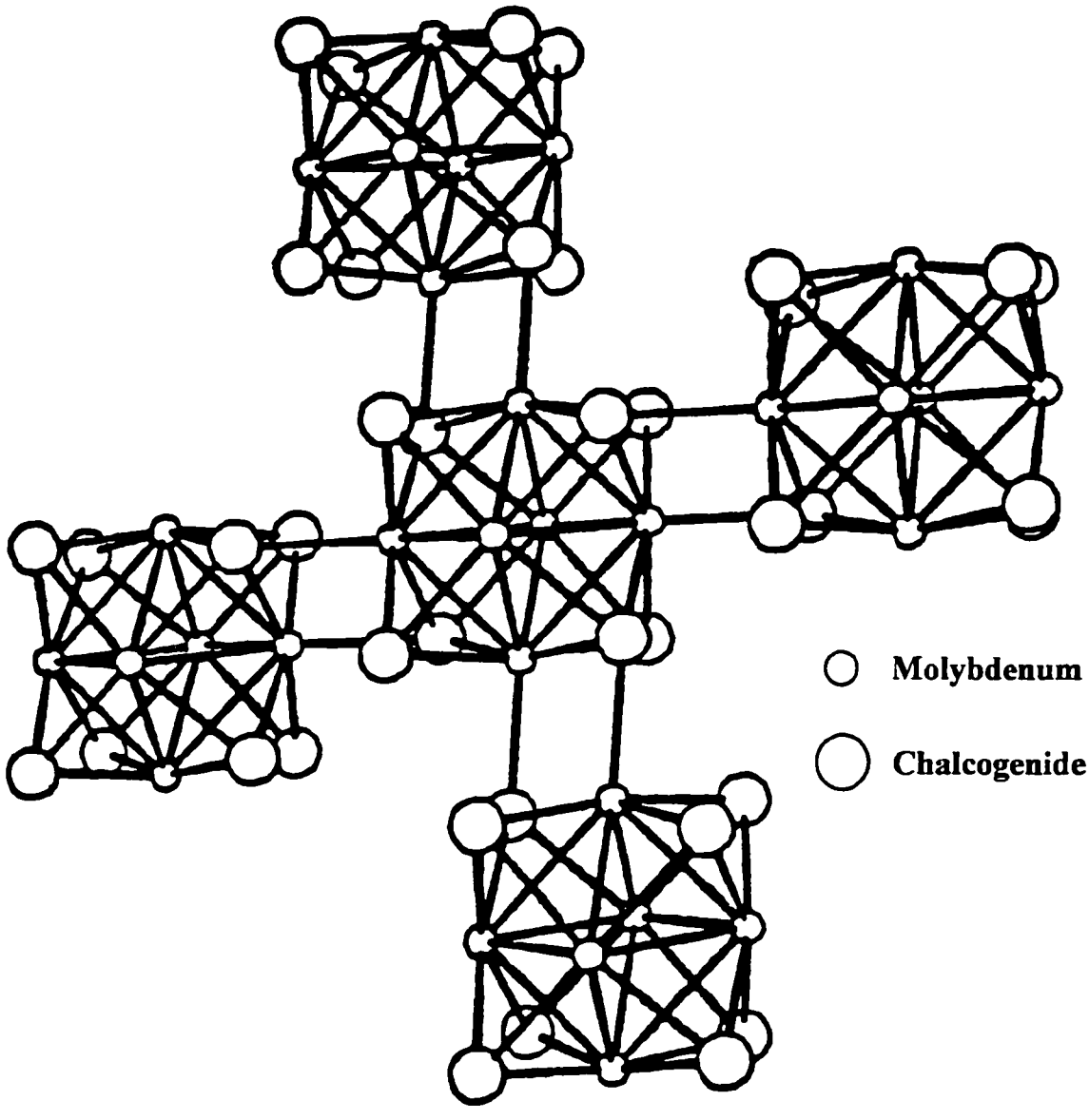

Figure 3. Structure of the Chevrel phases showing four of the six neighboring clusters

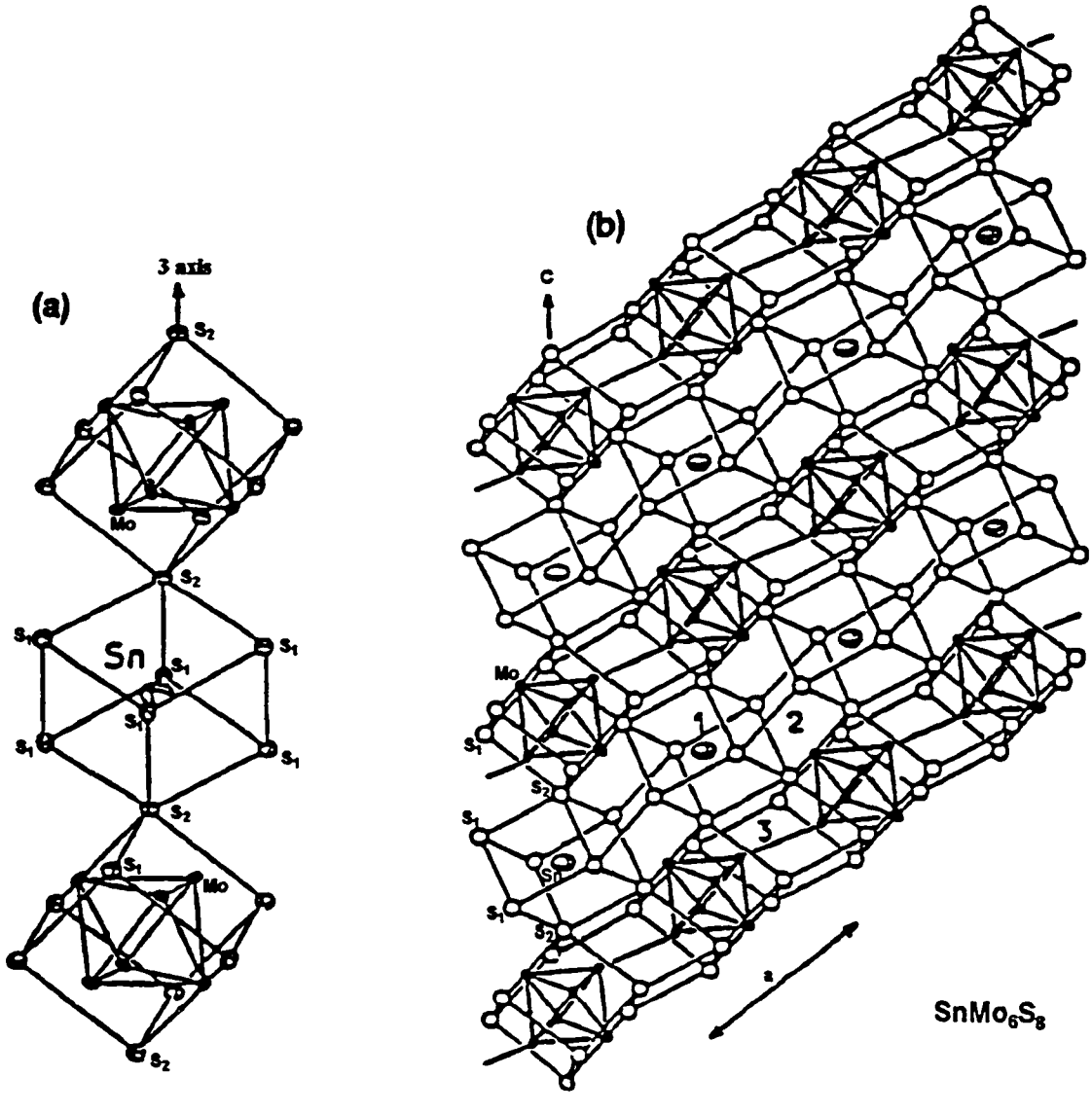

Figure 4. (a) The stacking of the Mo_6S_8 units and S_8 cubic sites along the threefold axis. Here, the Sn atoms are located at the cell origin. (b) View of the projection of the $SnMo_6S_8$ structure on the hexagonal $(11\bar{2}0)$ plane. Cavities can be noticed in the chalcogen atom network where sites 1 and 2 are partially filled by ternary metals and the inter-cluster Mo-Mo bond occurs through site 3.

all interconnected and form infinite channels along the rhombohedral axes. The large metal atoms exclusively fill site 1 to yield stoichiometric (x~1) compounds, while the smaller cations occupy both types of sites. This resulting partial occupancy yields non-stoichiometric compounds (x>1).

The occupancy of these cavities by the ternary metal is the only overall structural difference between the binary and ternary Chevrel phases. Therefore, the ternary phase can be viewed as the insertion of metal cations into the binary lattice. This concept can be exploited in the preparation of the metastable Mo_6S_8 phase via the acidic leaching of a small cation ternary molybdenum sulfide as shown in equation 1.[27,28]

$$M_xMo_6S_8 + 2x\ HCl \rightarrow Mo_6S_8 + x\ H_2 + x\ MCl_2$$

$$(M = Co, Cu, Fe, Ni) \qquad (1)$$

The high ionic mobility of the small ternary metal cations allows for the relative ease of chemical or electrochemical insertion and removal at room temperature. A variety of metastable ternary Chevrel phases can be prepared from the reaction with the binary Mo_6S_8 phase as shown in equation 2.[3,30]

$$x\ M + Mo_6S_8 \rightarrow M_xMo_6S_8 \qquad (2)$$

electrochemical - Li, Na, small cations at 25°C
chemical - Li (n-BuLi) at 25°C
Hg at 350°C

Electrochemical insertion of large cations into the binary Mo_6S_8 phase has not succeeded; yet, thermal insertion is possible with higher temperatures (470°C) and long reaction times (1-3 weeks).[31]

The physical properties of the Chevrel phase compounds are greatly dependent on the ternary metal cation. This influence is the result of a transfer of valence electrons from the "ionic" metal to the electron-deficient, metallic Mo_6Y_8 network.[1] Band structure calculations[32,33] on the Chevrel phases have indicated that the conduction band is made up of E_g cluster HOMO's and lies just below the 24 electron gap. The calculations suggested that the addition of more electrons to the cluster via a higher cation concentration or higher cation charge would cause a decrease in the intracluster Mo-Mo distance. This trend was observed experimentally, as evidenced for $Pb_{0.92}Mo_6S_8$ - 2.710 Å and Mo_6S_8 - 2.807 Å.[2] Yvon has shown that the intercluster Mo-Mo distances increase with the addition of electrons via charge transfer.[1] From band structure calculations, the conduction band of E_g character possesses δ-type symmetry ($d_{x^2-y^2}$) and results in very little interaction with neighboring clusters.[32] Therefore, the addition of electrons causes strengthening of the intracluster bonding (cluster contraction) and concomitant lengthening of the intercluster Mo-Mo distances.

Magnetic properties and the conductance of these materials have also been found to be dependent on the type of ternary metal cation that is present. Magnetic susceptibility studies have shown that the addition of a diamagnetic cation (e.g. Cu^+, Pb^{2+}) results in an overall diamagnetic species with a residual temperature-

independent paramagnetism. The addition of a magnetic metal cation (e.g. Fe^{2+}, RE^{3+}) gives rise to Curie-Weiss behavior.[26] The ternary Chevrel phase compounds have all been found to be metallic conductors. The only materials showing semiconductor behavior are the pseudobinary rhenium substituted molybdenum phase - $Re_4Mo_2Y_8$.[34] Even the 20 electron Mo_6Y_8 binary phases are metallic. This result agrees with the calculations which show that the conduction band is not purely e_g in character, but contains some chalcogenide p character and thus is not completely empty.[32] Many of the Chevrel phases also show superconductivity.

Molecular Complexes of Hexamolybdenum Chalcogenides and Chalcohalides

Until quite recently, molecular complexes with the Mo_6Y_8 cluster unit seen in the Chevrel phases have not been found.[19-22] Prior to the establishment of the molecular Mo_6Y_8 units, only molecular complexes of mixed sulfide-chloride clusters had been observed. The first molecular chalcohalide was reported by Michel and McCarley.[14] The Mo_6SCl_7 cluster was prepared by the sulfidation of Mo_6Cl_{12} and isolated as crystals of $(pyH)_3[(Mo_6SCl_7)Cl_6]$ and $(pyH)_3[(Mo_6SCl_7)Cl_6]\cdot 3pyHCl$. Since sulfur and chlorine are indistinguishable by x-ray diffraction, x-ray photoelectron spectroscopy (XPS) was used to determine that the sulfur atom occupied an inner bridging position in the cluster. The corresponding average intramolecular Mo-Mo bond distances of these two structures were equivalent (2.610 Å) and were found to agree quite well with values observed for the isoelectronic $Mo_6Cl_8^{4+}$ cluster of

Mo_6Cl_{12} (2.613 Å)[35] and the $Mo_6SCl_7^{3+}$ unit of $Mo_6Cl_{10}S$ (2.615 Å).[36] These clusters which possess 24 electrons for Mo-Mo bonding are all close to the estimated Mo-Mo single bond distance of 2.614 Å.

Michel also reported the crystal structure of what was believed to be $Mo_6S_6Cl_2(py)_6$.[15] This compound also showed no evidence for ordering of the sulfides and chlorides. The average intracluster Mo-Mo distance of 2.634 Å was close to the value estimated for a 22 electron cluster. Additional sulfidation of Mo_6Cl_{12} has yielded a series of mixed molybdenum chalcohalides with the general formula $Mo_6S_xCl_{8-x}L_y$ ($3 \leq x \leq 8$, y-variable) where incomplete sulfur substitution often leads to a mixture of cluster products.[15-20]

Recently, Saito *et al.* published the crystal structure of $Mo_6S_8(PEt_3)_6$ which was prepared by the reductive dimerization of trimeric Mo_3S_4 clusters.[21]

$$Mo_3S_7Cl_4 + 8\ PEt_3 \xrightarrow{\text{toluene}} Mo_3S_4Cl_4(PEt_3)_5 + 3SPEt_3 \qquad (3)$$

$$2\ Mo_3S_4Cl_4(PEt_3)_5 + 4\ Mg \xrightarrow{\text{THF}} Mo_6S_8(PEt_3)_6 + 4MgCl_2 + 4PEt_3 \qquad (4)$$

The selenide analogue was prepared by the same method, as well as a report on the one electron reduction to form $[PPN][Mo_6Y_8(PEt_3)_6]$ (Y=S, Se; PPN=$(Ph_3P)_2N$).[22]

Concurrently, McCarley *et al.* reported on the successful preparation of a series of molecular compounds with the Mo_6S_8 cluster unit via sulfidation of Mo_6Cl_{12}.[19,20] Adducts of pyridine (py), propylamine ($PrNH_2$), triethylphosphine (PEt_3), piperidine (pip), tetrahydrothiophene (THT), pyrrolidine (pyrr), and 4-methylpyridine were

prepared and the structures of the phosphine, thiophene, piperidine, and pyrrolidine complexes were determined. The sulfidation of the Mo_6Cl_{12} cluster has a distinct advantage as a general preparation technique due to the range of adducts which can be prepared. Another advantage lies in the high yields attainable because of the relative stability of the metal cluster during the sulfidation, as evidenced by very little, if any, cluster decomposition. The presence of the coordinating ligands appears to help stabilize the Mo_6S_8 cluster unit.

The first synthetic route used to prepare the completely sulfided cluster unit is shown below in equation 5, 6. Later, it was discovered that this $Mo_6S_8(py)_{\sim 4}$ had

$$Mo_6Cl_{12} + 8\ NaSH + 4\ NaOBu \xrightarrow{BuOH/py} \xrightarrow{MeOH\ wash} Mo_6S_7Cl(py)_x \qquad (5)$$

$$Mo_6S_7Cl(py)_x + 2\ NaSH \xrightarrow{BuOH/py} \xrightarrow{MeOH\ wash} Mo_6S_8(py)_{\sim 4} \qquad (6)$$

been misformulated. Both the previous two-step route and a new one-step method with higher stoichiometric amounts of the sulfiding agent, NaSH, resulted in a similar product which contained sodium, $Na_{2y}Mo_6S_{8+y}(py)_x$.

As shown in the reaction below, propylamine adducts without sodium, $Mo_6S_8(PrNH_2)_6$, can be prepared from this pyridine complex via ligand exchange.

$$Na_{2y}Mo_6S_{8+y}(py)_x + xs\ PrNH_2 \rightarrow Mo_6S_8(PrNH_2)_n + x\ py + yNa_2S \qquad (7)$$

And subsequent ligand exchange reactions with the propylamine adduct produced the other molecular complexes.

From the crystal structures of these molecular adducts, it is observed that the Mo_6S_8 cluster units are isolated with no intercluster interactions. The average intracluster Mo-Mo bond distances are found in the range from 2.6584 Å to 2.640 Å. These bond lengths are quite close to the value of 2.662 Å which is estimated for a 20-electron octahedral cluster.

Molecular Complexes of Hexatungsten Sulfides

Following the success in preparing the molecular Mo_6S_8 cluster unit, similar attempts were made to prepare the analogous tungsten complexes.[23,24] Complete substitution of the sulfide for chloride was achieved by using the stoichiometry of 1 W_6Cl_{12} : 12 NaSH : 6 NaOBu in neat pyridine. The resulting powder was poorly crystalline. However, single crystals of $W_6S_8(py)_6$ could be prepared by higher temperature (200°C) heating in pyridine. Unlike their molybdenum analogues, the product recovered from the 1:12:6 reaction did not contain sodium, and the sulfide substitution reaction for tungsten chloride is more rapid than that of the molybdenum compound. Ligand displacement of the pyridine adduct by triethylphosphine and tetrahydrothiophene produced crystalline molecular complexes also with the general formula $W_6S_8L_6$ (L = py, PEt_3, THT).

Single crystal structures for $W_6S_8(py)_6$, $W_6S_8(PEt_3)_6$, and $W_6S_8(THT)_6$ have been determined. The W-W bond distances in the these W_6S_8 clusters are longer than those in $W_6Cl_8^{4+}$, by an amount in agreement with a bond order of 0.833 in the former as compared to 1.0 in the latter, based on 20 and 24 electrons, respectively, for W - W bonding. The nearly perfect octahedral symmetry of the cluster units, and their diamagnetic susceptibility, clearly indicate that there is no orbital degeneracy in the ground state of the complexes.

Far-infrared spectroscopy was found to be a useful tool to monitor the extent of sulfidation and coordinated ligand exchange of the hexatungsten clusters. The W_6S_8 cluster unit shows a strong band around 380 cm^{-1}, which is assigned as the IR-allowed T_{1u} W-S stretching modes. This band is the characteristic band for the tungsten sulfide cluster complexes. In comparison, the W_6Cl_{12} starting material shows strong bands in the region of 280-320 cm^{-1}.

Substitution of coordinated pyridine ligands by triethylphosphine has been achieved but not the reverse. However, the pyridine and tetrahydrothiophene complexes can be interconverted. Based upon the comparison of W-L bond distances, these results suggested that the strength between tungsten and the organic terminal ligands appeared to have the following order: $PEt_3 > THT \geq py$.

CHAPTER 1. SYNTHESIS, CHARACTERIZATION, AND STRUCTURE OF TUNGSTEN SULFIDE CLUSTER COMPOUNDS

A paper to be submitted to Inorganic Chemistry

Xiaobing Xie and Robert E. McCarley

Abstract

The soluble and weakly-coordinated complexes $W_6S_8(pip)_6$ and $W_6S_8(BuNH_2)_6$ were prepared by reacting W_6Cl_{12} with NaSH and NaOBu in piperidine and butylamine, respectively. Crystals for the piperidine complex were grown from the reaction filtrate. Crystallographic data for this complex are as follows: $W_6S_8(pip)_6 \cdot 7pip$, tetragonal, $I\bar{4}$, a = 19.410(4) Å, c = 22.553(9) Å, Z = 4. A new sodium ternary tungsten sulfide, $Na_{2x}(W_6S_8)S_x(MeOH)_y$, was obtained when acetonitrile was used as the solvent in the sulfidation reaction. Furthermore, the tin compound, $Sn_x(W_6S_8)S_x(MeOH)_y$, was prepared via ion-exchange. Infrared and XP spectra supported the presence of the W_6S_8 cluster units in these ternary tungsten sulfides. These compounds are the first examples of ternary tungsten sulfides that contain the W_6S_8 cluster unit.

Introduction

The Chevrel phases of the general formula $M_xMo_6Y_8$ (M = ternary metal cation, $1 \leq x \leq 4$, Y=S, Se or Te), are an important class of compounds because of their interesting chemical and physical properties. Among these are numerous examples of high H_{c2} superconductors,[1] ordered magnetic phases,[2] solid electrolytes (fast ion conductors)[3], and hydrodesulfurization catalysts.[4] Structurally, the compounds consist of 3-dimensionally interlinked Mo_6Y_8 cluster units sharing chalcogenide ions between bridging and terminal positions[5] as indicated by the formulation $(Mo_6Y_2^iY_{6/2}^{i-a})Y_{6/2}^{a-i}$.[6] The interlinking joins each cluster with six adjoining cluster units in a rhombohedral (sometimes lower symmetry) stacking. The ternary metal ions M^{n+}, with n = 1 to 4, find positions within the interstices of this network in either large cation (*e.g.* Pb^{2+}, Sn^{2+} or La^{3+}) or small cation (*e.g.* Li^+, Cu^+ or Ni^{2+}) sites.[7] Electron transfer from the cations gives formal charges of 1- to 4- on the $Mo_6Y_8^{n-}$ anionic network, and consequently metal cluster electron counts of 20 to 24 can be realized.[8] The 20 electron case is realized in the binary phases Mo_6Y_8, of which the sulfide is metastable and must be prepared by indirect means,[9] the selenide and telluride members are stable and easily prepared by direct combination of the elements.[10]

Up to the present time, there has been no report concerning the successful preparation of the tungsten analogues W_6S_8 or $M_xW_6Y_8$. It is generally understood that these compounds must be unstable with respect to disproportionation (into W and WY_2 or W, WY_2 and $MY_{n/2}$). Thus, if success is to be achieved, preparation of the tungsten analogues must be pursued by low temperature approaches. In this laboratory work

has been successful in developing the chemistry of molecular complexes $M_6S_8L_6$ for both the molybdenum[11] and tungsten[12] cluster units. These complexes are projected to be useful in the development of low temperature routes to the ternary phases $M_xMo_6S_8$ and $M_xW_6S_8$. Such routes also could lead to methods for the deposition of films, coatings and highly dispersed or high surface area solids useful in electronic or catalytic applications.

Tungsten(II) chloride $(W_6Cl_8)Cl_4$ was chosen as a starting material, because it is structurally similar to the Chevrel phases, in that it also contains octahedral cluster units, $(W_6Cl_8)^{4+}$. Substitution of sulfide for chloride in W_6Cl_8, if it can be done successfully without decomposition of the cluster, should be an efficient method for the synthesis of $W_6S_8L_6$.

Prior to this work, substitution of sulfide for chloride in W_6Cl_8 had led to the discovery of molecular complexes of hexatungsten sulfide clusters,[13] $W_6S_8(py)_6$, $W_6S_8(PEt_3)_6$, and $W_6S_8(THT)_6$. It was found that sodium hydrosulfide was a good sulfiding reagent, especially in combination with a proton acceptor like sodium alkoxide. With the use of an excess amount of sodium hydrosulfide and sodium alkoxide (for example, twelve moles of sodium hydrosulfide and six moles of sodium n-butoxide per mole of cluster), the completely sulfided cluster $W_6S_8L_6$ can be synthesized in almost quantitative yield.

In this paper, the synthesis, characterization and structure of a new tungsten sulfide complex, $W_6S_8(pip)_6$, and ternary salts containing the tungsten sulfide cluster unit are presented.

Experimental

Materials

The reagents and products are air and moisture sensitive. Therefore, all manipulations were performed by the use of an inert-atmosphere (N_2 or Ar) drybox, a high-vacuum manifold, and Schlenk techniques, unless otherwise stated. W_6Cl_{12} was prepared by literature methods.[13,14] NaSH was prepared by the reaction of H_2S with NaOEt in ethanol according to the method described by Brauer.[15] NaOEt was obtained by the reaction of sodium metal with ethanol and used as the solid after vacuum removal of the solvent.

All solvents were purified and dried prior to use. Also, the solvents were deoxygenated by use of the freeze-thaw process: freeze to liquid nitrogen temperature, evacuate the gaseous material, and then thaw to obtain the liquid. This process was repeated three times prior to distillation of the purified solvent onto Linde 3- or 4-Å Molecular Sieves and stored under vacuum or a nitrogen atmosphere. Pyridine (Fisher), piperidine (Fisher), n-propylamine (Aldrich), n-butylamine (Aldrich), and acetonitrile (Fisher) were purified by refluxing over calcium hydride for at least 4 hours. Toluene (Fisher) and dichloromethane (Fisher) were refluxed over phosphors pentoxide. Without heating, tetrahydrofuran (Fisher) was dried by stirring with sodium metal and benzophenone. Ethanol was dried by stirring with sodium metal, and methanol (Mallinckrodt) was dried by refluxing over sodium methoxide. For use in a procedure, the solvents were vacuum distilled or

syringed under a flowing nitrogen gas atmosphere.

Physical Measurements

Infrared spectroscopy

All infrared spectra were collected using Nujol mulls and the samples were prepared in the drybox and were temporarily stored under nitrogen before being placed in the sample chamber of the instrument. Infrared (4000-200 cm^{-1}) spectra were recorded with a Bomem MB-102 Fourier transform infrared spectrometer manufactured by Hartman and Braun. Samples were prepared as Nujol mulls and the mulls were pressed between two cesium iodide plates. The sample chamber of the instrument was continuously purged with dry, compressed air and reference spectra were collected in the empty chamber.

X-ray photoelectron spectroscopy

XP spectra were collected by James Anderegg at room temperature with a Physical Electronics Industries 5500 multitechnique surface analysis system. This system was equipped with a hemispherical analyzer, a toroidal monochromator, and multichannel detector which sampled a 2 mm^2 area. The samples were pressed on an indium substrate and loaded into an air-sensitive sample holder in the dry-box. Then the sample holder was transferred into the chamber of the spectrometer. After the system was completely evacuated, the sample holder was opened and the

sample was excited with monochromatic Mg K-α radiation (1253.6 eV) at the power of 300 W. The photoelectron binding energies were calibrated with C 1s = 284.6 eV.

X-ray powder diffraction

Powder X-ray diffraction (XRD) data were obtained with a Philips ADP3520 θ-2θ diffractometer using Cu *K*α radiation. The air-sensitive samples were loaded into a specially designed sample holder and sealed under N_2 while in the drybox.

Analytical Procedures

Tungsten was determined gravimetrically as the trioxide. If ternary metal cations were not present, samples were placed in tared crucibles and decomposed initially with dilute (3M) nitric acid. Concentrated nitric acid was then added to ensure complete oxidation and the samples evaporated to dryness. After ignition in a muffle furnace at 800°C, the resulting WO_3 solid was weighed. If ternary metal cations were present, the samples were dissolved in 0.5 M KOH basic solutions with the aid of hydrogen peroxide. The solutions were then treated with equal volumes of concentrated nitric acid and 2 mL of hydrogen peroxide to form a peroxy-acid complex. The hydrated oxide, $WO_3 \cdot nH_2O$, was then completely precipitated by slowly decomposing this complex at 100°C and collected in tared ceramic filter crucibles. The materials were then dried to constant weight at 800°C.

Chlorine was determined by potentiometric titration with a standardized silver nitrate solution after dissolving the samples in hot KOH-H_2O_2 solution and neutralization. A silver/silver chloride electrode was used as the reference electrode and a silver wire as the working electrode. The endpoint was determined by using the second derivative method.

Sodium analysis was performed by atomic absorption spectroscopy using a Perkin-Elmer 305B spectrometer. All the reference solutions and the sample solution were prepared by using deionized water. The sample was dissolved in a KOH basic solution with the aid of hydrogen peroxide. The resulting sample solution had a concentration of about 18 μg sample per mL. The reference solutions were a series of standardized NaCl solutions, whose sodium ion (Na^+) concentration ranged from 0.1001μg/mL to 1.001μg/mL. A Hollow Cathode lamp was used as the light source, and the operating wavelength was 589 nm. Sodium is ionized in an air-acetylene flame.

Synthetic Procedures

Preparation of $W_6S_8(pip)_6$

W_6Cl_{12} (0.50 g, 0.328 mmol), NaSH (0.22 g, 3.93 mmol), and NaOEt (0.133 g, 1.97 mmol) were weighed in the drybox and transferred into a 100-mL Schlenk reaction flask equipped with a water-cooled condenser. By distillation, 50 mL of piperidine were added to the reactants and the mixture was refluxed for 3-4 days. A

dark-brown solid and dark-red solution were separated by filtration. The solvent was then removed from the filtrate under dynamic vacuum, and after drying overnight *in vacuo,* 0.33 g of brown powder was obtained. IR (Nujol, cm^{-1}): 3200 (m), 1350 (w), 1304 (m), 1270 (m), 1178 (m), 1084 (m), 1062 (s), 1039 (w), 1021 (s), 994 (m), 980 (w), 940 (w), 870 (s), 805 (ms), W-S 376 (ms), 227 (ms). A test for chloride was negative. Brown single crystals of $W_6S_8(pip)_6 \cdot 7pip$ were grown from the reaction filtrate by allowing it to stand at room temperature for a couple of days. About 0.46 g of brown insoluble powder was obtained upon filtration of the original reaction mixture. After 2-3 days of methanol extraction, about 0.25 g of brown powder was recovered. Both infrared and XP spectra indicated that this insoluble product was the $W_6S_8(pip)_6$ complex.

Sulfidation reactions in butylamine

A typical preparation involved loading W_6Cl_{12} (0.50 g, 0.328 mmol), NaSH (0.183 g, 3.28 mmol), and NaOEt (0.113 g, 1.64 mmol) in a 100 mL reaction flask. Then approximately 50 mL of butylamine were vacuum-distilled onto the solid. The mixture was refluxed for 3 days and, upon filtering, a dark brown solution and about 0.22 g white solid resulted. The butylamine solvent was removed under dynamic vacuum, and the resulting black powder was dried *in vacuo* for one day. Approximately, 0.55 g of black solid was recovered from the filtrate. Elemental analyses, infrared, and XP spectra were obtained on this black powder. Anal. Found: W, 56.33%. A test for chloride was negative. IR (Nujol, cm^{-1}): 1570 (m),

1350 (w), 1304 (m), 1152 (m), 1062 (s), 1033 (w), 946 (m), 462(m), W-S 376 (ms). The insoluble white solid was presumably composed of the by-product NaCl and unreacted NaSH.

The black powder recovered from the reaction filtrate was loaded into a reaction flask and 50 mL of toluene was syringed into the flask. Then the mixture was stirred at room temperature overnight. A dark brown filtrate and black powder were separated by filtration. After the toluene solvent was stripped away from the filtrate *in vacuo*, a black powder remained. IR (Nujol, cm^{-1}): 1566 (m), 1149 (m), 1055 (ms), 1019 (s), 938 (m), W-S 374 (s).

Preparation of $Na_{2x}(W_6S_8)S_x(MeOH)_y$

W_6Cl_{12} (2.34 g, 1.53 mmol), NaSH (1.02 g, 18.2 mmol), and NaOEt (0.625 g, 9.2 mmol) were loaded in a Schlenk reaction flask equipped with a water-cooled condenser. By distillation, 50 mL of acetonitrile were added to the reactants and the mixture was refluxed for 3-4 days. A black solid and faint yellow solution were separated by filtration. The solid was extracted with methanol for several days to remove the NaCl by-product, and the remaining solid was dried *in vacuo*. The product (2.06 g) showed an absence of Cl by chlorine analyses. The presence of sodium was confirmed by XPS. The product was found to be slightly soluble in methanol and amorphous to X-rays. IR (Nujol, cm^{-1}): $\nu(C\text{-}O)_{MeOH}$ 960 (br), ν(W-S) 376. Anal. Calcd. for $Na_{2.1}(W_6S_8)S_{1.05}(MeOH)_{5.4}$: Na, 2.98%; W, 68.19%. Found: Na, 3.02%; W, 66.50%; $Na/W_6 = 2.12$. Similar reactions were also examined in butanol.

Preparation of $Sn_x(W_6S_8)S_x$ by ion-exchange.

The procedure for the ion-exchange reaction involved transfer in the drybox of weighed amounts of $Na_{2x}(W_6S_8)S_x(MeOH)_y$ (1.00 g) and an excess of the metal salt $SnCl_2$ into a 100-mL Schlenk reaction flask. Then 30 mL of tetrahydrofuran (THF) were vacuum-distilled onto the solids. After the mixture was stirred at room temperature for 1-2 days, a black solid and faint yellow solution were obtained. The resulting solid was extracted with methanol in order to remove the NaCl by-product and any unreacted metal salt. After drying under dynamic vacuum, a black powder was obtained. The product was found to be insoluble in common solvents and amorphous to X-rays. IR (Nujol, cm^{-1}): $\nu(C\text{-}O)_{MeOH}$ 958 (br), ν(W-S) 376. An XP spectrum showed the absence of Na and presence of Sn.

X-ray Structure Determinations

A crystal of $W_6S_8(pip)_6 \cdot 7pip$ was chosen from material still in contact with the mother solution. The crystal was encased in epoxy cement, attached to the tip of a glass fiber, and immediately inserted into the low-temperature nitrogen stream of the diffractometer for data collection. The cell constants were determined from 25 randomly located and centered reflections. The structures were solved by direct methods using SHELXS[16] and refined on F by full-matrix, least-squares techniques with the TEXSAN package.[17] Pertinent crystallographic data are listed in Table 1.

Table 1. Crystallographic Data for the $W_6S_8(pip)_6 \cdot 7pip$ Cluster Complex.

compound	$W_6S_8(pip)_6 \cdot 7$ pip	radiation (Mo, $K\alpha$) Å	0.71069
chemical formula	$C_{65}H_{143}N_{13}S_8W_6$	T, °C	-70
formula weight	2466.51	2θ range, deg	5-60
space group	$I\bar{4}$ (No. 82)	total data	6723
a, Å	19.410 (4)	unique data	6387
c, Å	22.553 (9)	data obsd.	3539 ($I>4.0\sigma(I)$)
V, Å^3	8496 (5)	R^a	0.0509
Z	4	$R_w{}^b$	0.0498
ρ_{calcd}, g/cm^3	1.928	diff. peaks, e/Å^3	1.84, -1.98
μ, cm^{-1}	83.40	no. parameter	360
abs. correction	DIFABS	data/parameter	9.83
trans. Factors	0.8710 - 1.0945		

$^aR = \Sigma||F_o|-|F_c||/\Sigma|F_o|$.

$^bR_w = [\Sigma w(|F_o|-|F_c|)^2/\Sigma w|F_o|^2]^{1/2}$; $w = 1/\sigma^2(|F_o|)$.

Structure determination for $W_6S_8(pip)_6 \cdot 7pip$

Single crystals of $W_6S_8(pip)_6 \cdot 7pip$ were grown from a portion of the reaction filtrate by allowing it to stand at room temperature for several days. A black rectangular crystal, with dimensions of 0.3 x 0.4 x 0.5 mm^3, was mounted on a glass fiber, and data collection proceeded at -70°C. Data were collected with a Rigaku AFC6R diffractometer using Mo Kα radiation, over the range $5° < 2\theta < 60°$ for one octant (*-h,-k,-l*), using the ω-2θ scan technique. Three standard reflections were monitored every 300 reflections and showed no intensity variation over the

collection period. A total of 6723 reflections were collected, of which 6387 were unique (R_{int} = 0.150) and 3539 were observed with $I > 4\sigma(I)$. The linear absorption coefficient, μ, for Mo $K\alpha$ radiation is 83.4 cm^{-1}. First, an empirical absorption correction using the φ scan technique was applied after the structure solution. After all of the atoms were located and refined isotropically, an absorption correction using the DIFABS program[18] was applied and resulted in the relative transmission factors ranging from 0.87 to 1.10. The data were corrected for Lorentz and polarization effects.

The tetragonal space group $I\bar{4}$ was chosen on the basis of systematic absences and intensity statistics. Two other space groups were possible, *I4/m* and *I*4, but neither provided a good SHELXS solution as a reasonable starting model. Initial tungsten atom positions were input on the basis of the SHELXS direct methods output. Subsequently, the other non-hydrogen atomic positions were located directly from the electron density difference maps. Most atoms were refined with anisotropic thermal parameters, except for several nitrogen and carbon atoms in the piperidine molecules. Idealized hydrogen positions were calculated and placed in the refinement with C-H distances equal to 1.04 Å and N-H distances equal to 0.96 Å, but their parameters were held constant during subsequent cycles.

The asymmetric unit was found to be $W_3S_4(pip)_3 \cdot 3.5pip$, where three of the solvent piperidine molecules were well-behaved and displayed the chair conformation, but the remaining half-piperidine molecule was disordered. This disorder occurred about a crystallographic two-fold axis and was modeled with

atoms C(71), N(71), C(72), N(72), C(73), and N(73). The carbon/nitrogen atoms of this solvent molecule were given occupancies with the 0.83333:0.16667 ratio. This disordered half-piperidine molecule once joined with its symmetry equivalent displayed the boat conformation. The W_6S_8 cluster unit was centered on a 2-fold position (4e). The final cycle of full-matrix least-squares refinement was based on 3539 observed reflections and 360 variable parameters and converged with unweighted and weighted agreement factors of: R = 0.051 and R_w = 0.050, respectively. The atomic coordinates and equivalent isotropic thermal parameters of the non-hydrogen atoms are given in Table 2, and the anisotropic thermal parameters are shown in Table 3.

Results and Discussion

Synthesis of $W_6S_8(pip)_6$.

Previous research on sulfide substitution into the $W_6Cl_8^{4+}$ cluster units showed that NaSH was a good sulfiding agent. By using the reaction stoichiometry of 1:12:6 (W_6Cl_{12}:NaSH:NaOEt), one-step preparations of the $W_6S_8L_6$ cluster complexes were achieved. However, among the resulting complexes, the pyridine complex, $W_6S_8(py)_6$, was very insoluble and the coordinating pyridine ligands were strongly bonded to the tungsten atoms. However, the synthesis of more soluble and weakly ligated adducts

Table 2. Atomic Coordinates and Equivalent Isotropic Thermal Parameters ($Å^2$) of the Non-Hydrogen Atoms for $W_6S_8(pip)_6 \cdot 7pip$

atom	x	y	z	B_{eq}[a]
W(1)	0.09666(5)	0.00747(5)	0.26678(6)	1.27(2)
W(2)	-0.00481(7)	0.06858(7)	0.32520(4)	1.27(3)
W(3)	-0.00539(7)	0.06796(6)	0.20683(5)	1.22(3)
S(1)	0.0797(3)	0.1334(3)	0.2644(5)	2.0(1)
S(2)	0.0997(3)	-0.1197(3)	0.2663(5)	2.0(1)
S(3)	0.0886(4)	0.0054(5)	0.3747(3)	1.9(2)
S(4)	0.0908(4)	0.0069(5)	0.1583(3)	2.1(2)
N(1)	0.2167(10)	0.026(1)	0.267(1)	1.8(4)
N(2)	-0.007(1)	0.153(1)	0.394(1)	1.9(5)
N(3)	-0.020(1)	0.148(1)	0.133(1)	1.9(5)
N(4)	-0.024(1)	0.276(1)	0.306(1)	2.6(6)
N(5)	0.818(1)	0.171(2)	0.139(1)	3.6(6)
N(6)	0.210(1)	0.140(1)	0.164(1)	3.3(7)
C(11)	0.330(1)	-0.014(2)	0.230(2)	4.2(9)
C(12)	0.253(2)	-0.030(1)	0.239(2)	3.6(8)
C(13)	0.360(2)	-0.002(2)	0.278(3)	8(1)
C(14)	0.321(2)	0.059(2)	0.319(1)	3.4(8)
C(15)	0.250(2)	0.040(2)	0.320(2)	3.0(8)
C(21)	0.047(2)	0.159(2)	0.435(2)	3.9(8)
C(22)	0.048(2)	0.230(2)	0.470(2)	6(1)
C(23)	-0.069(2)	0.159(2)	0.427(3)	6(1)
C(24)	-0.014(3)	0.229(2)	0.507(2)	6(1)
C(25)	-0.075(3)	0.215(2)	0.477(3)	9(1)

[a] $B_{eq} = (8/3)\pi^2[U_{11}(aa^*)^2 + U_{22}(bb^*)^2 + U_{33}(cc^*)^2 + 2U_{12}aa^*bb^*\cos\gamma + 2U_{13}aa^*cc^*\cos\beta + 2U_{23}bb^*cc^*\cos\alpha]$

Table 2. (continued)

atom	x	y	z	B_{eq}
C(31)	0.005(2)	0.122(2)	0.072(1)	2.6(6)
C(32)	0.007(2)	0.219(2)	0.140(2)	4.3(9)
C(33)	0.016(2)	0.239(3)	0.033(2)	6(1)
C(34)	-0.018(2)	0.174(2)	0.019(1)	2.7(7)
C(35)	-0.006(2)	0.269(2)	0.092(2)	5(1)
C(41)	0.027(3)	0.325(2)	0.297(2)	8(1)
C(42)	0.022(2)	0.390(2)	0.340(2)	6(1)
C(43)	-0.040(2)	0.418(2)	0.334(2)	4.0(10)
C(44)	-0.097(2)	0.369(2)	0.336(2)	6(1)
C(45)	-0.091(2)	0.309(1)	0.294(2)	4.1(9)
C(51)	0.792(3)	0.232(3)	0.164(2)	7(1)
C(52)	0.764(3)	0.284(3)	0.136(2)	7(1)
C(53)	0.731(2)	0.250(2)	0.083(2)	4(1)
C(54)	0.750(3)	0.195(3)	0.054(2)	6(1)
C(55)	0.769(2)	0.140(2)	0.095(3)	6(1)
C(61)	0.223(2)	0.212(2)	0.171(2)	4(1)
C(62)	0.296(2)	0.232(2)	0.167(2)	4.0(9)
C(63)	0.322(2)	0.218(2)	0.108(2)	4(1)
C(64)	0.296(3)	0.146(2)	0.086(2)	6(1)
C(65)	0.228(2)	0.127(2)	0.100(2)	3.9(8)
C(71)[b]	0.570(4)	0.028(4)	0.476(3)	12(1)
C(72)[b]	0.490(4)	0.066(4)	0.440(3)	11(1)
C(73)[b]	0.443(3)	0.042(4)	0.469(3)	10(1)
N(71)[b]	0.5701	0.0275	0.4759	12.8
N(72)[b]	0.4899	0.0655	0.4405	12.0
N(73)[b]	0.4431	0.0421	0.4693	10.3

[b]Disordered positions

Table 3. Anisotropic Thermal Parameters[a] ($Å^2$) of the Non-Hydrogen Atoms for $W_6S_8(pip)_6 \cdot 7pip$

atom	U_{11}	U_{22}	U_{33}	U_{12}	U_{13}	U_{23}
W(1)	0.0129(4)	0.0168(5)	0.0184(5)	-0.0002(4)	-0.0006(6)	0.0006(7)
W(2)	0.0178(8)	0.0160(8)	0.0145(5)	0.0024(8)	0.0009(5)	-0.0011(5)
W(3)	0.0151(7)	0.0168(8)	0.0145(5)	-0.0019(8)	0.0002(5)	0.0016(5)
S(1)	0.027(3)	0.020(3)	0.027(4)	0.000(3)	0.000(4)	-0.006(4)
S(2)	0.018(3)	0.019(3)	0.039(4)	0.004(2)	0.003(4)	-0.010(4)
S(3)	0.028(4)	0.025(4)	0.018(3)	0.008(4)	-0.006(3)	-0.009(4)
S(4)	0.021(4)	0.034(5)	0.024(4)	-0.006(4)	0.006(3)	-0.004(4)
N(3)	0.02(1)	0.01(1)	0.04(2)	0.007(10)	-0.01(1)	-0.02(1)
N(4)	0.04(2)	0.04(2)	0.02(1)	0.01(1)	0.00(1)	0.02(1)
N(6)	0.02(1)	0.06(2)	0.04(2)	-0.02(1)	-0.01(1)	0.03(2)
C(11)	0.01(1)	0.06(2)	0.09(3)	0.00(1)	-0.01(2)	-0.03(3)
C(12)	0.05(2)	0.04(2)	0.05(2)	-0.03(1)	-0.02(2)	0.02(2)
C(13)	0.02(2)	0.06(3)	0.25(8)	0.02(2)	0.02(3)	0.11(4)
C(14)	0.02(2)	0.09(3)	0.02(2)	-0.01(2)	-0.01(1)	-0.01(2)
C(15)	0.03(2)	0.04(2)	0.05(2)	0.01(1)	-0.01(2)	-0.01(2)
C(23)	0.06(3)	0.05(3)	0.14(5)	0.00(2)	-0.01(3)	-0.03(3)
C(25)	0.16(5)	0.01(2)	0.20(6)	-0.01(3)	0.17(5)	-0.01(3)
C(32)	0.09(3)	0.02(2)	0.06(2)	-0.03(2)	-0.05(2)	0.02(2)
C(33)	0.04(2)	0.13(4)	0.06(3)	-0.06(3)	-0.03(2)	0.05(3)
C(34)	0.05(2)	0.04(2)	0.02(2)	0.02(2)	0.01(1)	0.01(1)
C(35)	0.13(4)	0.01(2)	0.06(3)	-0.03(2)	0.01(3)	0.00(2)
C(41)	0.16(5)	0.08(3)	0.08(3)	-0.07(3)	-0.10(3)	0.04(2)

Table 3. (continued)

atom	U_{11}	U_{22}	U_{33}	U_{12}	U_{13}	U_{23}
C(42)	0.11(4)	0.04(2)	0.09(4)	-0.05(3)	-0.05(3)	0.04(2)
C(43)	0.06(2)	0.03(2)	0.07(3)	0.01(2)	0.02(2)	-0.02(2)
C(44)	0.04(2)	0.10(4)	0.09(4)	0.03(2)	0.00(2)	0.04(3)
C(45)	0.06(2)	0.01(1)	0.08(3)	0.00(2)	0.00(2)	0.02(2)
C(51)	0.09(4)	0.13(5)	0.08(4)	0.06(3)	-0.07(3)	-0.05(3)
C(52)	0.17(6)	0.07(3)	0.05(3)	-0.02(4)	-0.05(4)	-0.01(3)
C(53)	0.06(3)	0.03(2)	0.09(4)	-0.02(2)	0.03(3)	-0.01(2)
C(54)	0.13(5)	0.08(3)	0.04(3)	0.00(3)	-0.02(3)	-0.02(3)
C(55)	0.05(2)	0.02(2)	0.18(6)	-0.02(2)	0.01(3)	-0.01(3)
C(61)	0.08(3)	0.02(2)	0.08(3)	0.00(2)	-0.02(3)	-0.02(2)
C(62)	0.05(2)	0.05(2)	0.05(3)	-0.03(2)	0.01(2)	-0.01(2)
C(63)	0.05(2)	0.03(2)	0.10(4)	0.00(2)	0.03(2)	0.04(2)
C(64)	0.14(5)	0.07(3)	0.04(3)	0.00(3)	0.02(3)	0.02(3)

[a]The coefficients U_{ij} of the anisotropic thermal parameter expression are defined as: $\exp[-2\pi^2(a^{*2}U_{11}h^2+b^{*2}U_{22}k^2+C^{*2}U_{33}l^2+2a^*b^*U_{12}hk+2a^*c^*U_{13}hl+2b^*c^*U_{23}kl)]$

was desirable for use as precursors in the conversion to tungsten analogues of the Chevrel phases $M_xMo_6S_8$.

The piperidine complex, $W_6S_8(pip)_6$, was obtained by refluxing the starting materials (1:12:6 mole ratio) in neat piperidine. A portion of a desired product can be recovered from the reaction filtrate due to its relatively high solubility and the remainder of the desired product can be recovered from the insoluble fraction after removal of NaCl by extensive methanol extraction. The infrared spectrum of this complex is shown in Figure 1. The characteristic W-S stretching band for W_6S_8 cluster units[12,13] was observed at 378 cm^{-1}. Coordinated piperidine exhibits several distinctive bands in the mid-IR region. The XP spectrum of the material recovered from the filtrate indicated that a small amount of unknown compound, whose $W4f_{7/2}$ BE was 32.6 eV, was present. This impurity could also be evidenced by a weak band around 460 cm^{-1} in the infrared spectrum. The identity of this impurity will be discussed later.(see below)

Sulfidation Reactions in Butylamine

Primary amines, such as propylamine and butylamine, are believed to be more labile and weakly coordinated ligands than the secondary amines like piperidine. Therefore, the sulfidation reactions of tungsten chloride, W_6Cl_{12}, were also attempted in propylamine and butylamine. Since the boiling point of propylamine is only 48°C, it required a much longer reaction time to accomplish complete sulfide substitution for chloride. Butylamine, with a higher boiling point of 78°C, seemed to

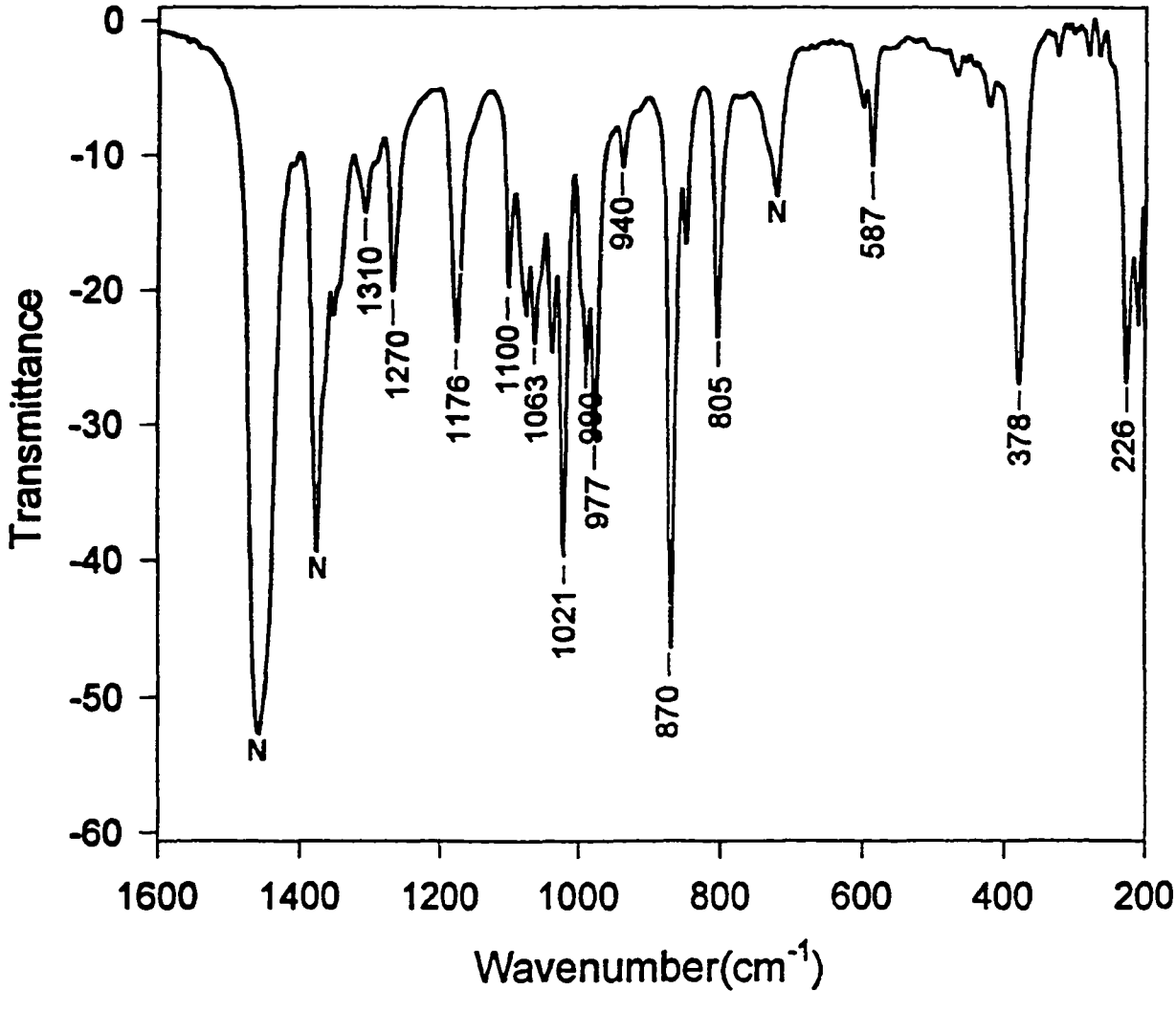

Figure 1. Infrared spectrum of $W_6S_8(pip)_6$ in the range 200-1600 cm^{-1}. The bands labeled as "N" are due to Nujol.

be a good solvent to carry out the sulfidation reaction. The reaction mixture with a stoichiometry of 1:10:5 (W_6Cl_{12}:NaSH:NaOEt) was refluxed in butylamine for three days. A dark brown filtrate and white solid were obtained upon filtration. Most of the tungsten products were thus soluble in butylamine.

The infrared spectrum for the amine materials recovered from the reaction filtrate is shown in Figure 2. In the far-IR region, besides the characteristic band for the W_6S_8 cluster at 376 cm^{-1}, there is another medium strong band at 462 cm^{-1}. This usually weak band was also visible in the far-IR spectra of the soluble products from reactions for other tungsten sulfide cluster derivatives. Furthermore, as illustrated in Figure 3, this soluble product is actually a mixture, as evidenced by two types of tungsten in the XP spectrum. Type I was identified as that in the $W_6S_8L_6$ cluster unit, with BE (W $4f_{7/2}$) = 30.8 eV. The other, type II, with BE (W $4f_{7/2}$) = 32.6 eV, has not been identified, but corresponds to tungsten sulfides with the tungsten oxidation state close to four. It was once thought to arise from an impurity of WS_2 produced by cluster decomposition. However, WS_2 is not soluble in these organic solvents, plus crystalline WS_2 only shows a strong and sharp band at 356 cm^{-1} in the far-IR.

When this mixture was stirred in toluene overnight at room temperature, a dark brown solution and black solid were separated upon filtration. Based on evidence from the infrared and XP spectra, the cluster complex, $W_6S_8(BuNH_2)_6$, was the soluble component in toluene, while the insoluble portion was the compound with a higher tungsten oxidation state. Therefore, toluene served as an efficacious solvent to separate these two compounds. The insoluble product had a characteristic band

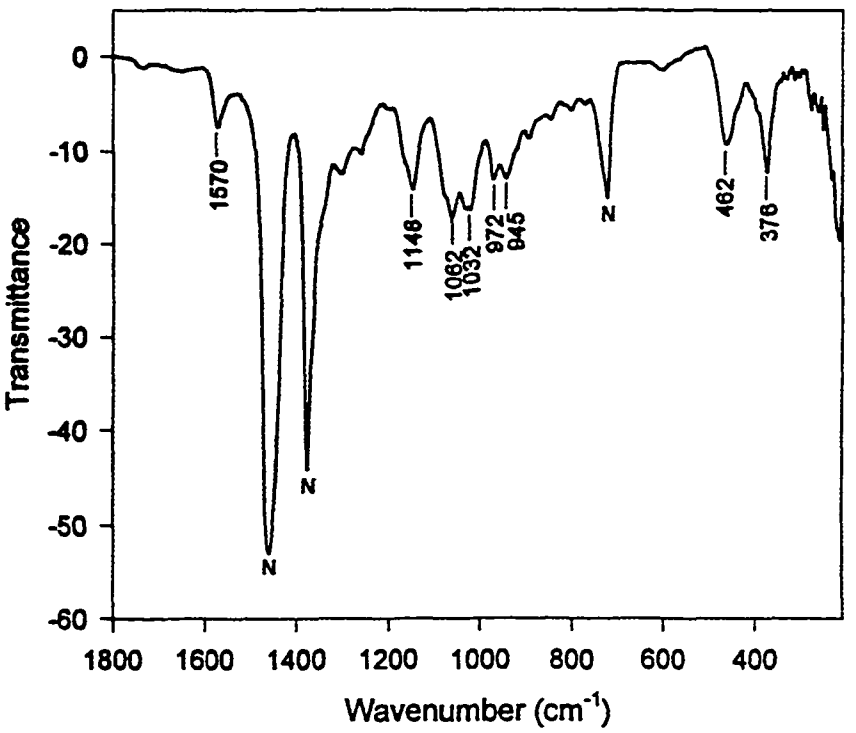

Figure 2. Infrared spectrum of the soluble amine products from the 1:10:5 reaction with W_6Cl_{12}, NaSH, and NaOEt. The bands labeled as "N" are due to Nujol

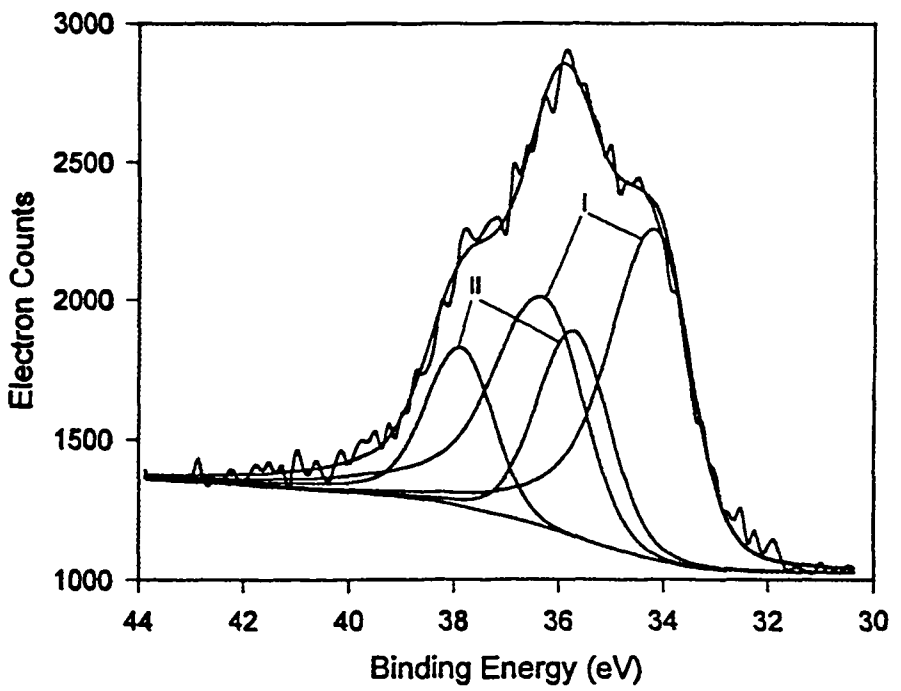

Figure 3. XP spectrum of the soluble product from butylamine, showing two types of tungsten, I and II.

in the IR spectrum around 460 cm^{-1} and the XP spectrum showed that it contained only one type of tungsten with BE ($W4f_{7/2}$) = 32.6 eV. The weight ratio of the soluble product to the insoluble product was about one. The butylamine complex, $W_6S_8(BuNH_2)_6$, is quite soluble in many organic solvents. However, all efforts at growing single crystals of $W_6S_8(BuNH_2)_6$ failed.

According to Müller,[19] compounds containing clusters like $[Mo_3S_{13}]^{2-}$ exhibit a characteristic infrared vibration at about 460 cm^{-1} which arises from the presence of a triply bridging (apical) S above the plane of the triangular Mo_3 cluster unit. Thus, it is possible that the band observed around 460 cm^{-1} for the unknown compound may be assigned as the vibrational mode of $\nu(W\text{-}\mu_3\text{-}S)$ in a new trinuclear complex. The pyridine, piperidine, and triethylphosphine derivatives of this unknown tungsten complex were also obtained by ligand exchange reactions. The resulting derivative complexes were quite soluble in common organic solvents. However, all efforts of growing single crystals of this unknown complex were unsuccessful.

Synthesis of $Na_{2x}(W_6S_8)S_x(MeOH)_y$

The most important result of this research involved the preparation of the first ternary salt of tungsten sulfide, $Na_{2x}(W_6S_8)S_x$, with W_6S_8 cluster units. The reaction appears to proceed as shown in equation 1. Acetonitrile was chosen as the solvent for

$$W_6Cl_{12} + (8+x)NaSH + (4+x)NaOEt \xrightarrow{MeCN} Na_{2x}(W_6S_8)S_x + 12NaCl + 2H_2 + (4+x)EtOH \qquad (1)$$

this reaction since it was a relatively poor coordinating ligand. When good coordinating ligands, such as pyridine and piperidine, were used as solvents, only the molecular $W_6S_8L_6$ cluster complexes were obtained.

The best results for the preparation of the analogous molybdenum compounds has been obtained with the use of butanol as a solvent.[20] However in the preparation of this tungsten compound, butanol was found to cause cluster decomposition, as evidenced by the presence of a broad band around 500 cm^{-1} in the IR spectra and a band indicative of WS_2 in the XP spectrum of the product. This decomposition was minimized when the reactions were conducted in acetonitrile, which has a lower boiling point (82°C). The lower refluxing temperature presumably prevented the decomposition of the cluster units. Fortunately, the sulfidation of W_6Cl_{12} is more facile than that of Mo_6Cl_{12}, which makes the lower temperature of refluxing acetonitrile advantageous.

The use of excess NaSH assures oxidation of the cluster units to the 20-electron neutral cluster core $(W_6S_8)^0$. Formation of these sodium salts results from coordination of sulfide ions in the terminal positions of the cluster units. Since the NaCl by-product is removed from the precipitated materials with methanol washing, some methanol is retained by coordination in the terminal positions or incorporated into the lattice. Unfortunately, washing with methanol also causes some cluster decomposition as evidenced by the presence of a small amount of material with a higher tungsten oxidation state in the W $4f_{7/2}$ XP spectrum. Atomic absorption analysis for sodium showed that there were about two sodium atoms per cluster unit. Compounds of the general formula $Na_2(W_6S_8)S{\cdot}y$MeOH are thus obtained, with y in the range of 4 to 5.

Furthermore, these materials are amorphous and generally quite reactive in air.

As illustrated in Figure 4, the IR spectrum for this sodium salt shows a strong band at 376 cm^{-1}, characteristic of the W-S stretching mode of T_{1u} symmetry for the W_6S_8 cluster units. The broad bands around 900-1000 cm^{-1} indicated the presence of methanol in this material.

Ion - Exchange Reactions

Earlier work on the preparation of molybdenum analogues suggested that ternary salts of tungsten sulfide could be obtained by ion-exchange reactions in methanol. However, methanol was found to cause decomposition of the W_6S_8 cluster unit. Therefore, an alternate solvent had to be used for these ion-exchange reactions. Because $SnCl_2$ is soluble in THF, THF was chosen as the solvent to prepare the ternary tin salt, $Sn_x(W_6S_8)S_x$. After washing the product with methanol, the absence of Na and the presence of Sn by XPS analysis indicated that complete ion-exchange was achieved.

Ion-exchange reactions with other metal salts, such as $Pb(NO_3)_2$, $NiCl_2$, and $CoCl_2$ were also attempted. However, these metal salts were not soluble in common organic solvents other than alcohol. Thus, methanol had to be used as the solvent for these ion-exchange reactions. After the mixture of $Na_{2x}W_6S_{8+x}$ and metal salts was stirred in methanol for one day, the XP spectrum of the product clearly indicated that cluster decomposition had occurred and a large amount of WS_2 was present in the sample.

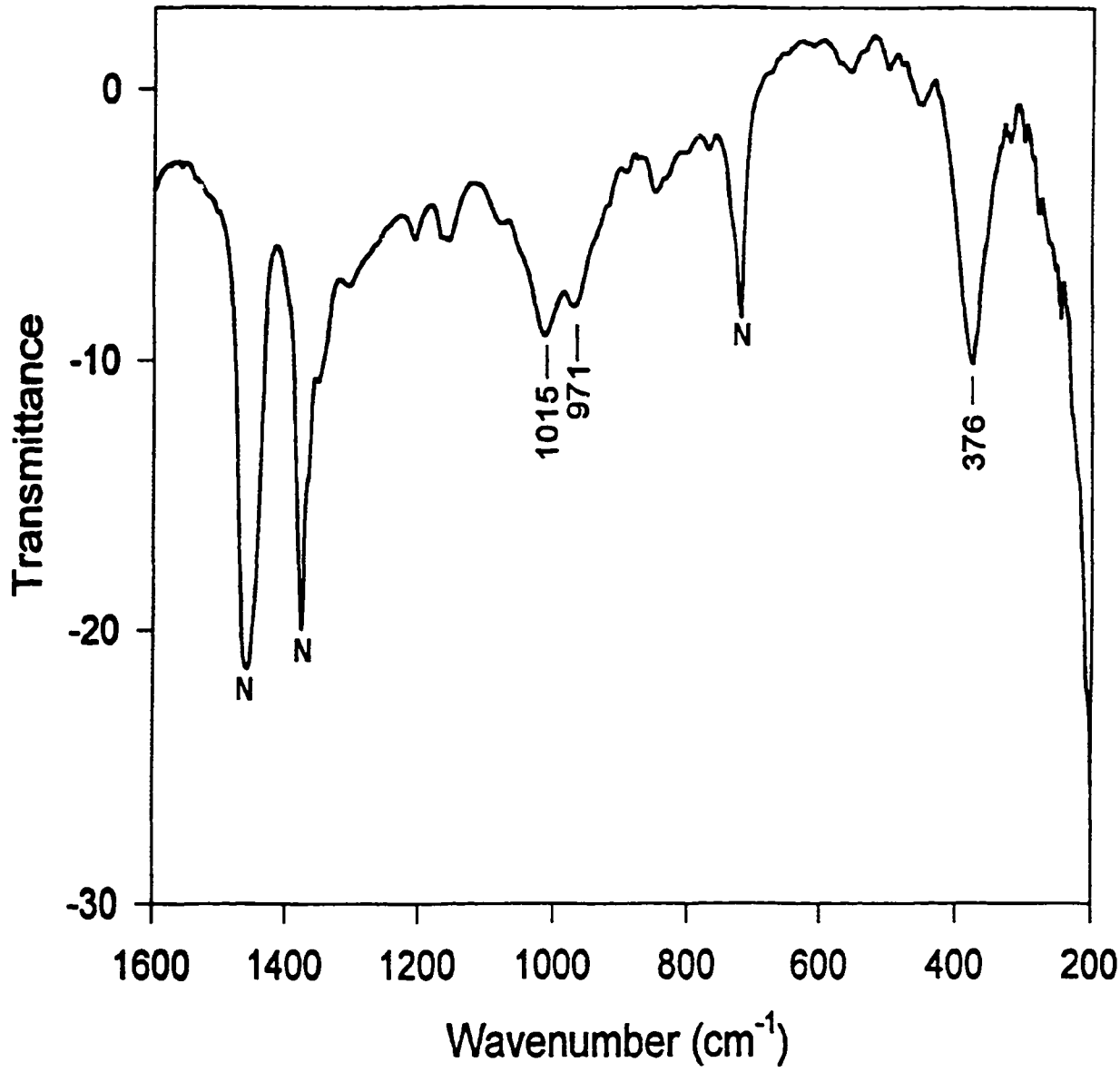

Figure 4. Infrared spectrum of $Na_{2x}(W_6S_8)S_x(MeOH)_y$ in the range 200-1600 cm^{-1}. The bands labeled as "N" are due to Nujol.

Ligand - Exchange Reactions

Earlier research into ligand-exchange reactions focused on the pyridine, triethylphosphine, and tetrahydrothiophene adducts.[13] It was established that the bonding between the hexatungsten cluster and the organic ligands decreased in the following order: PEt_3 > THT ≥ py. These experimental results and bond order calculations based on W-P, W-S and W-N distances seemed to indicated that the best materials for subsequent deligation should be the nitrogen-based ligands.

The piperidine ligands in $W_6S_8(pip)_6$ were readily displaced by pyridine to form the insoluble $W_6S_8(py)_6$ complex after $W_6S_8(pip)_6$ was refluxed in neat pyridine for several hours. Apparently the complete substitution of pyridine for piperidine was achieved, as illustrated in equation 2. Conversion of $W_6S_8(py)_6$ to the piperidine

$$W_6S_8(pip)_6 \xrightarrow{\text{pyridine}} W_6S_8(py)_6 + 6pip \qquad (2)$$

adduct, $W_6S_8(pip)_6$ was also examined. Upon refluxing in piperidine, $W_6S_8(py)_6$ was found to be unchanged, since the characteristic bands for the coordinated pyridine remained in the IR spectrum of the product. These results suggest that bonding between the hexatungsten cluster and pyridine is stronger than the bonding with piperidine.

The ligand displacement of butylamine by piperidine in $W_6S_8(BuNH_2)_6$ was also achieved, by refluxing the butylamine adduct and neat piperidine overnight.. An infrared spectrum of the product confirmed the complete displacement of butylamine by piperidine. The overall process is given in equation 3

$$W_6S_8(BuNH_2)_6 \xrightarrow{\text{piperidine}} W_6S_8(pip)_6 + 6BuNH_2 \qquad (3)$$

These experimental results indicated that butylamine was the most labile ligand and the bonding between the hexatungsten cluster and the organic ligands appeared to have the following order: PEt_3 > THT ≥ py >pip > $BuNH_2$. An identical conclusion was also reached in the studies of the ligand exchange reactions in the molybdenum sulfide analogues, $Mo_6S_8L_6$.[6]

Crystal Structures

The molecular complexes reported here contain the hexatungsten cluster unit $W_6S_8L_6$. This cluster unit can be viewed as an octahedron of tungsten atoms with eight triply-bridging sulfur atoms capping the octahedral faces. Each tungsten also possesses an additional terminal coordination site located at the vertex of the octahedron, which is occupied by the nitrogen donor ligands.

$W_6S_8(pip)_6 \cdot 7pip$ crystallizes in the tetragonal space group $I\bar{4}$ with 4 molecules per unit cell. The W_6S_8 cluster unit is centered on a 2-fold position (4e site symmetry). A diagram of the cluster is shown in Figure 5. The piperidine ligands, in the chair conformation, coordinate to the tungsten atoms such that the W-N bond occupies the equatorial position on the N atom. Selected bond distances and bond angles are listed in Table 4 and Table 5, respectively. From these tables, it can be seen that the deviations from strict octahedral symmetry are quite small. The average bond distances (Å) and maximum deviations are as follows: W-W, 2.662(2) ave., 0.015; W-S, 2.462(8) ave., 0.023; and W-N, 2.30(2) ave., 0.06. It is

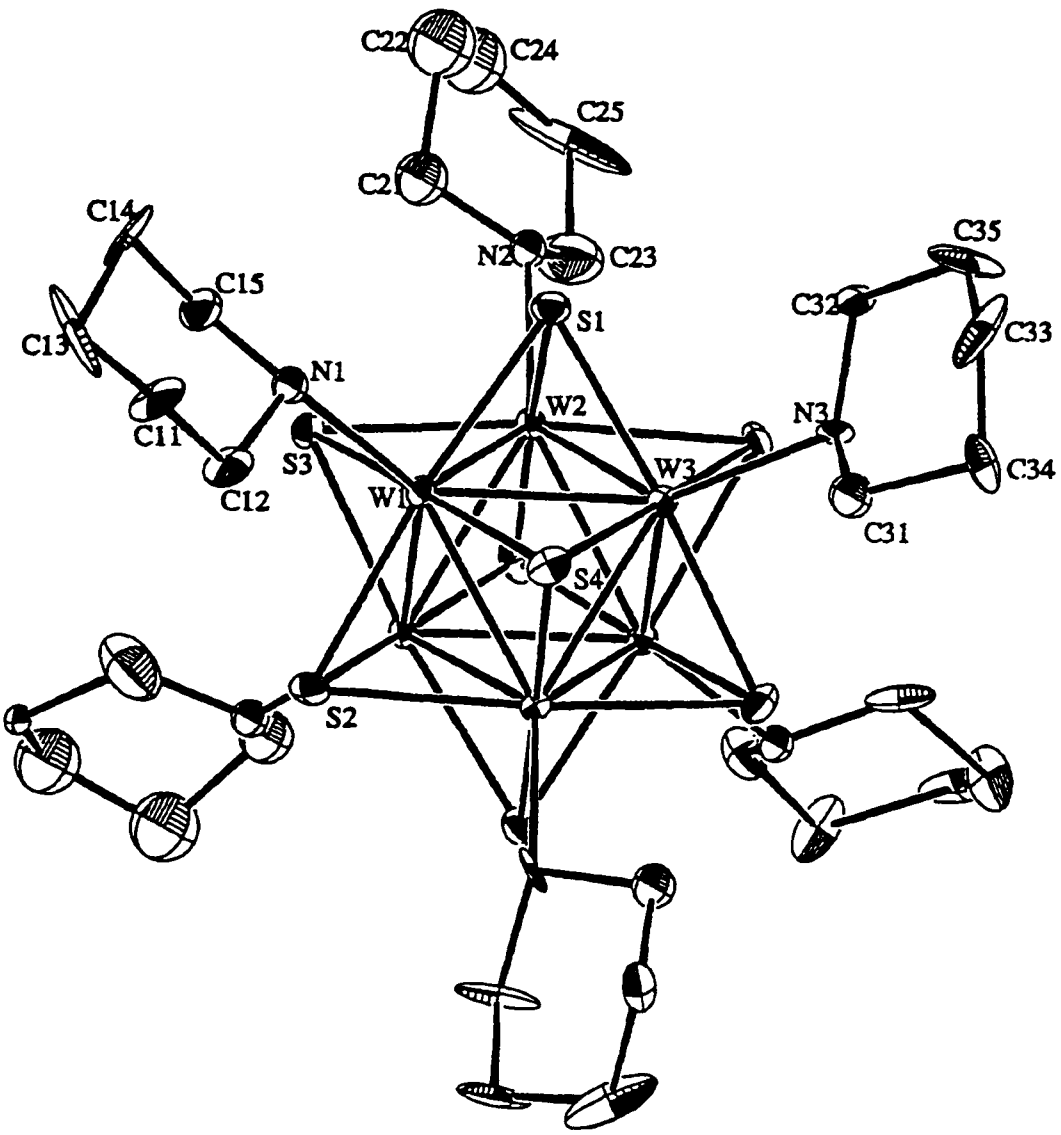

Figure 5. Molecular structure of $W_6S_8(pip)_6$. Thermal ellipsoids are shown at 35% probability level. Hydrogen atoms have been omitted for clarity.

Table 4. Selected Bond Distances (Å) in $W_6S_8(pip)_6 \cdot 7pip$

W(1) - W(2)	2.650(2)			W(1) - S(1)	2.466(6)
W(1) - W(2A)	2.663(2)			W(1) - S(2)	2.470(6)
W(1) - W(3)	2.670(2)			W(1) - S(3)	2.439(7)
W(1) - W(3A)	2.666(2)			W(1) - S(4)	2.449(8)
W(2) - W(2A)	2.669(2)			W(2) - S(1)	2.481(8)
W(2) - W(3)	2.670(2)			W(2) - S(2A)	2.478(8)
W(3) - W(3A)	2.647(2)			W(2) - S(3A)	2.441(8)
av. W-W	2.662(2)			W(2) - S(3)	2.457(8)
W(1) - N(1)	2.36(2)			W(3) - S(1)	2.455(8)
W(2) - N(2)	2.26(3)			W(3) - S(2A)	2.481(8)
W(3) - N(3)	2.29(2)			W(3) - S(4A)	2.461(9)
av. W-N	2.30(2)			W(3) - S(4)	2.467(8)
				av. W-S	2.462(8)

<u>coordinated piperidine</u>

N(1) - C(12)	1.45(4)	N(2) - C(21)	1.40(5)	N(3) - C(31)	1.55(4)
N(1) - C(15)	1.37(5)	N(2) - C(23)	1.41(5)	N(3) - C(32)	1.49(4)
C(11) - C(12)	1.53(4)	C(21) - C(22)	1.59(6)	C(31) - C(34)	1.62(4)
C(11) - C(13)	1.26(8)	C(22) - C(24)	1.46(7)	C(32) - C(35)	1.47(5)
C(13) - C(14)	1.67(6)	C(23) - C(25)	1.58(7)	C(33) - C(34)	1.47(6)
C(14) - C(15)	1.43(4)	C(24) - C(25)	1.40(8)	C(33) - C(35)	1.50(6)

<u>piperidine - solvent of crystallization</u>

N(4) - C(41)	1.39(6)	N(5) - C(51)	1.40(6)	N(6) - C(61)	1.43(5)
N(4) - C(45)	1.48(4)	N(5) - C(55)	1.50(6)	N(6) - C(65)	1.50(5)
C(41) - C(42)	1.59(6)	C(51) - C(52)	1.31(8)	C(61) - C(62)	1.46(6)
C(42) - C(43)	1.33(6)	C(52) - C(53)	1.52(7)	C(62) - C(63)	1.45(6)
C(43) - C(44)	1.46(6)	C(53) - C(54)	1.29(6)	C(63) - C(64)	1.57(6)
C(44) - C(45)	1.52(6)	C(54) - C(55)	1.47(7)	C(64) - C(65)	1.41(7)

Table 5. Selected Bond angles (deg) in $W_6S_8(pip)_6 \cdot 7pip$

W(2) - W(1) - W(2A)	60.30(5)	S(1) - W(1) - S(3)	91.7(3)
W(2) - W(1) - W(3)	60.24(5)	S(1) - W(1) - S(4)	88.7(3)
W(2A) - W(1) - W(3A)	60.12(5)	S(2) - W(1) - S(3)	89.4(3)
W(3) - W(1) - W(3A)	59.46(4)	S(2) - W(1) - S(3)	89.5(3)
W(1) - W(2) - W(2A)	60.10(5)	S(1) - W(2) - S(2A)	89.5(3)
W(1) - W(2) - W(3)	60.26(5)	S(1) - W(2) - S(3)	90.9(3)
W(1A) - W(2) - W(2A)	59.60(4)	S(2A) - W(2) - S(3A)	89.2(3)
W(1A) - W(2) - W(3)	60.00(5)	S(3A) - W(2) - S(3)	89.5(3)
W(1) - W(3) - W(2)	59.50(5)	S(1) - W(3) - S(2A)	90.1(3)
W(1) - W(3) - W(3A)	60.20(4)	S(1) - W(3) - S(4)	88.5(3)
W(1A) - W(3) - W(2)	59.88(5)	S(2A) - W(3) - S(4A)	89.0(3)
W(1A) - W(3) - W(3A)	60.34(4)	S(4A) - W(3) - S(4)	91.6(3)
avg W - W - W	60.00(5)	avg S - W - S	89.8(3)
W(2) - W(1) - W(3A)	89.87(5)	S(1) - W(1) - S(2)	173.5(2)
W(2A) - W(1) - W(3)	90.24(5)	S(3) - W(1) - S(4)	173.6(3)
W(1) - W(2) - W(1A)	90.20(5)	S(1) - W(2) - S(3A)	172.8(3)
W(2A) - W(2) - W(3)	89.76(5)	S(2A) - W(2) - S(3)	172.7(3)
W(2) - W(3) - W(3A)	90.24(5)	S(1) - W(3) - S(4A)	173.6(3)
W(1) - W(3) - W(1A)	89.69(5)	S(4) - W(3) - S(2A)	172.9(3)
avg W - W - W	90.00(5)	avg S - W - S	173.2(3)
W(1) - S(1) - W(2)	64.8(2)	S(1) - W(1) - N(1)	88.8(5)
W(1) - S(1) - W(3)	65.7(2)	S(2) - W(1) - N(1)	97.5(5)
W(2) - S(1) - W(3)	65.5(2)	S(3) - W(1) - N(1)	93.4(8)
W(1) - S(2) - W(2A)	65.1(2)	S(4) - W(1) - N(1)	93.0(8)
W(1) - S(2) - W(3A)	65.2(2)	S(1) - W(2) - N(2)	91.4(7)
W(3A) - S(2) - W(2A)	65.1(2)	S(2A) - W(2) - N(2)	93.7(7)
W(1) - S(3) - W(2A)	66.2(2)	S(3) - W(2) - N(2)	93.6(7)
W(1) - S(3) - W(2)	65.5(2)	S(3A) - W(2) - N(2)	95.8(7)
W(2) - S(3) - W(2A)	66.0(2)	S(1) - W(3) - N(3)	96.8(6)
W(1) - S(4) - W(3A)	65.8(2)	S(2A) - W(3) - N(3)	91.5(6)
W(1) - S(4) - W(3)	65.8(2)	S(4A) - W(3) - N(3)	89.6(6)
W(3) - S(4) - W(3A)	65.0(2)	S(4) - W(3) - N(3)	95.6(6)
avg W - S - W	65.5(2)	avg S - W - N	93.4(7)

worthwhile to point out that $W_6S_8(pip)_6 \cdot 7pip$ is isomorphous with $Mo_6S_8(pip)_6 \cdot 7pip$. As expected, the W-W and W-S distances are slightly longer than the Mo-Mo and Mo-S distances in the molybdenum analogue and very close to those in the previously found hexatungsten cluster complexes,[13] $W_6S_8(py)_6$, $W_6S_8(PEt_3)_6$, and $W_6S_8(THT)_6$.

A cell packing diagram of $W_6S_8(pip)_6$ without solvent molecules is shown in Figure 6. The molecules of the cluster complexes are well separated from each other in the lattice. The spaces between clusters are occupied by solvent molecules.

Conclusion

This paper describes the preparation, and characterization of the first ternary salt of the W_6S_8 cluster unit, $Na_{2x}(W_6S_8)S_x(MeOH)_y$, and the molecular complexes, $W_6S_8(pip)_6$ and $W_6S_8(BuNH_2)_6$.

As previous research showed, one mole of W_6Cl_{12}, twelve moles of NaSH, and six moles of NaOEt refluxing in an organic solvent with the presence of good coordinating ligands is an efficient one-step synthetic recipe for preparing the molecular complexes, $W_6S_8L_6$. New molecular complexes, $W_6S_8(pip)_6$, and $W_6S_8(BuNH_2)_6$, were obtained by refluxing the starting materials in piperidine and butylamine, respectively. Compared to previous $W_6S_8L_6$ complexes, these two new

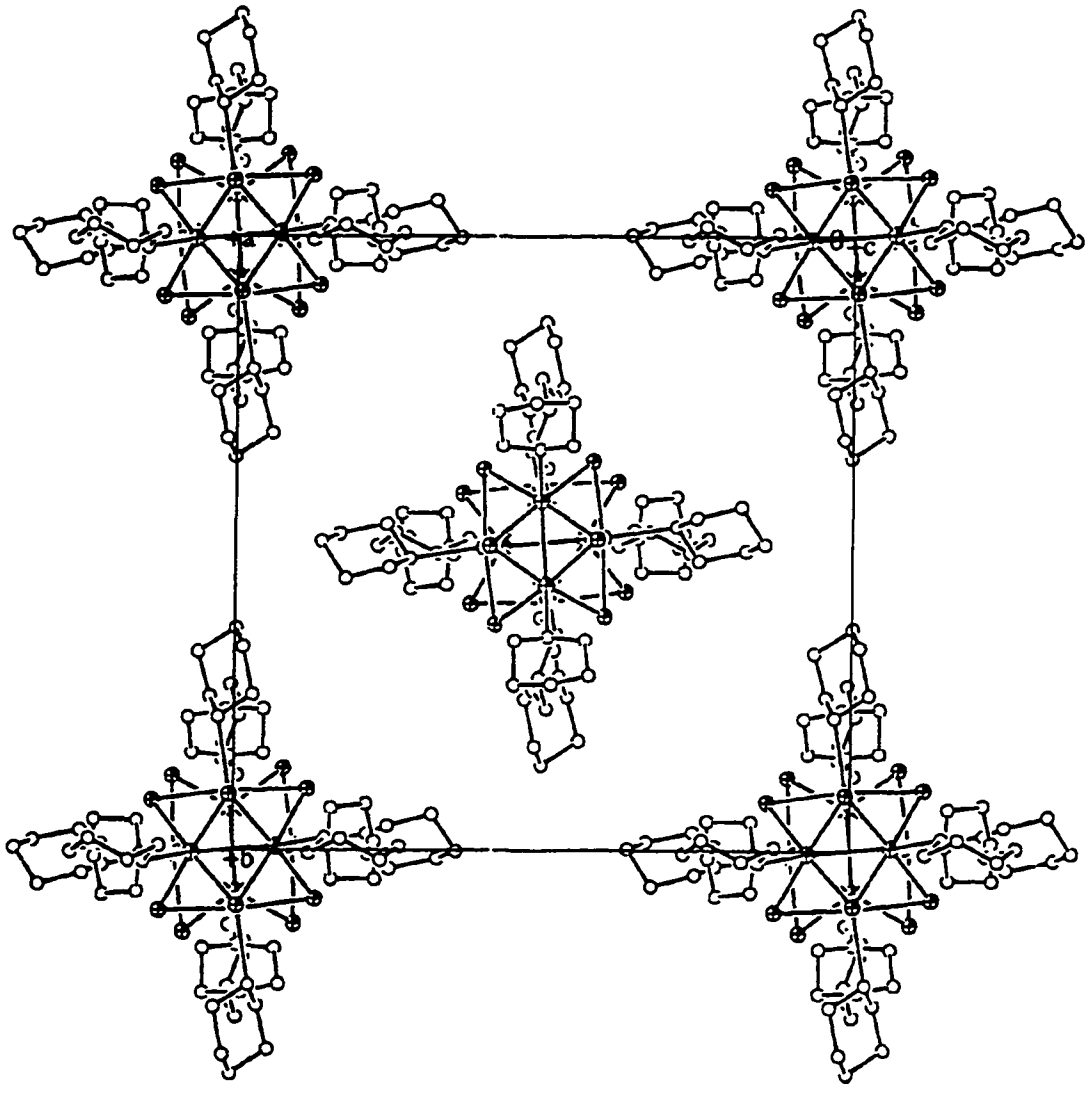

Figure 6. The unit cell of compound $W_6S_8(pip)_6 \cdot 7(pip)$ as viewed along the c axis. Solvent molecules have been omitted for clarity. Thermal ellipsoids are shown at 20% probability level.

cluster complexes display two advantages. First of all, the terminal ligands on these two complexes, especially butylamine, are bonded to the cluster core more loosely than those previously reported. Therefore, these two new complexes are expected to be good candidates for subsequent deligation reactions. Secondly, these new complexes are more soluble in common organic solvents than the other nitrogen-based ligand complex, $W_6S_8(py)_6$.

When poor coordinating ligands, such as acetonitrile, were used as the solvent for the sulfidation reaction, the sodium ternary compound, $Na_{2x}(W_6S_8)S_x(MeOH)_y$, was obtained. Formation of these sodium salts resulted from coordination of sulfide ions in the terminal positions of the cluster units. Some methanol from methanol extraction is retained by coordination in the terminal positions or incorporated into the lattice. Unfortunately, washing with methanol also causes some cluster decomposition. Therefore, WS_2 is often found as an impurity in the reaction product.

The most useful spectroscopic data are provided by the W 4f photoelectron spectra. The derived binding energies of 30.8 ($4f_{7/2}$) and 33.0 eV ($4f_{5/2}$) are characteristics of the W_6S_8 unit and compare with the $4f_{7/2}$ BEs of 32.7 eV for WS_2, and 35.4 eV for WO_3. Therefore, this 2 eV difference between the cluster unit and WS_2 makes WS_2 easily detectable when it occurs as an impurity.

The crystal structure of $W_6S_8(pip)_6 \cdot 7pip$ is isomorphous with its molybdenum analogue. The structures of the products recovered from the sulfidation reaction in butylamine were not determined because crystals could not be obtained for X-ray structure work. However, other data suggest that $W_6S_8(BuNH_2)_6$ and a trinuclear

cluster of tungsten (IV) are the principal products of the latter reaction.

References

(1) Chevrel, R.; Sergent, M. *Topics in Current Physics*, Fischer, Ø. and Maple, M. B., Eds.; **1982**, Vol. 32, Chapter 2 Springer-Verlag: Heidelberg.

(2) Peña, O.; Sergent, M. *Prog. Solid St. Chem.* **1989**, *19*, 165.

(3) Mulhern, P. J.; Haering, R. R. *Can. J. Phys.* **1984**, *62*, 527.

(4) (a) McCarty, K. F.; Schrader, G. L. *Ind. Eng. Chem. Prod. Res. Dev.* **1984**, *23*, 519. (b) McCarty, K. F.; Anderegg, J. W.; Schrader, G. L. *J. Catal.* **1985**, *93*, 375.

(5) The Mo_6Y_8 cluster unit is composed of six Mo atoms bonded to form an octahedron. The *bridging* ligands Y which cap the face of the octahedron are each bonded to three Mo atoms. Each Mo atom can form one additional bond directed radially outward from the cluster to a *terminal* ligand.

(6) The terminology used here is given by A. Simon, *Chem. Unserer Zeit* **1976**, *10*, 1.

(7) K. Yvon, *in* "Current Topics in Materials Science" (E. Kaldis, Ed.), **1979**, Vol. 3, p.53. Elsevier, Amsterdam.

(8) Here the MCE consists of only the electrons remaining in the 4d orbitals of Mo and used for Mo-Mo bonding after the valence levels of the S atoms are filled.

(9) (a) Chevrel, R.; Sergent, M.; Prigent, J. *Mater. Res. Bull.* **1974**, *9*, 1487. (b) Schöllhorn, R.; Kümpers, Plorin, D. *Less-Common Met.* **1978**, *58*, 55.

(10) (a) Opalovski, A. A.; Fedorov, V. E. *Izv. Akad. Nauk. SSSR Neorg. Mater.* **1966**,2, 443. (b) Spiesser, M.; Rouxel, J. *C. R. Acad. Seances Ser. Sci.* **1967**, *C 265,* 92.

(11) Hilsenbeck, S. J.; Young Jr., V. G.; McCarley, R. E. *Inorg. Chem.* **1994**, *33*, 1822.

(12) Zhang, X.; McCarley, R. E. *Inorg. Chem.* **1995**, *34*, 2678.

(13) Zhang, X. Ph.D. Dissertation, Iowa State University, Ames, IA, 1991.

(14) Ehrlich, G. M.; Rauch, P. E.; DiSalvo, F. J. *Inorg. Synth.* **1995**, *30*, 1.

(15) Brauer, G. *in* "Handbuch der Preparativen Anorganischen Chemie" **1975**, P. 371, Enke Verlag, Stuttgart.

(16) Scheldrick, G. M. *Crystallographic Computing 3*; Oxford University Press: Oxford, U.K., 1985.

(17) *TEXSAN: Single Crystal Structure Analysis Software*, Version 1.6c; Molecular Structure Corp.: The Woodlands, TX 77381, 1985 & 1992.

(18) *DIFABS*: Walker, N. & Stuart, *Acta Cryst.* **1983**, *A39*, 158.

(19) Müller, A. *in* "Analytical Applications of FT-IR to Molecular and Biological System" (Durig, J. R., Ed.) **1980**, P. 257. D. Reidel Dordrecht.

(20) McCarley, R. E.; Hilsenbeck, S. J.; Xie, X. *J. Solid. State Chem.* **1995**, *117*, 269.

CHAPTER 2. SYNTHESIS, STRUCTURE, AND CHARACTERIZATION OF N-LIGANDED TUNGSTEN SELENIDE CLUSTER COMPLEXES $W_6Se_8L_6$

A paper published in a revised form in Inorganic Chemistry

Xiaobing Xie and Robert E. McCarley

Abstract

Two new W_6Se_8 cluster units were synthesized via the reaction of W_6Cl_{12} with Na_2Se in the refluxing amine solvents pyridine (py) and piperidine (pip). Crystals for both complexes were grown from the reaction filtrates. Crystallographic data for theses complexes are as follows: $W_6Se_8(pip)_6 \cdot 8pip$, cubic, $I\bar{4}3d$, a = 31.150(4) Å, Z = 12; $W_6Se_8(py)_6 \cdot 6py$, trigonal, $R\bar{3}$, a = 19.654(2) Å, c = 11.100(5) Å, Z = 3. W - W and W - Se bond distances show little variation among the complexes with average values of 2.691 (1) and 2.574(1) Å, respectively. Photoelectron spectra give characteristic tungsten binding energies at 30.8 eV (W $4f_{7/2}$) and 33.0 eV (W $4f_{5/2}$). IR spectra show a strong band at 243 cm^{-1}, attributable to the T_{1u} W - Se stretching modes.

Introduction

The synthesis of tungsten chalcogenide cluster complexes, $W_6Y_8L_6$(Y = S, Se, Te; L = donor ligand) and their possible conversion into the ternary compounds $M_xW_6Y_8$, has become a major scientific goal. This attention is derived from the relation of these compounds to the well-known Chevrel phases, $M_xMo_6Y_8$, which exhibit a range of interesting physical and chemical properties,[1-4] The essential structural elements in these Chevrel phase compounds are the Mo_6Y_8 units with octahedral Mo_6 clusters which have a variable electron population of 20 to 24 electrons in the Mo-Mo bonding orbitals. The production of the Chevrel phases has generally involved solid-state reactions at higher temperatures (1000 - 1300°C).

In contrast to the abundance of these molybdenum compounds, no example of the tungsten analogues, W_6Y_8 or $M_xW_6Y_8$, has been reported. It is generally understood that these compounds cannot be obtained at high temperatures because they are unstable with respect to disproportionation (into W and WY_2 or W, WY_2, and $MY_{n/2}$, where n is the valence of M). Thus, these phases may be isolated only at lower temperatures where they are either thermodynamically stable or metastable and kinetically trapped.

We have initiated research towards preparation of these tungsten analogues at low temperatures through molecular precursors. W_6Cl_{12}, which contains the $(W_6Cl_8)^{4+}$ cluster unit, was successfully converted by sulfide substitution to the cluster complex without decomposition.[5-7] The preparation and structural characterization of $W_6S_8L_6$ molecular complexes, where L is an organic donor ligand

such as pyridine,[5,6] piperidine,[7] triethylphosphine,[8] or tetrahydrothiophene[8] were accomplished in this laboratory. Likewise, the molybdenum sulfide cluster complexes, $Mo_6S_8L_6$, were also developed.[9] Concurrently, a low-yield synthesis of $W_6S_8(PEt_3)_6$ via "reductive dimerization" of a complex formed between $W_3S_7Cl_4$ and triethylphosphine was reported by Saito *et al.*[10]

However, no example of either the tungsten selenide or telluride molecular complexes such as $W_6Se_8L_6$ or $W_6Te_8L_6$ has been reported. The present paper describes the syntheses, characterization, and structures of the first two new molecular complexes of the tungsten selenide clusters, $W_6Se_8(pip)_6$, $W_6Se_8(py)_6$.

Experimental

Materials

The reagents and products are air and moisture sensitive. Therefore, all manipulations were performed by the use of an inert-atmosphere drybox, a high-vacuum manifold, and Schlenk techniques, unless otherwise stated. W_6Cl_{12} was prepared by literature methods.[5,6] Na_2Se was prepared by the reaction of sodium metal and selenium in refluxing tetrahydrofuran with catalytic amounts of naphthalene.[11]

All solvents were purified and dried prior to use. Also, the solvents were de-oxygenated by use of the freeze-thaw process: freeze to liquid nitrogen temperature, evacuate the gaseous material, and then thaw. This process was repeated three times prior to the distillation of the purified solvent onto Linde 3- or 4-Å Molecular Sieves and stored under vacuum or a nitrogen atmosphere. Pyridine (Fisher), piperidine (Fisher), acetonitrile (Fisher) and triethylphosphine (Strem) were purified by refluxing over calcium hydride for at least 4 hours. Toluene (Fisher) and chloroform were refluxed over phosphorus pentoxide. Without heating, tetrahydrofuran (Fisher) was dried by stirring with sodium metal and a benzophenone indicator. Methanol (Mallinckrodt) was dried by refluxing over sodium methoxide. When used, the solvents were vacuum-distilled or syringed under a flowing nitrogen gas atmosphere.

Physical Measurements

Infrared spectroscopy

The samples were prepared in the drybox and were temporarily stored under nitrogen before being placed in the sample chamber of the instrument. Mid-infrared (4000-200 cm^{-1}) spectra were recorded with a Bomem MB-102 Fourier transform infrared spectrometer manufactured by Hartman and Braun. Samples were prepared as Nujol mulls and pressed between two cesium iodide plates. The

sample chamber of the instrument was continuously purged with dry, compressed air and the reference spectra were collected in the empty chamber. Far-infrared (650-100 cm^{-1}) spectra were recorded separately with an IBM IR/98 Fourier transform infrared spectrometer. Thick sample mulls were placed on a polyethylene film in the drybox, and the film was mounted on a sample holder. Then the sample was transferred to the sample chamber. Data were collected for these samples while the sample chamber was under vacuum, and Nujol on the polyethylene film was used as a reference.

Nuclear magnetic resonance spectroscopy

^1H NMR spectra were collected on a Unity 300-MHz spectrometer. The samples were handled in an inert atmosphere glove-box and dissolved in deuterated chloroform just prior to the NMR study.

X-ray photoelectron spectroscopy

XP spectra were collected by James Anderegg at room temperature with a Physical Electronics Industries 5500 multitechnique surface analysis system. This system was equipped with a hemispherical analyzer, a toroidal monochromator, and multichannel detector which sampled a 2 mm^2 area. The samples were pressed on an indium substrate and loaded into an air-sensitive sample holder in the dry-box. Then the sample holder was transferred into the chamber of the spectrometer. After the system was completely evacuated, the sample holder was opened and the

sample was excited with monochromatic Mg $K\alpha$ radiation (1253.6 eV) at the power of 300 W. The photoelectron binding energies were calibrated with C 1s = 284.6 eV.

X-ray powder diffraction

Powder X-ray diffraction (XRD) data were obtained with a Philips ADP3520 θ-2θ diffractometer using Cu $K\alpha$ radiation. The air-sensitive samples were loaded into a specially designed sample holder and sealed under N_2 while in the drybox.

Analytical Procedures

Tungsten was determined gravimetrically as the trioxide. If ternary metal cations were not present, the samples were placed in tared crucibles and decomposed initially with dilute (3M) nitric acid. Concentrated nitric acid was then added to ensure complete oxidation and the samples evaporated to dryness. After ignition in a muffle furnace at 800°C, the resulting WO_3 solid was weighed. If ternary metal cations were present, the sample was dissolved in 0.5 M KOH with the aid of hydrogen peroxide. The solutions were then treated with equal volumes of concentrated nitric acid and hydrogen peroxide to form a peroxy-acid complex. The hydrated oxide, $WO_3 \cdot nH_2O$, was then completely precipitated by slowly decomposing this complex at 100°C and collected in tared ceramic filter crucibles. Then the materials were dried to constant weight at 800°C.

Chlorine was determined by potentiometric titration with a standardized silver nitrate solution after dissolving the sample in KOH-H_2O_2 solution and neutralization. A silver/silver chloride electrode was used as the reference, and a silver wire as the working electrode. The endpoint was determined by using the second derivative method. Additional microanalyses for carbon, hydrogen, and nitrogen were obtained from Oneida Research Services.[12]

Synthetic Procedures

Preparation of $W_6Se_8(pip)_6$

W_6Cl_{12} (0.250 g, 0.164 mmol), and Na_2Se (0.164 g, 1.31 mmol) were weighed in the drybox and transferred into a 100-mL Schlenk reaction flask equipped with a water-cooled condenser. By distillation, 40 mL of piperidine were added to the reactants and the mixture was refluxed for 3-4 days. A tan solid and purple-red solution were separated by filtration. The solvent was then removed from the filtrate under dynamic vacuum, and after drying overnight *in vacuo,* 0.30 g of a dark red powder (74% yield) was obtained. IR (Nujol, cm^{-1}): 1350 (w), 1304 (m), 1261 (m), 1185 (w), 1171 (w), 1082 (w), 1054 (m), 1041 (w), 1019 (s), 976 (s), 935 (w), 868 (s), 805 (ms), ν(W-Se) 243 (s), 202 (ms), 150 (w). Anal. Calcd for $W_6Se_8(pip)_6$,: C,16.04; H, 2.94; N, 3.74. Found: C, 16.70; H, 3.24; N, 3.35. A test for chloride was negative.

The tan insoluble product obtained by filtration of the reaction mixture was washed with methanol for 2-3 days to remove NaCl, and about 0.18 g of black solid was recovered.

Preparation of $W_6Se_8(py)_6$

W_6Cl_{12} (0.250 g, 0.164 mmol), and Na_2Se (0.164 g, 1.31 mmol) were weighed in the drybox and transferred into a 100-mL Schlenk reaction flask equipped with a water-cooled condenser. By distillation, 40 mL of pyridine were added to the reactants and the mixture was refluxed for 3-4 days. A brown solid and reddish brown solution were separated by filtration. The filtrate was evaporated and dried overnight under dynamic vacuum to remove the solvent. About 0.21 g of dark brown powder (56% yield) was thus recovered. IR (Nujol, cm^{-1}): 1594 (w), 1348 (w), 1306 (w), 1211 (s), 1168 (w), 1146 (m), 1065 (ms), 1038 (ms), 969 (w), 935 (w), 750 (s), 687 (s), ν(W-Se) 245 (ms), 202 (w). Anal. Calcd for $W_6Se_8(py)_6$: C, 16.3; H, 1.36; N, 3.80. Found: C, 15.0; H, 1.42, N, 3.03. A test for chloride was negative. The insoluble product obtained by filtration of the reaction mixture was washed with methanol for 2-3 days to remove the NaCl by-product, and about 0.2 g of brown powder was recovered. XPS data were collected for this brown powder in order to obtain evidence for the formation of W metal by disproportionation (see below).

Reaction of $W_6Se_8(pip)_6$ with pyridine

About 0.05 grams of $W_6Se_8(pip)_6$ were placed onto the frit of an extractor and about 20 mL of pyridine (py) were distilled into the receiving flask. After approximately 4-6 hours of extraction, the solid completely dissolved and provided a dark red solution. Single crystals were grown by allowing this solution to stand at-20°C for a week.

A larger scale reaction, under the same conditions as described previously, resulted in the formation of the dark red solution. After drying under dynamic vacuum, the infrared spectrum of the recovered brown material indicated only pyridine coordination.

Reaction of $W_6Se_8(py)_6$ with piperidine

About 0.068 grams of $W_6Se_8(py)_6$ were loaded into a 100 mL round-bottom flask, and about 15 mL of piperidine (pip) were distilled into the flask. Then, the mixture was stirred at room temperature for 12 hours. Only about 40% of the starting material was soluble and formed a red solution. After drying the solution under dynamic vacuum, an infrared spectrum was obtained for the product.

X-ray Structure Determinations

In each case, a crystal was chosen from material still in contact with the mother solution. The crystal was encased in epoxy cement, attached to the tip of a glass

fiber, and immediately inserted into the low-temperature nitrogen stream of the diffractometer for data collection. The cell constants were determined from 25 randomly located and centered reflections. The structures were solved by direct methods using SHELXS[13] and refined on F by full-matrix, least-squares techniques with the TEXSAN package.[14] Pertinent crystallographic data are listed in Table 1.

Structure determination for $W_6Se_8(pip)_6 \cdot 8pip$

Single crystals of $W_6Se_8(pip)_6 \cdot 8pip$ were grown from a portion of the reaction filtrate by allowing it to stand at room temperature for several days. A dark red tetrahedral crystal, with dimensions of 0.5 x 0.5 x 0.5 mm^3, was mounted on a glass fiber, and data collection proceeded at -50°C. Data were collected with an Enraf-Nonius CAD4 diffractometer using Mo Kα radiation, over the range $4° < 2\theta < 50°$ for one octant (*-h,-k,-l*), using the ω-2θ scan technique. Three standard reflections were monitored every 250 reflections and showed no intensity variation over the collection period. A total of 14212 reflections were collected, of which 2555 were unique (R_{int} = 0.150) and 1248 were observed with $I > 3\sigma(I)$. The linear absorption coefficient, μ, for Mo $K\alpha$ radiation is 97.6 cm^{-1}. First, an empirical absorption correction using the φ scan technique was applied after the structure solution. After all of the atoms were located and refined isotropically, an absorption correction using the DIFABS program[15] was applied and resulted in the relative transmission factors ranging from 0.75 to 1.16. The data were corrected for Lorentz and polarization effects.

Table 1. Crystallographic Data for the $W_6Se_8L_6$ Cluster Complexes

compound	$W_6Se_8(pip)_6 \cdot 8pip$	$W_6Se_8(py)_6 \cdot 6py$
chemical formula	$C_{70}H_{154}N_{14}Se_8W_6$	$C_{60}H_{60}N_{12}Se_8W_6$
formula weight	2926.86	2683.99
space group	$I\bar{4}3d$ (No. 220)	$R\bar{3}$ (No. 148)
a, Å	31.150(4)	19.654(2)
c, Å		15.100(5)
V, Å^3	30225.(11)	5051.(2)
Z	12	3
ρ_{calcd}, g/cm^3	1.929	2.647
μ, cm^{-1}	97.62	145.90
radiation (Mo $K\alpha$)	0.71069Å	0.71069Å
T, °C	-50	-65
2θ range, deg	4-50	4-55
total data	14212	4159
unique data	2555	2601
data observed	1248 [$I>3\sigma(I)$]	1764 [$I>4\sigma(I)$]
no. parameter	146	130
data/parameter	8.5	13.6
abs. correction	DIFABS	DIFABS
trans. factors	0.75-1.16	0.93-1.06
R^a	0.0415	0.0295
$R_w{}^b$	0.0397	0.0254
diff. peaks, e/Å^3	1.32, -0.65	1.45, -1.12

[a] $R = \Sigma||F_o|-|F_c||/\Sigma|F_o|$.

[b] $R_w = [\Sigma w(|F_o|-|F_c|)^2/\Sigma w|F_o|^2]^{1/2}$; $w = 1/\sigma^2(|F_o|)$.

The cubic space group $I\bar{4}3d$ was chosen on the basis of systematic absences and intensity statistics. Initial tungsten atom positions were input on the basis of the SHELXS direct methods output. Subsequently, the other non-hydrogen atomic positions were located directly from the electron density difference maps. These atoms were refined with anisotropic thermal parameters, except for two free piperidine solvent molecules. Idealized hydrogen positions were calculated and placed in the refinement, but their parameters were held constant during subsequent cycles. The asymmetric unit was found to be $W_2Se_2(pip)_2 \cdot 2pip$, where one coordinated piperidine molecule was located on a 2-fold axis (24d site symmetry) and displayed planar conformation. The other piperidine molecules were found in the chair conformation. Refinement of one solvent piperidine molecule (N4, C41 to C45) was poorly-behaved, therefore a rigid group was applied to improve the refinement. The atomic coordinates and equivalent isotropic thermal parameters of the non-hydrogen atoms are given in Table 2, and the anisotropic thermal parameters are shown in Table 3. The relatively large B_{eq} values for the heavier atoms (W and Se), and the planar conformation of the two piperidine ligands suggested that this crystal was probably a twin by merohedry.[16] Therefore, refinement of twinning was explored by using the SHELXL-93 program.[17] However, no improvement was obtained by applying this twin refinement. Thus, only the results without the twin refinement are reported here. The final cycle of full-matrix least-squares refinement was based on 1248 observed reflections and 146 variable parameters and converged with unweighted and weighted agreement factors of: R =

Table 2. Atomic Coordinates and Equivalent Isotropic Thermal Parameters ($Å^2$) of the Non-Hydrogen Atoms for $W_6Se_8(pip)_6 \cdot 8pip$

atom	x	y	z	B_{eq}[a]
W(1)	0.2500	0.31382(5)	0.0000	3.72(4)
W(2)	0.30858(3)	0.37601(4)	-0.01689(3)	3.84(3)
Se(1)	0.2887(1)	0.4331(1)	-0.0727(1)	4.73(8)
Se(2)	0.2910(1)	0.31652(9)	-0.07151(9)	4.62(8)
N(1)	0.2500	0.2411(3)	0.0000	4.7(8)
N(2)	0.3801(8)	0.380(1)	-0.031(1)	8.3(9)
N(3)	0.228(1)	0.026(2)	0.133(1)	15(1)
N(4)	0.921(2)	0.064(2)	0.330(1)	35
C(11)	0.238(1)	0.217(1)	-0.0361(9)	6.1(7)
C(12)	0.237(1)	0.1701(8)	-0.040(1)	9(1)
C(13)	0.2500	0.149(2)	0.0000	10(2)
C(21)	0.399(1)	0.349(2)	-0.051(2)	13(1)
C(22)	0.445(1)	0.347(1)	-0.069(2)	11(1)
C(23)	0.466(1)	0.388(2)	-0.074(2)	10(1)
C(24)	0.447(1)	0.421(2)	-0.053(2)	17(2)
C(25)	0.396(1)	0.421(1)	-0.044(1)	6(1)
C(31)	0.220(3)	0.072(3)	0.112(3)	22(2)
C(32)	0.175(3)	0.068(3)	0.101(3)	25(2)
C(33)	0.176(3)	0.029(3)	0.063(3)	23(2)
C(34)	0.183(5)	-0.007(5)	0.081(4)	37(5)
C(35)	0.229(2)	-0.006(2)	0.089(2)	16(1)
C(41)	0.926(1)	0.085(2)	0.375(2)	23
C(42)	0.915(2)	0.015(2)	0.335(2)	31

Table 2. (continued)

atom	x	y	z	B_{eq} [a]
C(43)	0.875(2)	0.006(1)	0.363(2)	25
C(44)	0.880(2)	0.027(2)	0.407(2)	23
C(45)	0.886(2)	0.076(2)	0.402(1)	19

[a] $B_{eq} = (8/3)\pi^2[U_{11}(aa^*)^2 + U_{22}(bb^*)^2 + U_{33}(cc^*)^2 + 2U_{12}aa^*bb^*\cos\gamma + 2U_{13}aa^*cc^*\cos\beta + 2U_{23}bb^*cc^*\cos\alpha]$

Table 3. Anisotropic Thermal Paprameters[a] ($Å^2$) of the Non-Hydrogen Atoms for $W_6Se_8(pip)_6 \cdot 8pip$

atom	U_{11}	U_{22}	U_{33}	U_{12}	U_{13}	U_{23}
W(1)	0.055(1)	0.0428(9)	0.043(1)	0.0000	-0.0027(9)	0.0000
W(2)	0.0449(7)	0.0471(7)	0.0538(7)	0.0006(7)	0.0032(6)	-0.0020(6)
Se(1)	0.062(2)	0.061(2)	0.057(2)	0.000(0)	0.011(2)	0.009(2)
Se(2)	0.067(2)	0.057(2)	0.052(2)	0.007(2)	0.005(2)	-0.005(2)
N(1)	0.09(2)	0.04(2)	0.05(2)	0.0000	-0.04(2)	0.0000
N(2)	0.05(2)	0.08(2)	0.18(3)	0.00(2)	0.06(2)	-0.05(2)
C(12)	0.11(3)	0.02(1)	0.23(5)	0.02(2)	-0.05(3)	0.04(2)
C(13)	0.16(6)	0.06(4)	0.18(6)	0.0000	-0.02(6)	0.0000
C(21)	0.08(3)	0.18(5)	0.25(6)	0.02(3)	0.08(4)	0.05(4)
C(22)	0.10(4)	0.11(3)	0.21(5)	0.00(3)	0.04(3)	-0.05(4)
C(23)	0.06(3)	0.14(4)	0.19(5)	0.02(3)	0.04(3)	-0.03(4)
C(24)	0.07(3)	0.29(8)	0.30(7)	-0.13(4)	0.07(4)	-0.09(6)
C(25)	0.09(3)	0.09(3)	0.07(2)	0.03(2)	0.00(2)	0.02(2)

[a]The coefficients U_{ij} of the anisotropic thermal parameter expression are defined as: $\exp[-2\pi^2(a^{*2}U_{11}h^2+b^{*2}U_{22}k^2+C^{*2}U_{33}l^2+2a^*b^*U_{12}hk+2a^*c^*U_{13}hl+2b^*c^*U_{23}kl)]$

0.041 and R_w = 0.040, respectively.

Structure determination for $W_6Se_8(py)_6 \cdot 6(py)$

Single crystals of $W_6Se_8(py)_6 \cdot 6py$ were grown from a portion of the filtrate by allowing it to stand at -20°C for several days. A dark red rhombohedral crystal, with dimensions of 0.35 x 0.35 x 0.24 mm^3, was mounted on a glass fiber, and data collection proceeded at -65°C. Data were collected with a Rigaku AFC6R diffractometer using Mo Kα radiation, over the range $3° < 2\theta < 55°$ in the hemisphere ($\pm h, \pm k, +l$), using the ω-2θ scan technique. Three standard reflections were monitored every 150 reflections and showed no intensity variation over the collection period. A total of 4159 reflections were collected, of which 2601 were unique (R_{int} = 0.040) and 1764 were observed with $I > 4\sigma(I)$. The linear absorption coefficient, μ, for Mo $K\alpha$ radiation is 145.90 cm^{-1}. First, an empirical absorption correction using the φ scan technique was applied after the structure solution. After all of the atoms were located and refined isotropically, an absorption correction using the DIFABS program[15] was applied and resulted in the relative transmission factors ranging from 0.38 to 1.15. The data were corrected for Lorentz and polarization effects.

The trigonal space group $R\bar{3}$ was chosen on the basis of systematic absences and intensity statistics. Initial tungsten atom positions were input on the basis of the SHELXS direct methods output. Subsequently, the non-hydrogen atomic positions were located directly from the electron density difference maps. All non-hydrogen

atoms were refined with anisotropic thermal parameters. Idealized hydrogen positions were calculated and placed in the refinement, but their parameters were held constant during subsequent cycles. The final cycle of full-matrix least-squares refinement was based on 1764 observed reflections and 130 variable parameters and converged with unweighted and weighted agreement factors of: R = 0.029 and R_w = 0.025, respectively. The asymmetric unit was found to be $W_1Se_2(py)_1 \cdot 1py$. The atomic coordinates and equivalent isotropic thermal parameters of the non-hydrogen atoms are given in Table 4, and the anisotropical thermal parameters are shown in Table 5.

Results and Discussion

Synthesis of $W_6Se_8(pip)_6$ and $W_6Se_8(py)_6$

Previous research on sulfide substitution in the $(W_6Cl_8)^{4+}$ cluster units (W_6Cl_{12}) showed that NaSH was a good sulfiding agent.[5-8] However, NaSH also served as an oxidizing agent for the tungsten during the sulfide substitution. Piperidine and pyridine were used as solvents since they possessed sufficiently high boiling points to conveniently promote the reaction at reflux temperatures, and also acted as good ligands for binding in the terminal positions of the W_6Y_8 cluster units, thus stabilizing and solubilizing the cluster complexes.

Table 4. Atomic Coordinates and Equivalent Isotropic Thermal Parameters ($Å^2$) of the Non-Hydrogen Atoms for $W_6Se_8(py)_6 \cdot 6py$

atom	x	y	z	B_{eq}[a]
W(1)	0.07349(2)	-0.01052(2)	0.07258(2)	1.083(7)
Se(1)	0.0000	0.0000	0.2086(1)	1.41(2)
Se(2)	0.13995(5)	-0.02052(5)	-0.07045(6)	1.44(2)
N(1)	0.1637(4)	-0.0213(4)	0.1574(5)	1.8(2)
N(10)	0.5756(5)	0.0585(6)	0.8196(6)	3.3(2)
C(1)	0.1439(5)	-0.0607(5)	0.2340(7)	2.1(2)
C(2)	0.1971(7)	-0.0674(6)	0.2883(7)	2.9(2)
C(3)	0.2751(7)	-0.0292(7)	0.2647(8)	3.2(3)
C(4)	0.2970(5)	0.0137(6)	0.1847(8)	3.0(2)
C(5)	0.2387(5)	0.0155(5)	0.1353(7)	2.2(2)
C(11)	0.6299(6)	0.1327(7)	0.8113(8)	3.6(3)
C(12)	0.6422(6)	0.1740(5)	0.7325(8)	3.0(2)
C(13)	0.5980(6)	0.1380(6)	0.6609(8)	3.2(2)
C(14)	0.5423(6)	0.0586(6)	0.6699(8)	3.2(3)
C(15)	0.5342(6)	0.0233(6)	0.7470(9)	3.1(2)

[a] $B_{eq} = (8/3)\pi^2[U_{11}(aa^*)^2 + U_{22}(bb^*)^2 + U_{33}(cc^*)^2 + 2U_{12}aa^*bb^*\cos\gamma + 2U_{13}aa^*cc^*\cos\beta + 2U_{23}bb^*cc^*\cos\alpha]$

Table 5. Anisotropic Thermal Parameters[a] ($Å^2$) of the Non-Hydrogen Atoms for $W_6Se_8(py)_6 \cdot 6py$

atom	U_{11}	U_{22}	U_{33}	U_{12}	U_{13}	U_{23}
W(1)	0.0132(2)	0.0147(2)	0.0137(2)	0.0074(1)	-0.0006(2)	0.0004(2)
Se(1)	0.0199(4)	0.0199	0.0138(8)	0.0099	0.000	0.0000
Se(2)	0.0175(4)	0.0220(4)	0.0185(5)	0.0124(3)	0.0015(4)	-0.0009(3)
N(1)	0.021(4)	0.028(4)	0.021(4)	0.014(3)	-0.001(3)	0.005(4)
N(10)	0.036(5)	0.053(6)	0.035(6)	0.021(5)	0.001(4)	0.010(5)
C(1)	0.034(5)	0.031(5)	0.019(5)	0.021(4)	-0.002(4)	0.000(4)
C(2)	0.056(7)	0.040(6)	0.024(6)	0.033(5)	-0.007(5)	0.005(5)
C(3)	0.054(7)	0.053(7)	0.036(7)	0.043(6)	-0.017(6)	-0.004(6)
C(4)	0.017(4)	0.042(6)	0.052(8)	0.014(4)	-0.013(5)	-0.006(6)
C(5)	0.028(5)	0.034(5)	0.025(6)	0.019(4)	-0.005(4)	0.006(4)
C(11)	0.038(6)	0.058(8)	0.039(8)	0.022(6)	-0.003(6)	-0.006(6)
C(12)	0.034(6)	0.028(5)	0.039(7)	0.005(4)	0.004(5)	0.004(5)
C(13)	0.035(6)	0.051(7)	0.032(7)	0.019(5)	-0.001(5)	0.006(6)
C(14)	0.042(6)	0.041(6)	0.038(7)	0.021(5)	0.002(6)	-0.002(6)
C(15)	0.030(5)	0.028(5)	0.055(8)	0.011(4)	0.003(6)	0.005(6)

[a]The coefficients U_{ij} of the anisotropic thermal parameter expression are defined as: $\exp[-2\pi^2(a^{*2}U_{11}h^2+b^{*2}U_{22}k^2+c^{*2}U_{33}l^2+2a^*b^*U_{12}hk+2a^*c^*U_{13}hl+2b^*c^*U_{23}kl)]$

Ideally, if Na_2Se is used as the selenium source instead of NaSeH, it would lead to the formation of $W_6Se_8^{4-}$ or $W_6Se_8L_6^{4-}$ as indicated by equation 1. However, the

$$W_6Cl_{12} + 8Na_2Se \xrightarrow{L} Na_4W_6Se_8L_6 + 12NaCl \qquad (1)$$

material recovered from the filtrate contained the neutral cluster molecules, $W_6Se_8(pip)_6$ or $W_6Se_8(py)_6$, based on spectroscopic analyses (XPS and IR) and X-ray diffraction. A ^1H NMR study on the $W_6Se_8(pip)_6 \cdot x$ pip complex in $CDCl_3$ provided a spectrum similar to that of $Mo_6S_8(pip)_6 \cdot x$ pip.[9a] Lattice piperidine are evident by peaks at 2.60 ppm (α-CH_2) and 1.37 ppm (β-,γ-CH_2). No evidence was found for the formation of. $Na_4W_6Se_8L_6$

The reactions leading to formation of the 20-electron W_6Se_8 cluster unit are still not clear. However, one possibility is that the 24-electron $(W_6Se_8)^{4-}$ unit undergoes disproportionation to form elemental tungsten and $W_6Se_8L_6$ as indicated in equation 2. In the case with L = pyridine, the insoluble residue isolated after separation of

$$4Na_4W_6Se_8L_6 \longrightarrow 3W_6Se_8L_6 + 6W + 8Na_2Se \qquad (2)$$

the soluble products $W_6Se_8(py)_6$ and NaCl provided XP spectra for both W 4f and Se 3d transitions. The W $4f_{7/2}$ binding energies (eV) were found at 31.1 (strong), 32.5 (strong) and 34.7 (weak), corresponding to W metal, WSe_2 and WO_3, respectively. The last is regarded as only a surface impurity. Thus it appears that some elemental tungsten is formed when the reaction is conducted in pyridine. For the reaction conducted in piperidine, the similarly recovered residue provided XPS data with only one W $4f_{7/2}$ peak at 32.5 eV. This corresponds most closely to WSe_2 with W $4f_{7/2}$ at 32.3 eV determined on our spectrometer. Apparently, some WSe_2

results from the reactions in both solvents. Formation of WSe_2 could occur by further disproportionation of the tungsten in the $W_6Se_8(amine)_6$ compounds or possibly through oxidation by the amines or methanol, with liberation of H_2.

X-ray Photoelectron Spectroscopy

XPS was used to obtain tungsten binding energies and gain further information about possible cluster retention or degradation. If decomposition of the cluster unit "W_6Se_8" did occur to form the thermodynamically favored WSe_2 during any reactions, distinct evidence for this should be found in the resolved W 4f binding energy values. For example, the W 4f XPS of $W_6Se_8(py)_6$ (shown in Figure 1) illustrates that only one type of tungsten is necessary to fit this spectrum. The derived binding energies (BE) of 30.8 eV ($4f_{7/2}$) and 32.9 eV ($4f_{5/2}$) are characteristic of the W_6Y_8 unit. For comparison, the W $4f_{7/2}$ BE for WSe_2 is 32.3 eV. This 1.5 eV difference in BE should make WSe_2 easily detectable when it occurs as an impurity. The XPS binding energies for related compounds are tabulated in Table 6. The materials recovered from the filtrates of the 1:8 (W_6Cl_{12}:Na_2Se) reactions provided an XPS which showed W 4f binding energies corresponding only to those of pure $W_6Se_8L_6$ cluster complexes. However, for the insoluble reaction products, as discussed above for the reaction in pyridine, the XPS showed that three different kinds of tungsten were present. Although the component at 31.1 eV was assigned as tungsten metal, we note that the W $4F_{7/2}$ binding energy for tungsten metal[18] is

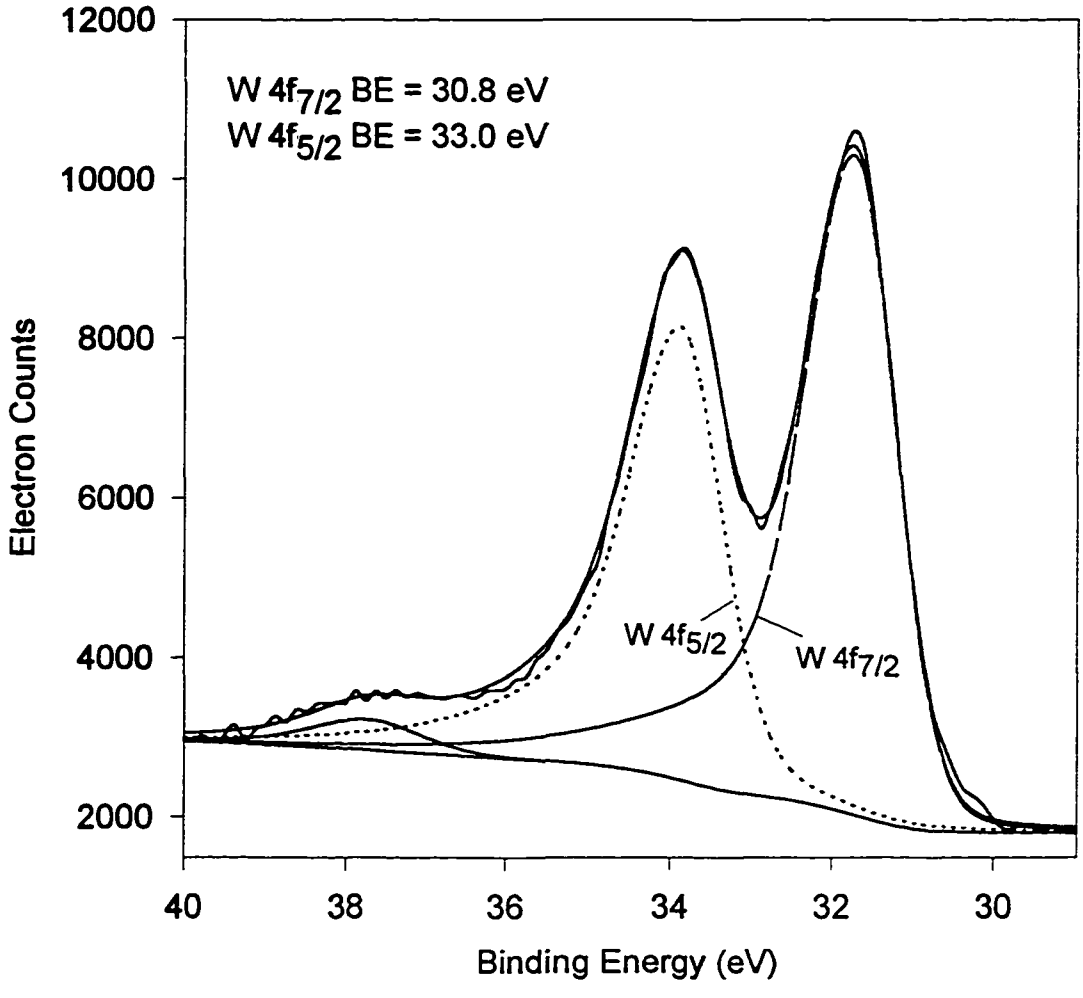

Figure 1. W 4f X-ray photoelectron spectrum of $W_6Se_8(py)_6$. The observed spectrum is given by the upper wiggly solid line, the fitted components are given by the lower dashed line ($4f_{7/2}$) and dotted line ($4f_{5/2}$), and the sum of fitted components is given by the upper smooth solid line.

Table 6. XPS Binding Energies (eV) for the W_6Y_8 Cluster Complexes and Related Compounds[a]

Compound	W $4f_{7/2}$ (eV)	W $4f_{5/2}$ (eV)	S $2p_{3/2}$ (eV)	Se $3d_{5/2}$ (eV)
$W_6S_8(py)_6$	30.5	32.6	160.6	–
$W_6Se_8(py)_6$	30.8	32.9	–	53.6
$W_6S_8(pip)_6$	30.5	32.6	160.6	–
$W_6Se_8(pip)_6$	30.8	32.9	–	53.7
WS_2	32.7	34.8	162.4	–
WSe_2	32.3	34.4	–	54.6
W_6Cl_{12}	32.4	34.5	–	–
W metal	31.4	33.5	–	–

[a]Data have been corrected to the C 1s binding energy of 284.6 eV.

nearly the same as that for $W_6Se_8(amine)_6$, 31.4 and 30.8 eV, respectively.

Ligand-Exchange Reactions

The complex $W_6Se_8(pip)_6$ can be readily extracted with neat pyridine to form a red solution. Single crystals of $W_6Se_8(py)_6 \cdot 6py$ were grown from this solution by allowing it to stand at -20°C for several days. Apparently the complete substitution of pyridine for piperidine was achieved, as illustrated in equation 4.

$$W_6Se_8(pip)_6 \xrightarrow{\text{pyridine}} W_6Se_8(py)_6 + 6pip \qquad (4)$$

Conversion of $W_6Se_8(py)_6$ to the piperidine adduct was also examined. Upon the extraction with piperidine, the $W_6Se_8(py)_6$ was found to be somewhat soluble, and formed a reddish brown solution. However, upon removal of the liquid after one day, several characteristic bands of the coordinated pyridine remained in the IR spectrum of the product. These results suggest that bonding between the hexatungsten cluster and pyridine is stronger than the bonding with piperidine. A similar conclusion was reached in the studies of the ligand exchange reactions between pyridine and piperidine in the sulfide analogues, $M_6S_8L_6$ (M = Mo or W).[7,9]

Infrared Spectra

Infrared spectroscopy has proven to be a powerful characterization method. As an example, the mid-IR and far-IR spectra of the $W_6Se_8(pip)_6$ complex are shown in

Figure 2 and Figure 3, respectively. The IR bands in the mid-IR region (600 -3500 cm^{-1}) arise from coordinated ligands. It is in the far-IR region where two distinctive cluster vibrations occur. The stronger band at about 240 cm^{-1} is assigned as the IR-allowed T_{1u} W-Se stretching modes. This band is the characteristic band for the tungsten selenide cluster complexes. The tungsten sulfide analogues, $W_6S_8L_6$, exhibit a similar T_{1u} W-S stretching band at 376 cm^{-1}. The reduction from 376 to 240 cm^{-1} is about the change expected based upon the reduced masses of the respective diatomic W-Y vibrators. The other three bands at 200, 150, and 133 cm^{-1} must arise from other sets of T_{1u} modes involving either W-W or W-N stretching or W-Se bending vibrations. The assignment of these bands is not completely clear.

Crystal Structures

All of the molecular complexes reported here contain the hexatungsten cluster unit $W_6Se_8L_6$. This cluster unit can be viewed as an octahedron of tungsten atoms with eight triply-bridging selenium atoms capping the octahedral faces. Each tungsten also possesses an additional terminal coordination site located at the vertex of the octahedron, which is occupied by the nitrogen or phosphorus donor ligands.

$W_6Se_8(pip)_6 \cdot 8pip$ crystallizes in the cubic space group $I\bar{4}3d$ with 12 molecules per unit cell. The W_6Se_8 cluster unit is centered on a $\bar{4}$ position (12a site symmetry). A diagram of the cluster is shown in Figure 4. The piperidine ligand in

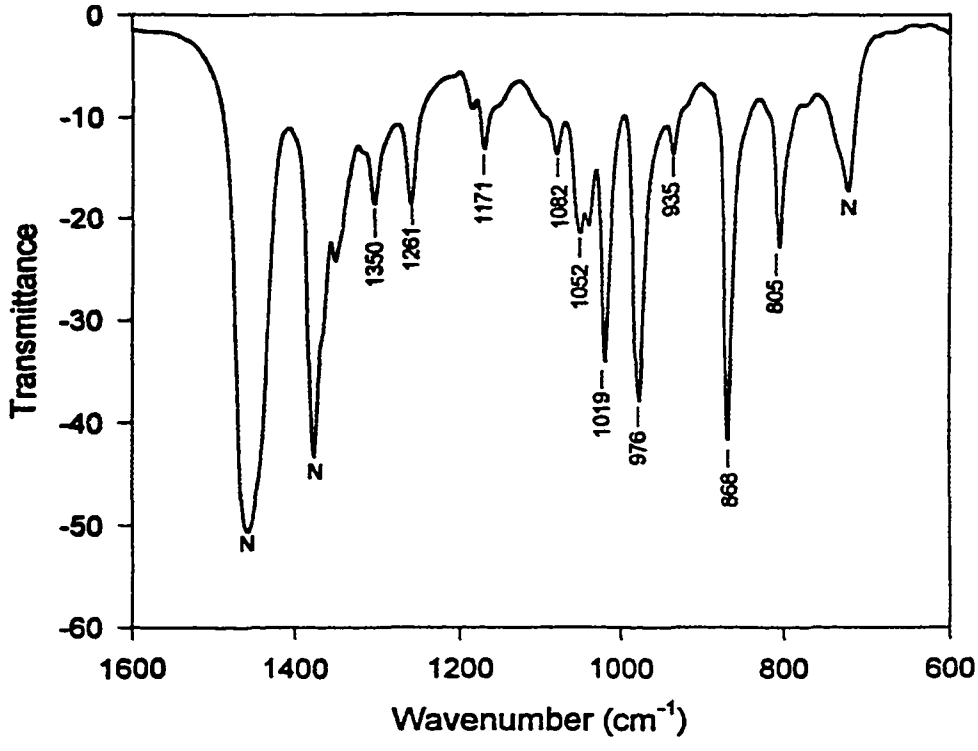

Figure 2. Mid-infrared spectrum of $W_6Se_8(pip)_6$.
The bands labeled as "N" are due to Nujol

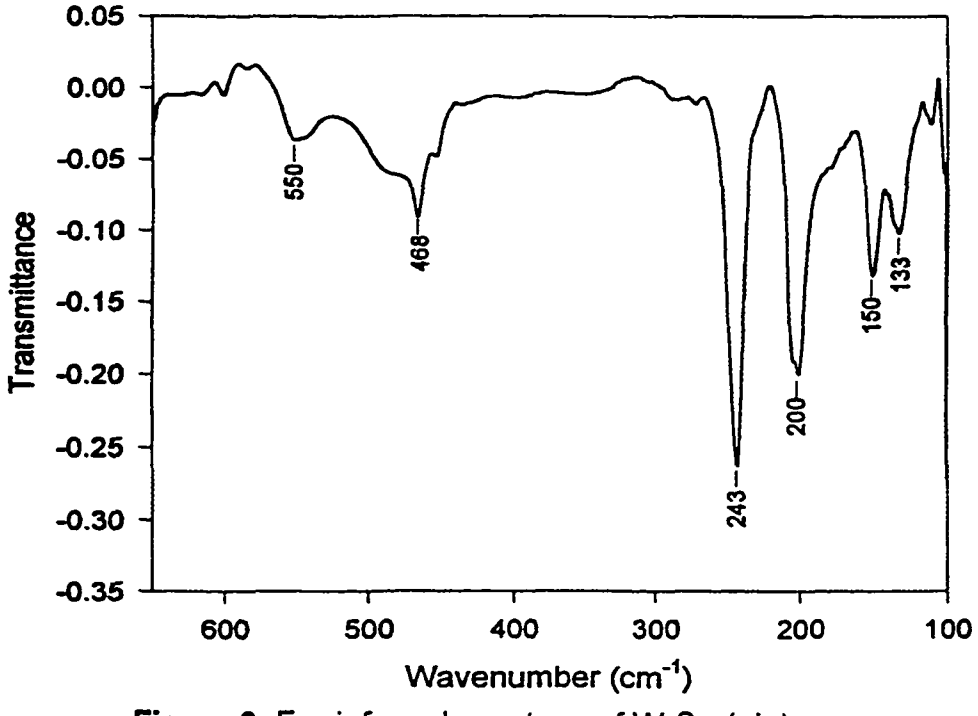

Figure 3. Far-infrared spectrum of $W_6Se_8(pip)_6$

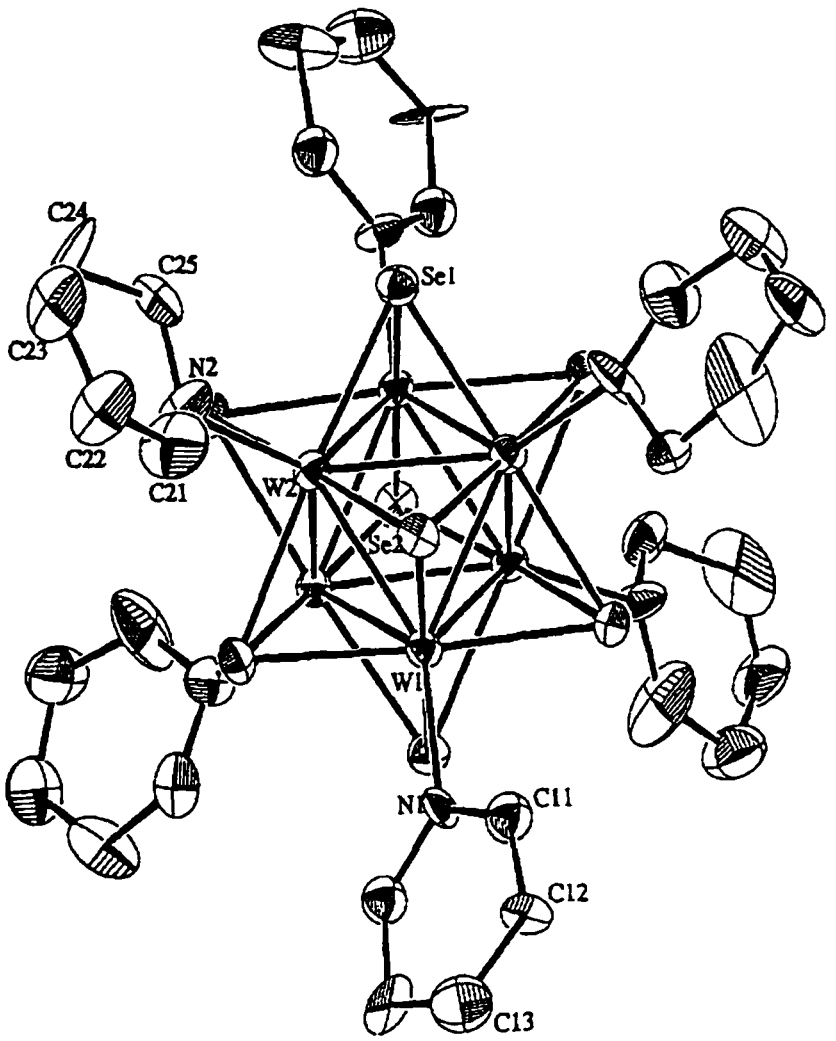

Figure 4. Molecular structure of $W_6Se_8(pip)_6$. Thermal ellipsoids are shown at 25% probability level. Hydrogen atoms have been omitted for clarity.

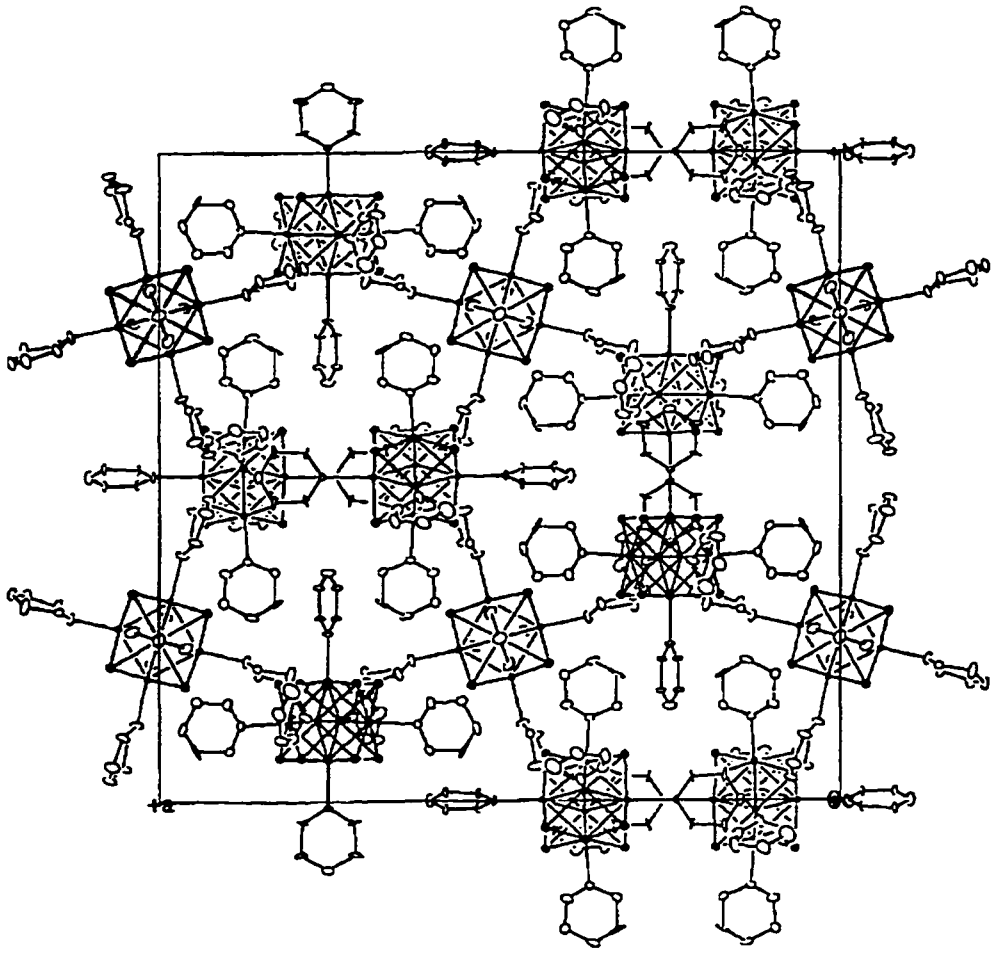

Figure 5 The unit cell of compound $W_6Se_8(pip)_6 \cdot 8(pip)$ as viewed along the c axis. Thermal ellipsoids are shown at 35% probability level. Free piperidine molecules are not shown for clarity.

a chair conformation coordinates to the tungsten atom such that the W-N bond occupies the equatorial position on the N atom. Selected bond distances and bond angles are listed in Table 7. From this table, it can be seen that the deviations from strict octahedral symmetry are quite small. The average bond distances (Å) and maximum deviations are as follows: W-W, 2.689(2) ave., 0.023; W-Se, 2.569(3) ave., 0.006; and W-N, 2.28(3) ave., 0.01.

In comparison, the sulfide analogue, $W_6S_8(pip)_6 \cdot 7pip$, crystallizes in the tetragonal space group $I\bar{4}$ with 8 molecules per unit cell.[7] It is notable that the average W-W bond distance of 2.662(2) Å in $W_6S_8(pip)_6$ is slightly shorter than that of 2.689(2) Å for $W_6Se_8(pip)_6$. Both the size of the chalcogen atom and electronic effects must be involved to give this result. EHMO calculations[19] suggest that the W-W overlap populations are higher for the W_6Se_8 cluster than for the W_6S_8 cluster, in spite of the longer W-W distance in the former.

The average W-Se distance of 2.569(3) Å is much longer than the average W-S distance of 2.461(3) Å for $W_6S_8(pip)_6$. In order to obtain a value for the covalent radius of W towards nonmetallic atoms, the Pauling radius of S, r(S) = 1.05 Å, is subtracted from the average W-S distance to obtain r(W) = 1.41 Å. Applying the latter value to estimate the W-Se distance [r(W) + r(Se) = 1.41 + 1.17 = 2.58 Å] produces a value that is very close to the experimental value, 2.57 Å. The average W-N distance of 2.28(3) Å in these selenide clusters is also close to the average values found for the sulfide clusters, 2.31(3)Å.

The $W_6Se_8(py)_6 \cdot 6py$ crystallizes in the trigonal space group $R\bar{3}$ with 3

Table 7. Selected Bond Lengths (Å) and Angles (deg) in $W_6Se_8(pip)_6 \cdot 8pip$[a]

W(1) - W(2)	2.713(2)	W(1) - Se(1A)	2.567(3)
W(1) - W(2A)	2.668(2)	W(1) - Se(2)	2.569(3)
W(2) - W(2A)	2.687(2)	W(2) - Se(1)	2.563(3)
av. W-W	2.689(2)	W(2) - Se(1A)	2.566(3)
W(1) - N(1)	2.26(3)	W(2) - Se(2A)	2.573(3)
W(2) - N(2)	2.28(3)	W(2) - Se(2)	2.575(3)
av. W-N	2.27(3)	av. W-Se	2.569(3)
W(2)-W(1)-W(2B)	88.87(6)	Se(1B)-W(1A)-Se(1)	175.7(1)
W(1)-W(2)-W(1A)	90.19(5)	Se(2)-W(1)-Se(2B)	176.3(1)
W(2)-W(1A)-W(2B)	90.76(7)	Se(1A)-W(2)-Se(1)	175.7(1)
W(2B)-W(2A)-W(2)	89.97(1)	Se(2)-W(2)-Se(2A)	175.8(1)
av. W-W-W	89.95(5)	av. Se-W-Se	175.9(1)
W(2)-W(1)-W(2A)	59.90(3)	Se(1A)-W(1)-Se(2)	88.1(1)
W(1)-W(2)-W(2A)	59.23(3)	Se(1A)-W(1)-Se(2B)	91.7(1)
W(1)-W(2A)-W(2)	60.87(3)	Se(1)-W(2)-Se(2A)	91.7(1)
av. W-W-W	60.00(3)	Se(1A)-W(2)-Se(2)	88.0(1)
		Se(1)-W(2)-Se(2)	90.0(1)
W(1A)-Se(1)-W(2)	62.69(8)	Se(1A)-W(2)-Se(2A)	90.0(1)
W(2)-Se(1A)-W(2A)	63.18(8)	av. Se-W-Se	89.9(1)
W(1)-Se(1A)-W(2)	63.81(8)		
W(1A)-Se(2A)-W(2)	62.52(8)	Se(1)-W(1A)-N(1A)	92.13(7)
W(1)-Se(2)-W(2)	63.65(8)	Se(2)-W(1)-N(1)	91.87(7)
W(2)-Se(2A)-W(2A)	62.92(8)	Se(1A)-W(2)-N(2)	90.4(8)
av. W-Se-W	63.13(8)	Se(2)-W(2)-N(2)	96.9(8)
		Se(2A)-W(2)-N(2)	86.8(8)
		Se(1)-W(2)-N(2)	93.6(8)
		av. Se-W-N	91.9(7)

[a]Equivalent atoms A and B generated by symmetry transformation:
A, 1/4-z,3/4-y,3/4+x; B, 1/2-x,y,-z.

per unit cell. The W_6Se_8 cluster unit is centered on a $\bar{3}$ position (3a site symmetry), with two of the eight bridging selenium atoms on the 3-fold axis. A diagram of the cluster unit is shown in Figure 6, and cell packing diagrams of $W_6Se_8(py)_6$ with and without solvated pyridine molecules are shown in Figure 7 and Figure 8, respectively. Selected bond distances and bond angles are listed in Table 8. The average W-W and W-Se bond distances are 2.694(1) Å and 2.578(2) Å, respectively.

In comparison, the insoluble sulfide analogue, $W_6S_8(py)_6$, crystallizes in the triclinic space group $P\bar{1}$ (Z=1) without any solvent of crystallization.[5] The solubility of $W_6Se_8(py)_6$ in pyridine is much higher than that of $W_6S_8(py)_6$, so crystals of the former could be obtained directly from the reaction filtrate. As evidenced in Figure 5, and Figure 8, the molecules of the selenide cluster complexes are well separated from each other in the lattice for both the piperidine and pyridine derivatives. The spaces in between are occupied by solvent molecules. However, in the insoluble $W_6S_8(py)_6$, the molecules are packed more closely and the coordinated pyridine molecules are thereby interleaved.[5] For both selenide and sulfide clusters, piperidine adducts are much more soluble in organic solvents than the pyridine adducts.

A summary of the average bond distances and bond angles in these four sulfide and selenide complexes is given in Table 9. Based on Pauling's relation,[20] $d(n) = d(1) - 0.6\log n$, the calculated W-W bond distance, d(n), for the W_6Y_8 unit with average bond order n = 20/24 = 0.833 is 2.677 Å, where d(1) = 2.630 Å is used as

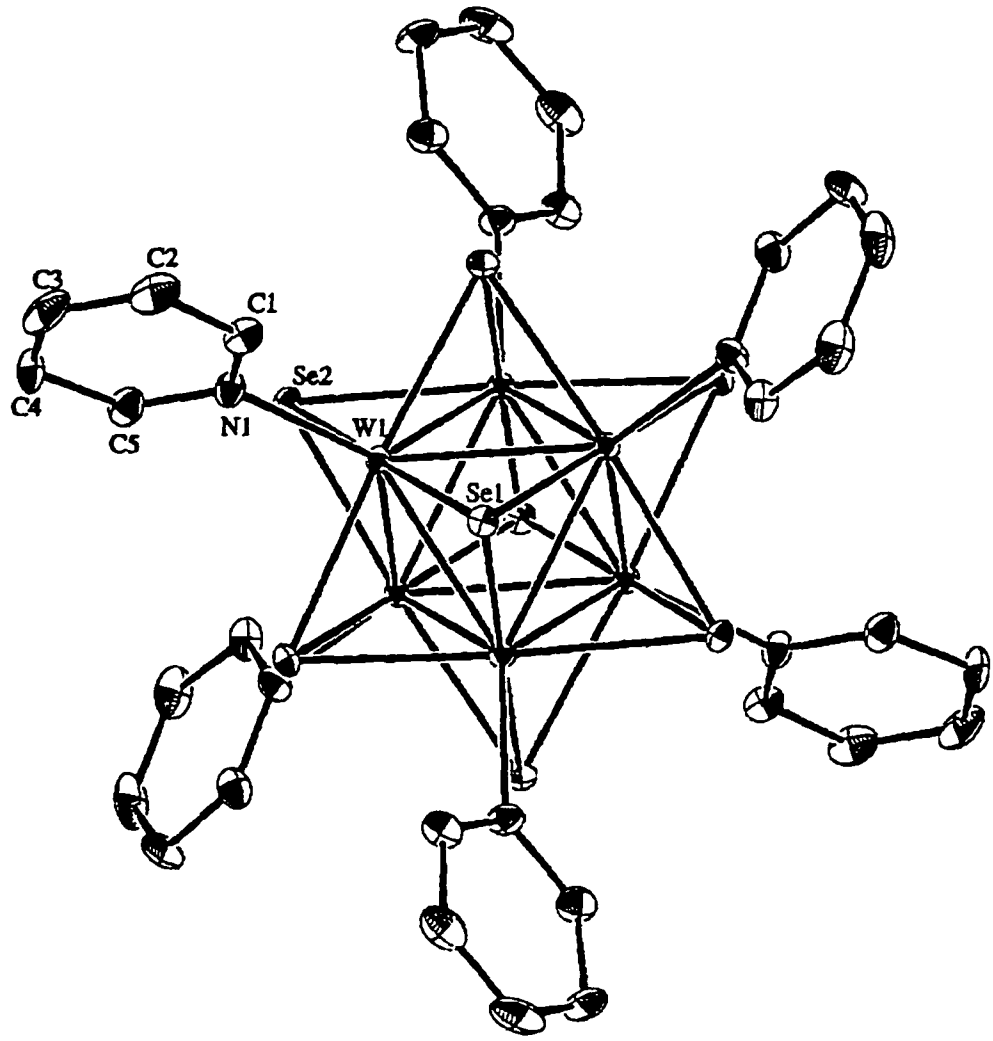

Figure 6. Molecular structure of $W_6Se_8(py)_6$. Thermal ellipsoids are shown at 35% probability level. Hydrogen atoms have been omitted for clarity.

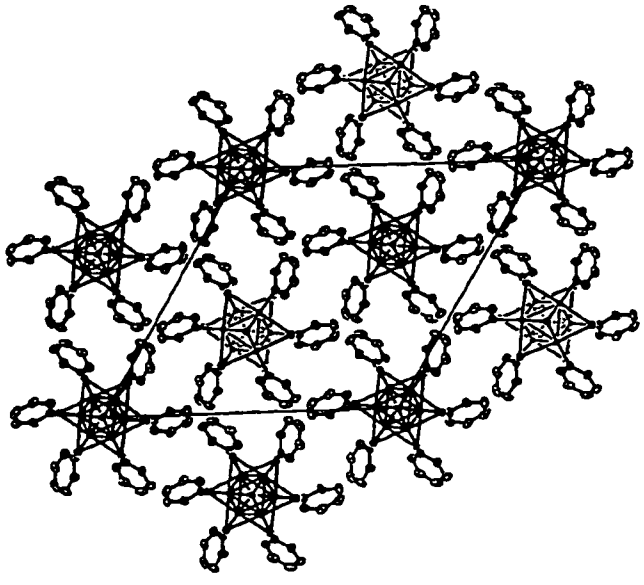

Figure 7 A view look down the c axis of the unit cell in $W_6Se_8(py)_6$. Thermal ellipsoids are shown at 35% probability level. Free pyridine molecules are not shown.

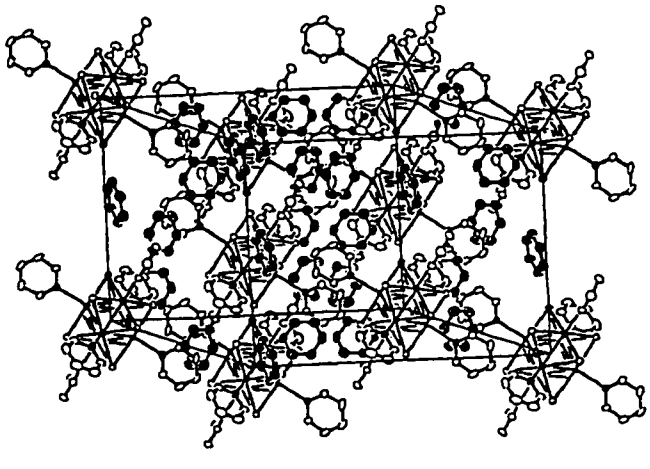

Figure 8 Packing diagram for $W_6Se_8(py)_6 \cdot 6py$. Thermal ellipsoids are at the 50% probability level. The carbon atoms in the uncoordinated pyridine solvent molecules are shown in striped ellipsoids and the corresponding nitrogen atoms are shown in shaded ellipsoids.

Table 8. Selected Bond Lengths (Å) and Angles (deg) in $W_6Se_8(py)_6 \cdot 6py$[a]

W(1)-W(1B)	2.6984(6)	W(1)-Se(1)	2.578(2)
W(1)-W(1C)	2.6891(9)	W(1)-Se(2)	2.582(1)
av. W-W	2.6938(8)	W(1)-Se(2C)	2.580(1)
		W(1)-Se(2D)	2.572(1)
W(1)-N(1)	2.281(7)	av. W-Se	2.578(1)
C(1)-C(2)	1.39(1)		
C(2)-C(3)	1.37(1)	N(1)-C(1)	1.34(1)
C(3)-C(4)	1.41(2)	N(1)-C(5)	1.32(1)
C(4)-C(5)	1.38(1)		

W(1C)-W(1A)-W(1D)	60.00(1)	W(1)-W(ID)-W(IA)	90.00(2)
W(1)-W(1B)-W(1C)	59.89(1)	W(1B)-W(1)-W(1D)	90.00(2)
W(1C)-W(1)-W(1D)	60.23(2)		
av. W-W-W	60.04(1)	Se(1)-W(1)-Se(2C)	89.52(2)
		Se(1)-W(1)-Se(2D)	89.70(3)
W(1)-Se(1)-W(1B)	63.12(4)	Se(2C)-W(1)-Se(2)	90.18(3)
W(1)-Se(2)-W(1C)	62.90(3)	Se(2D)-W(1)-Se(2)	90.36(3)
W(1)-Se(2)-W(1D)	62.79(3)	av. Se-W-Se	89.94(3)
W(1)-Se(2C)-W(1B)	63.18(2)		
av. W-Se-W	63.00(3)	Se(2)-W(1)-N(1)	90.9(2)
		Se(2C)-W(1)-N(1)	92.7(2)
Se(1)-W(1)-Se(2)	176.05(3)	Se(2D)-W(1)-N(1)	90.8(2)
Se(2D)-W(1)-Se(2C)	176.51(3)	Se(1)-W(1)-N(1)	93.0(2)
av. Se-W-Se	176.28(3)	av. Se-W-N	91.8(2)

[a]Equivalent atoms generated by symmetry transformation:

A, -x,-y,-z; B, -x+y,-x,z; C, y,-x+y,-z; D, x-y,x,-z

Table 9. Summary of Selected Average Bond Distances (Å) and Bond Angles (deg) for the $W_6Se_8L_6$ and $W_6Se_8L_6$ Cluster Complexes

formula	W-W	W-Y	W-L	Y-W-Y
$W_6Se_8(py)_6 \cdot 6py$	2.6938(8)	2.578(1)	2.281(7)	176.28(3)
$W_6S_8(py)_6$[5]	2.6617(2)	2.458(3)	2.255(5)	173.09(7)
$W_6Se_8(pip)_6 \cdot 8pip$	2.689(2)	2.569(3)	2.27(3)	175.9(1)
$W_6S_8(pip)_6 \cdot 7pip$[6]	2.6588(3)	2.461(4)	2.31(5)	173.0(2)

the W-W single-bond value. The observed W-W distances in the selenide clusters are slightly longer than this calculated distance. The average W-Se and W-N bond distances are essentially identical in these two new selenide cluster complexes after considering the statistical errors. However, the results of the ligand exchange reactions suggested that the W-N bonds in the pyridine adduct were stronger than that in the piperidine adduct. This stronger W-N bonding in the pyridine adduct, however does not result in any statistically significant difference in the W-W distance that might be expected based on the nature of the donor ligand. The cluster orbitals that are oriented toward the terminal ligands are somewhat antibonding with respect to the W-W bonds of the cluster. Increased donation of electron density to these orbitals should result in W-W bond lengthening. Besides the longer W-W and W-Se bond distances in the selenide complexes, another notable difference between sulfide and selenide cluster units is the average trans Y-W-Y bond angles. The average trans S-W-S and Se-W-Se bond angles are 173.0(1) and 176.1(1), respectively. Thus, the tungsten atom is closer to

coplanarity with four selenium atoms than with four sulfur atoms in the W_6Y_8 units. In both cases, the W atoms reside outside the square faces of the W_6Y_8 cube, as seen in the Y-W-N angles of >90°.

Conclusion

This paper describes the preparations, characterizations, and structures of the first molecular $W_6Se_8L_6$ (L = pyridine and piperidine) cluster complexes.

It was found that Na_2Se was a good selenium source. When a reaction is conducted between one mole of W_6Cl_{12} and ten moles of Na_2Se in the presence of amine ligand (pyridine or piperidine), substitution of selenide for chloride takes place, and tungsten selenide cluster complexes, $W_6Se_8L_6$, are formed in a reasonably high yield (50 - 70%). Although the mechanism of this type of substitution reaction is not quite clear, it is conceivable that the cluster unit, W_6Se_8, is formed through disproportionation of tungsten (II) starting material. It is also noteworthy that the tungsten selenide cluster complexes are more soluble than their sulfide analogues.

Far-infrared and X-ray photoelectron spectroscopy are two major means for characterization of these compounds. The cluster unit, W_6Se_8, shows a characteristic far-IR band at about 250 cm^{-1}, which can be assigned to the T_{1u} W - Se stretching modes. The tungsten sulfide cluster unit, W_6S_8, exhibits a similar T_{1u}

W - S stretching band at 376 cm^{-1}. The reduction from 376 to 250 cm^{-1} is about that expected on the basis of the reduced masses. XPS was used to obtained tungsten binding energies and gain further information about possible cluster retention or degradation. The tungsten binding energies of 30.8 eV ($4f_{7/2}$) and 32.9 eV ($4f_{5/2}$) are characteristic of the W_6Se_8 cluster unit.

The first structures for tungsten selenide cluster complexes, $W_6Se_8L_6$, have been determined. The W - W bond distances in these W_6Se_8 cluster units are slightly longer than those for $W_6S_8L_6$ clusters. The average W - Se bond distance is about 2.57 Å. And all the cluster units show nearly perfect octahedral symmetry.

References

(1) Chevrel, R.; Sergent, M. *Topics in Current Physics*, Fischer, Ø. and Maple, M. B., Eds.; Springer-Verlag: Heidelberg, 1982; Vol. 32, Chapter 2.

(2) Peña, O.; Sergent, M. *Prog. Solid St. Chem.* **1989**, *19*, 165.

(3) Mulhern, P. J.; Haering, R. R. *Can. J. Phys.* **1984**, *62*, 527.

(4) (a) McCarty, K. F.; Schrader, G. L. *Ind. Eng. Chem. Prod. Res. Dev.* **1984**, *23*, 519. (b) McCarty, K. F.; Anderegg, J. W.; Schrader, G. L. *J. Catal.* **1985**, *93*, 375.

(5) Zhang, X.; McCarley, R. E. *Inorg. Chem.* **1995**, *34*, 2678.

(6) Ehrlich, G. M.; Rauch, P. E.; DiSalvo, F. J. *Inorg. Synth.* **1995**, *30*, 1.

(7) Xie, X.; McCarley, R. E. Unpublished results.

(8) Zhang, X. Ph.D. Dissertation, Iowa State University, Ames, IA, 1991.

(9) (a) Hilsenbeck, S. J.; Young Jr., V. G.; McCarley, R. E. *Inorg. Chem.* **1994**, *33*, 1822. (b) McCarley, R. E.; Laughlin, S. K.; Spink, D. A.; Hur, N. *Abstracts of Papers*, 3rd Chemical Congress of North America, Toronto, Ontario, Canada, 1988; American Chemical Society: Washington, DC, 1988. (c) Zhang, X.; Hur, N.; Spink, D. A.; Michel, J. B.; Laughlin, S. K.; McCarley, R. E. Manuscript in preparation.

(10) Saito, T.; Yoshikawa, A.; Yamagata, T.; Imoto, H.; Unoura, K. *Inorg. Chem.* **1989**, *28*, 3588.

(11) Thompson, D. P.; Boudjouk, P. *J. Org. Chem.* **1988**, *53*, 2109.

(12) Oneida Research services, Inc., Whitesboro, NY.

(13) Scheldrick, G. M. *Crystallographic Computing 3*; Oxford University Press: Oxford, U.K., 1985.

(14) *TEXSAN: Single Crystal Structure Analysis Software*, Version 1.6c; Molecular Structure Corp.: The Woodlands, TX 77381, 1985 & 1992.

(15) *DIFABS*: Walker, N. & Stuart, *Acta Cryst.* **1983**, *A39*, 158.

(16) Catti, M.; Ferraris, G. *Acta Cryst.* **1976**, *A32*, 163.

(17) Sheldrick, G. M. SHELXL-93. *J. Appl. Crystallogr.* in press.

(18) A sample of tungsten metal prepared in this laboratory gave W $4f_{7/2}$ BE = 31.5 eV on the spectrometer described in the experimental section. This compares with a reported value of 31.4 eV in *Handbook of X-Ray Photoelectron Spectroscopy,* Perkin-Elmer Cooperation, Eden Prairie, Minnesota, 1992; p 173.

(19) Xie, X.; McCarley, R. E. unpublished research.

(20) Pauling, L. *The Nature of the Chemical Bond*, 3rd Ed.; Cornell Univ. Press: Ithaca, New York, 1960, p 400.

CHAPTER 3. PREPARATION AND STRUCTURE OF THE FIRST TUNGSTEN TELLURIDE COMPLEXES WITH THE OCTAHEDRAL M_6Y_8 CLUSTER UNITS: $W_6Te_8L_6$ AND $NaW_6Te_8L_6$

A paper to be submitted to Inorganic Chemistry

Xiaobing Xie and Robert E. McCarley

Abstract

The first examples of molecular telluride complexes, $W_6Te_8L_6$ (L = py and pip), and $[Na(py)_6]^+[W_6Te_8(py)_6]^-$ were discovered. $W_6Te_8(PEt_3)_6$ was established by ligand displacement of pyridine in $W_6Te_8(py)_6$. The cluster unit, W_6Te_8, showed a characteristic T_{1u} W-Te stretching mode around 180-200 cm^{-1}. The tungsten binding energy of 30.8 eV ($4f_{7/2}$) for $W_6Te_8L_6$ compared favorably with values for the sulfide and selenide analogues. Crystallographic data for these complexes are as follows: $W_6Te_8(pip)_6 \cdot 6pip$, hexagonal, $R\bar{3}$, a = 17.738(6) Å, c = 24.318(10) Å, Z = 3; $W_6Te_8(PEt_3)_6$, monoclinic, $C2/c$, a = 24.724(6) Å, b = 19.716(4) Å, c = 13.543(9) Å, Z = 4; $[Na(py)_6]^+[W_6Te_8(py)_6]^- \cdot 1py$, triclinic, $P\bar{1}$, a = 12.433(3) Å, b = 12.760(2) Å, c = 12.882(2) Å, α = 96.78(1)°, β = 100.03(1)°, γ = 98.58(1)°, Z = 1. The W-Te bond distances are very close to the average W-W bond distance of 2.74 Å in these telluride clusters. For the ionic complex, both the distorted tungsten octahedral

cluster and the shortening of W-W bond confirmed that it was a $21e^-$ cluster unit. The unique cationic unit $[Na(py)_6]^+$ is the first documented example of a sodium ion octahedrally coordinated with six pyridine molecules.

Introduction

The chemistry of molecular tungsten chalcogenide complexes with W_6Y_8 (Y = chalcogen atom) cluster units has attracted considerable interest. These compounds are closely related to the well-known molybdenum chalcogenide Chevrel phases, $M_xMo_6Y_8$, which exhibit diverse and interesting physical and chemical properties.[1-4] The preparation of the Chevrel phases has generally involved solid-state reactions at higher temperatures (1000 - 1300°C). However, there presently is no reported example of the tungsten analogues of the Chevrel phases, W_6Y_8 or $M_xW_6Y_8$. It is generally understood that these compounds are unstable at high temperatures with respect to disproportionation (into W and WY_2 or W, WY_2, and $MY_{n/2}$, where n is the valence of M). Thus, these phases may be isolated only at lower temperatures where they are either thermodynamically stable or metastable and kinetically trapped.

Recently, lower temperature synthetic routes via solution precursors have received a good deal of attention. Such routes not only provide a way to produce thin films, coatings, and small particles, either alone or on typical catalyst support materials, but also provide opportunities to approach meta-stable materials. Therefore, W_6Y_8 or

$M_xW_6Y_8$ might be obtained through these lower temperature synthetic routes.

The coordination chemistry of molecular molybdenum sulfide[5,7] and selenide[8] cluster complexes has been well-developed. Also recently, the preparation of molecular tungsten analogues for both the sulfide[9-11] and selenide[12] complexes were reported by our group. However, no example of the corresponding telluride molecular cluster complexes, such as $M_6Te_8L_6$ (M = Mo, W), has been reported. Furthermore, we have become especially interested in the possible low temperature conversion of these $W_6Y_8L_6$ complexes into the W_6Y_8 or $M_xW_6Y_8$ analogues of the Chevrel phase structure. However, this conversion has not yet been possible with the W_6S_8 and W_6Se_8 clusters complexes.[10c] We wished to examine the W_6Te_8 complexes for this purpose with the idea that the W_6Te_8 binary compound might be more stable towards disproportionation than the W_6S_8 and W_6Se_8 examples. The present paper describes the syntheses, characterizations, and structures of the new neutral molecular complexes of the tungsten telluride clusters, $W_6Te_8(pip)_6$,[13] $W_6Te_8(py)_6$, and $W_6Te_8(PEt_3)_6$, as well as a reduced ionic compound, $[Na^+(py)_6][W_6Te_8(py)_6^-]$.[13]

Experimental

Materials

The reagents and products are air and moisture sensitive. Therefore, all manipulations were performed by the use of an inert-atmosphere drybox, a high-vacuum manifold, and Schlenk techniques, unless otherwise stated. W_6Cl_{12} was prepared by literature methods.[10b,14] Na_2Te and Na_2Te_2 were prepared by the reactions of the stoichiometric amount of sodium and tellurium metal in *liq.* NH_3.[15] All solvents were purified and dried prior to use. Also, the solvents were deoxygenated by use of the freeze-thaw process: freeze to liquid nitrogen temperature, evacuate the gaseous material, and then thaw. This process was repeated three times prior to the distillation of the purified solvent onto Linde 3- or 4-Å Molecular Sieves and stored under vacuum or a nitrogen atmosphere. Pyridine (Fisher), piperidine (Fisher), and triethylphosphine (Strem) were purified by refluxing over calcium hydride for at least 4 h. Toluene (Fisher) and chloroform were refluxed over phosphorus pentoxide. Without heating, tetrahydrofuran (Fisher) was stirred with sodium metal and a benzophenone indicator. Methanol (Mallinckrodt) was dried by refluxing over sodium methoxide. When used, the solvents were vacuum-distilled or syringed under a flowing nitrogen gas atmosphere.

Physical Measurements

Infrared spectroscopy

All infrared spectra were collected as Nujol mulls. The samples were prepared in the drybox and were temporarily stored under nitrogen before being placed in the sample chamber of the instrument. Infrared (4000-200 cm^{-1}) spectra were recorded with a Bomem MB-102 Fourier Transform Infrared Spectrometer manufactured by Hartman and Braun. Sample mulls were pressed between two cesium iodide plates. The sample chamber of the instrument was continuously purged with dry, compressed air and the reference spectra were collected in the empty chamber. Far-infrared (650-100 cm^{-1}) spectra were recorded separately with an IBM IR/98 Fourier transform infrared spectrometer. Thick sample mulls were placed on a polyethylene film in the drybox, and the film was mounted on a sample holder. Then the sample was transferred to the sample chamber. Data were collected for these samples while the sample chamber was under vacuum, and Nujol on the polyethylene film was used as a reference.

X-ray photoelectron spectroscopy

XP spectra were collected by James Anderegg at room temperature with a Physical Electronics Industries 5500 multitechnique surface analysis system. This system was equipped with a hemispherical analyzer, a toroidal monochromator, and multichannel detector which sampled a 2 mm^2 area. The samples were pressed on

an indium substrate and loaded into an air-sensitive sample holder in the dry-box. Then the sample holder was transferred into the chamber of the spectrometer. After the system was completely evacuated, the sample holder was opened and the sample was excited with monochromatic Mg *Kα* radiation (1253.6 eV) at the power of 300 W. The photoelectron binding energies were calibrated with C 1s = 284.6 eV.

X-ray powder diffraction

Powder X-ray diffraction (XRD) data were obtained with a Philips ADP3520 θ-2θ diffractometer using Cu *Kα* radiation. The air-sensitive samples were loaded into a specially designed sample holder and sealed under N_2 while in the drybox.

Ultraviolet-visible spectroscopy

Electronic spectra were collected on a Hewlett-Packard 8453 UV-VIS scanning spectrophotometer located in Professor Mark Porter's group. The sample cells were equipped with stopcocks so that air sensitive samples could be stored in the cells. The samples of $W_6Y_8(pip)_6$ (Y=S, Se, Te) were dissolved in neat piperidine, transferred into sample cells under N_2 gas purge, and examined over the range of 300-1000 nm. A piperidine blank was used as the reference and subtracted from the sample spectra.

Magnetic susceptibility

The magnetic properties were examined on powder samples with a Quantum SQUID magneto-susceptometer. The samples were loaded into a 3 mm inner diameter fused silica tube that had been sealed on the bottom half with a 3 mm outer diameter fused silica rod. Another fused silica rod was placed on top of the sample, thus giving an arrangement where an uniform measurement could be made. The data were subsequently corrected for the diamagnetic contribution of the quartz.

Electron spin resonance spectroscopy

ESR spectra were recorded using a Bruker ESP-300 spectrometer. The spectral parameters were 100.0 kHz modulation frequency, 0.125 G modulation amplitude, 100 ms time constant, 1.25×10^4 receiver gain, 1300-4300 G sweep width, and a 5.243 s sweep time. All signals were averaged over sixty scans. The samples were loaded in a 3 mm outer diameter fused silica tube in a dry-box. The tube was then evacuated and sealed on a vacuum line.

Analytical Procedures

Tungsten was determined gravimetrically as the trioxide. The samples were dissolved in 0.5 M KOH basic solutions with the aid of hydrogen peroxide. The solutions were then treated with concentrated nitric acid and 2 mL of hydrogen

peroxide to form a peroxy-acid complex. The hydrated oxide, $WO_3 \cdot nH_2O$, was then completely precipitated by slowly decomposing this complex at 100°C and collected in tared ceramic filter crucible. After washing with dilute nitric acid and hydrochloric acid extensively to remove any TeO_2 or TeO_3 residues, the materials were then dried to constant weight at 800°C.

Chlorine was determined by potentiometric titration with a standardized silver nitrate solution after dissolving the samples in hot KOH-H_2O_2 solutions and neutralization. A silver/silver chloride electrode was used as the reference, and a silver rod as the working electrode. The endpoint was determined by using the second derivative method.

Synthetic Procedures

Preparation of $W_6Te_8(pip)_6 \cdot 6pip$

W_6Cl_{12} (0.300 g, 0.196 mmol), and Na_2Te (0.136 g, 0.784 mmol), and NaTe (0.118 g, 0.784 mmol) were weighed in the drybox and transferred into a 100-mL Schlenk reaction flask equipped with a water-cooled condenser. By distillation, 40 mL of piperidine were added to the reactants and the mixture was refluxed for 3 days. A black solid and dark-blue solution were separated by filtration. Single crystals of $W_6Te_8(pip)_6 \cdot 6pip$ were grown from a portion of the filtrate by allowing it to stand at -20°C for several weeks. The solvent was removed from the filtrate under dynamic vacuum and about

0.35 g of dark blue powder was recovered. IR (Nujol, cm^{-1}): 1353 (w), 1303 (m), 1260 (m), 1175 (w), 1082 (w), 1058 (m), 1041 (w), 1020 (s), 980 (s), 935 (w), 866 (s), 803 (s), ν(W-Te) 179 (s). A test for chloride was negative. UV-Vis (λ, piperidine): 566 nm.

Preparation of $W_6Te_8(py)_6$

W_6Cl_{12} (0.300 g, 0.196 mmol), Na_2Te (0.136 g, 0.784 mmol), and NaTe (0.118 g, 0.784 mmol) were weighed in the drybox and transferred into a 100-mL Schlenk reaction flask equipped with a water-cooled condenser. By distillation, 50 mL of pyridine were added to the reactants and the mixture was refluxed for 3 days. A black solid and faint yellow solution were separated by filtration. The black solid was extracted with methanol for two days to remove the NaCl by-product. Then about 0.45 g of black powder (88% yield) was recovered after being dried under dynamic vacuum for one day. All attempts to grow single crystals of this insoluble compound were unsuccessful. IR (Nujol, cm^{-1}): 1594 (w), 1348 (w), 1306 (w), 1208 (s), 1168 (w), 1146 (m), 1063 (ms), 1035 (ms), 965 (w), 932 (w), 746 (s), 685 (s), W-Te 180 (ms). A test for chloride was negative.

Preparation of $W_6Te_8(PEt_3)_6$

About 0.24 g of $W_6Te_8(pip)_6$ was loaded into a 100 mL Schlenk reaction flask equipped with a water-cooled condenser. By syringe, 40 mL of toluene and 0.15 mL of triethylphosphine were added and the mixture was refluxed for one day. The mixture was filtered while hot, thereby providing a small amount of solid and grape purple

solution. The toluene was then removed from the filtrate under dynamic vacuum, and after drying overnight *in vacuo,* 0.22 g of dark purple powder was collected. IR (Nujol, cm^{-1}): 1255 (m), 1168 (w), 1146 (m), 1033 (s), 759 (s) 713 (m), 404 (ms), 368 (s), 334 (w), W-Te 205 (m). Single crystals of $W_6Te_8(PEt_3)_6$ were obtained by redissolving 0.05 g of the purple solid into 6 mL $CHCl_3$ and allowing the solution to stand at -20°C for one week.

Preparation of $[Na(py)_6][W_6Te_8(py)_6]\cdot 1py$

W_6Cl_{12} (0.500 g, 0.327 mmol), and Na_2Te (0.453 g, 2.610 mmol) were weighed in the drybox and transferred into a 100-mL Schlenk reaction flask equipped with a water-cooled condenser. By vacuum distillation, 50 mL of pyridine were added to the reactants and the mixture was refluxed for 2 days. The mixture was then filtered while hot, and 0.622 g of a black solid and dark red solution were separated. Single crystals of $[Na(py)_6][W_6Te_8(py)_6]\cdot 1py$ were grown from the filtrate by allowing it to stand at room temperature for two days. The solvent was then removed from the filtrate under dynamic vacuum. After drying overnight *in vacuo,* 0.41 g black powder was obtained. A test for chloride was negative. The black insoluble product obtained by filtration of the reaction mixture was washed with methanol for two days to remove the NaCl by-product, and about 0.25g of black solid was recovered. A test for chloride was negative.

Reaction of $W_6Te_8(pip)_6$ with pyridine

About 0.20 g of the piperidine adduct $W_6Te_8(pip)_6$ was weighed in the drybox and transferred into a 100 mL Schlenk reaction flask, and 30 mL of pyridine was vacuum-distilled onto the solid. The solid was initially soluble in pyridine. After the mixture was refluxed for several hours or allowed to sit at room temperature for 2 days, a black solid and faint filtrate were obtained upon filtration. The black powder was then recovered and dried *in vacuo*. IR (Nujol, cm^{-1}): 1594 (w), 1348 (w), 1306 (w), 1208 (s), 1168 (w), 1146 (m), 1063 (ms), 1035 (ms), 965 (w), 932 (w), 746 (s), 685 (s), W-Te 182 (ms).

X-ray Structure Determinations

Single-crystal structure determinations were undertaken for three of the $W_6Te_8L_6$ cluster complexes. In each case, a crystal was chosen from material still in contact with the mother solution. The crystals were encased in epoxy cement, quickly attached to the tip of a glass fiber, and immediately inserted into the low-temperature nitrogen stream of the diffractometer for data collection. The cell constants were determined from 25 randomly located and centered reflections. The structures were solved by direct methods using SHELXS[16] and refined on F by full-matrix, least-squares techniques with the TEXSAN package.[17] Pertinent crystallographic data are listed in Table 1.

Table 1. Crystallographic Data for the $W_6Te_8L_6$ Cluster Complexes

compound	$W_6Te_8(pip)_6 \cdot 6pip$	$W_6Te_8(PEt_3)_6$	$[Na(py)_6][W_6Te_8(py)_6] \cdot 1py$
chemical formula	$C_{70}H_{154}N_{14}Te_8W_6$	$C_{36}H_{90}P_6Te_8W_6$	$C_{65}H_{65}NaN_{13}Te_8W_6$
formula weight	2926.86	2832.85	3175.21
space group	$R\bar{3}$ (#148)	$C2/c$ (#15)	$P\bar{1}$ (# 2)
a, Å	17.738(6)	24.724(6)	12.433(3)
b, Å		19.716(4)	12.760(2)
c, Å	24.318(10)	13.543(9)	12.882(2)
α, °			96.78(1)
β, °		108.56(3)	100.03(1)
γ, °			98.58(1)
V, Å^3	6638(2)	6258(4)	1968(1)
Z	3	4	1
ρ_{calcd}, g/cm^3	2.361	3.006	2.679
μ, cm^{-1}	103.99	148.30	116.99
radiation (Mo Kα) Å	0.71069	0.71069	0.71069
T, °C	-70	-70	-70
2θ rang, deg	4-45	3-55	3-55
total data	3294	15087	9508
unique data	1938	7465	9101
data observed	1203 [I>3.0σ(I)]	3361 [I>5.0σ(I)]	4575 [I>4.0σ(I)]
no. parameter	125	249	407
data/para.	9.6	13.5	11.2
abs. correction	DIFABS	DIFABS	DIFABS
trans. factors	0.88-1.11	0.81-1.22	0.72-1.47
R^a	0.045	0.027	0.034
R_w^b	0.041	0.030	0.030
diff. peaks, e/Å^3	1.85, -2.14	1.31, -1.67	1.95, -2.05

$^aR = \Sigma||F_o|-|F_c||/\Sigma|F_o|$.

$^bR_w = [\Sigma\omega(|F_o|-|F_c|)^2/\Sigma\omega|F_o|^2]^{1/2}$; $\omega = 1/\sigma^2(|F_o|)$

Structure determination for $W_6Te_8(pip)_6 \cdot 6pip$

A black crystal, with dimensions of 0.20 x 0.30 x 0.35 mm^3, was mounted on a glass fiber, and data collection proceeded at -70°C. Data were collected with a Rigaku AFC6R diffractometer using Mo $K\alpha$ radiation, over the range $4°<2\theta<45°$ in the hemisphere ($\pm h,+k,\pm l$) using the ω-2θ scan technique. Three standard reflections were monitored every 150 reflections and showed no intensity variation over the collection period. A total of 3294 reflections were collected, of which 1938 were unique (R_{int} = 0.068) and 1203 were observed with $I>3\sigma(I)$. The linear absorption coefficient, μ, for Mo $K\alpha$ radiation is 103.99 cm^{-1}. First, an empirical absorption correction using the φ scan technique was applied after the structure solution. After all of the atoms were located and refined isotropically, an absorption correction using the DIFABS program[18] was applied and resulted in the relative transmission factors ranging from 0.88 to 1.11. The data were corrected for Lorentz and polarization effects.

The trigonal space group $R\bar{3}$ was chosen on the basis of systematic absences and intensity statistics. Initial tungsten atom positions were input on the basis of the SHELXS direct methods[16] output. Subsequently, the other non-hydrogen atomic positions were located directly from the electron density difference maps. These atoms were refined with anisotropic thermal parameters, except the nitrogen atom on the piperidine ligand molecule. Idealized hydrogen positions were calculated and placed in the refinement with C-H distances equal to 0.95 Å and N-H distances equal to 0.86 Å, but their parameters were held constant during subsequent cycles. The final cycle of full-matrix least-squares refinement was based on 1203 observed reflections and 125

variable parameters and converged with unweighted and weighted agreement factors of: R = 0.045 and R_w = 0.041, respectively. The asymmetric unit was found to be $W_1Te_2(pip)_1 \cdot 1pip$. One of the tellurium atoms is located at a special position (C3), and all the other unique atoms are at general positions. The atomic coordinates and equivalent isotropic thermal parameters of the non-hydrogen atoms are given in Table 2, and the anisotropical thermal parameters of non-hydrogen atoms are shown in Table 3.

Structure determination for $W_6Te_8(PEt_3)_6$

Single crystals were grown from a chloroform solution of $W_6Te_8(PEt_3)_6$ by standing at -20°C. A black crystal, with dimensions of 0.10 x 0.20 x 0.35 mm^3, was mounted on a glass fiber, and data collection proceeded at -70°C. Data were collected with a Rigaku AFC6R diffractometer using Mo $K\alpha$ radiation, over the range $4° < 2\theta < 55°$ in the hemisphere ($\pm h, \pm k, +l$) using the ω-2θ scan technique. Three standard reflections were monitored every 200 reflections and showed 1.99% intensity decay over the collection period. A total of 15087 reflections were collected, of which 7465 were unique (R_{int} = 0.083) and 3361 were observed with $I > 5\sigma(I)$. The linear absorption coefficient, μ, for Mo $K\alpha$ radiation is 148.30 cm^{-1}. First, an empirical absorption correction using the φ scan technique was applied after the structure solution. After all of the atoms were located and refined isotropically, an absorption correction using the DIFABS program[18] was applied and resulted in the relative transmission factors ranging from 0.81 to 1.22. The data were corrected for Lorentz and polarization effects. A

Table 2. Atomic Coordinates and Equivalent Isotropic Thermal Parameters ($Å^2$) of the Non-Hydrogen Atoms for $W_6Te_8(pip)_6 \cdot 6pip$

atom	x	y	z	B_{eq}[a]
W(1)	0.02317(5)	0.09862(5)	0.04597(3)	1.86(2)
Te(1)	0.0000	0.0000	0.13788(8)	2.52(3)
Te(2)	0.04632(9)	0.19766(8)	-0.04723(5)	2.26(3)
N(1)	0.050(1)	0.2211(10)	0.0968(5)	2.3(3)
N(2)	0.282(1)	0.359(1)	-0.0486(8)	4.2(5)
C(11)	0.017(2)	0.204(1)	0.1561(9)	4.2(6)
C(12)	0.022(2)	0.281(2)	0.1854(10)	4.8(7)
C(13)	0.130(2)	0.298(1)	0.0929(9)	4.5(6)
C(14)	0.139(2)	0.379(2)	0.120(1)	5.7(7)
C(15)	0.108(3)	0.360(2)	0.179(1)	7(1)
C(21)	0.266(2)	0.419(2)	-0.086(1)	6.0(8)
C(22)	0.370(3)	0.479(2)	0.013(1)	8.2(10)
C(23)	0.355(3)	0.544(2)	-0.026(1)	9(1)
C(24)	0.270(2)	0.495(2)	-0.058(1)	7(1)
C(25)	0.364(2)	0.406(2)	-0.016(1)	7.3(10)

[a] $B_{eq} = (8/3)\pi^2[U_{11}(aa^*)^2 + U_{22}(bb^*)^2 + U_{33}(cc^*)^2 + 2U_{12}aa^*bb^*\cos\gamma + 2U_{13}aa^*cc^*\cos\beta + 2U_{23}bb^*cc^*\cos\alpha]$

Table 3. Anisotropic Thermal Parameters[a] ($Å^2$) of the Non-Hydrogen Atoms for $W_6Te_8(pip)_6 \cdot 6pip$

atom	U_{11}	U_{22}	U_{33}	U_{12}	U_{13}	U_{23}
W(1)	0.0246(6)	0.0227(5)	0.0237(4)	0.0121(4)	-0.0004(4)	-0.0026(4)
Te(1)	0.0383(9)	0.0383	0.019(1)	0.0192	0.0000	0.0000
Te(2)	0.0308(8)	0.0203(8)	0.0339(7)	0.0121(6)	-0.0011(6)	0.0036(6)
N(2)	0.06(1)	0.03(1)	0.08(1)	0.03(1)	0.00(1)	0.001(10)
C(11)	0.06(2)	0.03(1)	0.06(1)	0.02(1)	0.01(1)	0.01(1)
C(12)	0.07(2)	0.04(2)	0.06(2)	0.02(2)	0.02(1)	-0.02(1)
C(13)	0.08(2)	0.01(1)	0.05(1)	0.01(1)	0.04(1)	0.005(9)
C(14)	0.09(2)	0.04(2)	0.09(2)	0.02(1)	-0.01(2)	-0.05(1)
C(15)	0.18(4)	0.07(2)	0.06(2)	0.08(3)	-0.05(2)	-0.03(2)
C(21)	0.11(2)	0.07(2)	0.07(2)	0.06(2)	0.01(2)	0.01(1)
C(22)	0.12(3)	0.08(2)	0.07(2)	0.02(2)	-0.06(2)	-0.02(2)
C(23)	0.19(4)	0.03(2)	0.08(2)	0.00(2)	-0.04(2)	-0.01(2)
C(24)	0.14(3)	0.07(2)	0.10(2)	0.06(2)	-0.03(2)	-0.03(2)
C(25)	0.09(3)	0.09(2)	0.09(2)	0.03(2)	0.00(2)	0.01(2)

[a]The coefficients U_{ij} of the anisotropic thermal parameter expression are defined as:
$\exp[-2\pi^2(a^{*2}U_{11}h^2+b^{*2}U_{22}k^2+c^{*2}U_{33}l^2+2a^*b^*U_{12}hk+2a^*c^*U_{13}hl+2b^*c^*U_{23}kl)]$

correction for decay (1.99%) and a correction for secondary extinction (coefficient = $1.59x10^{-10}$) were also applied.

The monoclinic space group *C2/c* was chosen on the basis of systematic absences and intensity statistics. Initial tungsten atom positions were input on the basis of the SHELXS direct methods[16] output. Subsequently, the other non-hydrogen atomic positions were located directly from the electron density difference maps. These atoms were refined with anisotropic thermal parameters, except one carbon atom on a ligand molecule. Idealized hydrogen positions were calculated and placed in the refinement with C-H distances equal to 1.06 Å, but their parameters were held constant during subsequent cycles. The final cycle of full-matrix least-squares refinement was based on 3361 observed reflections and 249 variable parameters and converged with unweighted and weighted agreement factors of: R = 0.027 and R_w = 0.030, respectively. The asymmetric unit was found to be $W_3Te_4(PEt_3)_3$. The atomic coordinates and equivalent isotropic thermal parameters of the non-hydrogen atoms are given in Table 4, and the anisotropical thermal parameters of non-hydrogen atoms are shown in Table 5.

Structure determination for $[Na(py)_6][W_6Te_8(py)_6]\cdot 1(py)$

Single crystals were grown from the pyridine reaction filtrate by allowing it to stand at room temperature. A dark rectangular crystal, with dimensions of 0.20 x 0.20 x 0.40 mm^3, was mounted on a glass fiber, and data collection proceeded at -70°C. Data were collected with a Rigaku AFC6R diffractometer using Mo $K\alpha$ radiation, over the range $3°<2\theta<55°$ in the hemisphere ($+h,\pm k,\pm l$), using the ω-2θ scan technique. Three standard

Table 4. Atomic Coordinates and Equivalent Isotropic Thermal Parameters ($Å^2$) of the Non-Hydrogen Atoms for $W_6Te_8(PEt_3)_6$

atom	x	y	z	B_{eq}[a]
W(1)	0.30317(3)	0.18979(3)	0.96151(4)	1.08(1)
W(2)	0.29474(3)	0.32851(3)	0.98399(5)	1.12(1)
W(3)	0.29667(3)	0.24289(3)	1.14673(5)	1.07(1)
Te(1)	0.30360(5)	0.10510(5)	1.12276(7)	1.48(2)
Te(2)	0.39300(4)	0.26074(5)	1.09094(8)	1.40(2)
Te(3)	0.29989(5)	0.27541(5)	0.79932(7)	1.47(2)
Te(4)	0.21254(4)	0.11932(5)	0.83234(7)	1.41(2)
P(1)	0.3758(2)	0.1153(2)	0.9162(3)	1.81(8)
P(2)	0.3544(2)	0.4303(2)	0.9702(3)	2.01(9)
P(3)	0.3559(2)	0.2356(2)	1.3374(3)	1.66(8)
C(111)	0.4144(9)	0.0497(7)	1.013(1)	2.9(4)
C(112)	0.4573(9)	0.0789(8)	1.112(1)	3.7(5)
C(121)	0.3505(8)	0.0612(7)	0.800(1)	2.7(4)
C(122)	0.3286(9)	0.0996(7)	0.695(1)	2.8(4)
C(131)	0.4368(8)	0.1629(8)	0.894(1)	2.7(4)
C(132)	0.4813(10)	0.1216(10)	0.868(2)	4.1(4)
C(211)	0.3859(9)	0.4300(9)	0.868(1)	3.4(5)
C(212)	0.4353(9)	0.375(1)	0.884(2)	4.1(5)
C(221)	0.4138(7)	0.4497(7)	1.094(1)	2.3(4)
C(222)	0.4495(8)	0.5119(7)	1.091(2)	3.0(4)
C(231)	0.3196(8)	0.5129(7)	0.939(1)	3.0(4)
C(232)	0.2945(7)	0.5439(7)	1.022(1)	2.6(4)
C(311)	0.4294(8)	0.2631(9)	1.372(1)	3.0(4)
C(312)	0.4382(8)	0.3403(9)	1.358(1)	3.3(4)
C(321)	0.3309(8)	0.2842(8)	1.429(1)	2.3(4)
C(322)	0.3669(9)	0.2841(9)	1.545(1)	3.5(4)
C(331)	0.3701(8)	0.1502(8)	1.400(1)	2.5(4)
C(332)	0.3149(9)	0.1167(9)	1.406(1)	3.3(4)

[a] $B_{eq} = (8/3)\pi^2[U_{11}(aa^*)^2 + U_{22}(bb^*)^2 + U_{33}(cc^*)^2 + 2U_{12}aa^*bb^*\cos\gamma + 2U_{13}aa^*cc^*\cos\beta + 2U_{23}bb^*cc^*\cos\alpha]$

Table 5. Anisotropic Thermal Parameters[a] ($Å^2$) of the Non-Hydrogen Atoms for $W_6Te_8(PEt_3)_6$

atom	U_{11}	U_{22}	U_{33}	U_{12}	U_{13}	U_{23}
W(1)	0.0135(3)	0.0139(3)	0.0136(3)	-0.0005(2)	0.0041(3)	-0.0005(2)
W(2)	0.0145(3)	0.0133(3)	0.0151(3)	-0.0024(2)	0.0053(3)	0.0011(2)
W(3)	0.0129(3)	0.0145(3)	0.0123(3)	-0.0005(2)	0.0029(2)	0.0009(2)
Te(1)	0.0206(5)	0.0154(4)	0.0190(5)	0.0012(4)	0.0044(4)	0.0043(3)
Te(2)	0.0125(5)	0.0207(5)	0.0192(5)	-0.0014(4)	0.0040(4)	-0.0019(4)
Te(3)	0.0203(5)	0.0228(5)	0.0157(5)	-0.0024(4)	0.0098(4)	0.0015(4)
Te(4)	0.0188(5)	0.0156(4)	0.0183(5)	-0.0030(4)	0.0046(4)	-0.0038(3)
P(1)	0.020(2)	0.025(2)	0.021(2)	0.007(2)	0.003(2)	-0.004(2)
P(2)	0.026(3)	0.019(2)	0.035(2)	-0.005(21)	0.016(2)	0.002(2)
P(3)	0.019(2)	0.026(2)	0.015(2)	-0.001(2)	0.001(2)	-0.003(1)
C(111)	0.07(1)	0.022(8)	0.024(8)	0.034(9)	0.014(9)	0.011(6)
C(112)	0.06(1)	0.034(9)	0.05(1)	0.04(1)	0.01(1)	0.001(8)
C(121)	0.05(1)	0.023(8)	0.034(10)	-0.021(8)	0.018(9)	-0.013(7)
C(122)	0.06(1)	0.020(8)	0.017(8)	-0.002(8)	0.006(9)	-0.011(6)
C(131)	0.03(1)	0.05(1)	0.029(9)	0.001(9)	0.018(8)	-0.012(7)
C(211)	0.06(1)	0.04(1)	0.04(1)	-0.01(1)	0.04(1)	0.011(8)
C(212)	0.04(1)	0.06(1)	0.07(1)	-0.03(1)	0.02(2)	-0.01(1)
C(221)	0.021(9)	0.022(8)	0.042(10)	0.005(7)	0.004(8)	0.003(7)
C(222)	0.020(9)	0.018(8)	0.06(1)	-0.009(8)	-0.004(9)	-0.008(8)
C(231)	0.04(1)	0.021(8)	0.038(10)	-0.008(8)	-0.003(9)	0.027
C(232)	0.03(1)	0.019(8)	0.05(1)	0.001(8)	0.004(9)	-0.003(7)
C(311)	0.020(9)	0.05(1)	0.038(10)	-0.008(9)	0.000(8)	0.003(8)
C(312)	0.03(1)	0.04(1)	0.04(1)	-0.021(9)	-0.003(9)	-0.019(8)
C(321)	0.03(1)	0.047(10)	0.007(7)	-0.001(9)	0.007(7)	-0.005(6)
C(322)	0.06(1)	0.05(1)	0.028(9)	0.02(1)	0.012(10)	0.000(8)
C(331)	0.04(1)	0.029(8)	0.027(9)	0.016(8)	0.009(8)	0.004(7)
C(332)	0.06(1)	0.038(10)	0.028(9)	0.004(10)	0.012(10)	0.008(7)

[a]The coefficients U_{ij} of the anisotropic thermal parameter expression are defined as:

$\exp[-2\pi^2(a^{*2}U_{11}h^2+b^{*2}U_{22}k^2+c^{*2}U_{33}l^2+2a^*b^*U_{12}hk+2a^*c^*U_{13}hl+2b^*c^*U_{23}kl)]$

reflections were monitored every 200 reflections and showed no intensity variation over the collection period. A total of 9508 reflections were collected, of which 9101 were unique (R_{int} = 0.055) and 4575 were observed with $I>4\sigma(I)$. The linear absorption coefficient, μ, for Mo $K\alpha$ radiation is 116.99 cm^{-1}. First, an empirical absorption correction using the φ scan technique was applied after the structure solution. After all of the atoms were located and refined isotropically, an absorption correction using the DIFABS program[18] was applied and resulted in the relative transmission factors ranging from 0.73 to 1.47. The data were corrected for Lorentz and polarization effects. And a correction for secondary extinction was applied (coefficient = 1.17×10^{-6}).

The triclinic space group $P\bar{1}$ was chosen on the basis of intensity statistics. Initial tungsten atom positions were input on the basis of the SHELXS direct methods[16] output. Subsequently, the non-hydrogen atomic positions were located directly from the electron density difference maps. All non- hydrogen atoms were refined with anisotropic thermal parameters. Idealized hydrogen positions were calculated and placed in the refinement, but their parameters were held constant during subsequent cycles. The final cycle of full-matrix least-squares refinement was based on 4575 observed reflections and 407 variable parameters and converged with unweighted and weighted agreement factors of: R = 0.034 and R_w = 0.030, respectively. The asymmetric unit was found to be $[Na(py)_3][W_3Te_4(py)_3]\cdot 0.5py$. The atomic coordinates and equivalent isotropic thermal parameters of the non-hydrogen atoms are given in Table 6, and the anisotropical thermal parameters of non-hydrogen atoms are shown in

Table 6. Atomic Coordinates and Equivalent Isotropic Thermal Parameters ($Å^2$) of the Non-Hydrogen Atoms for $[Na(py)_6][W_6Te_8(py)_6]\cdot 1py$

atom	x	y	z	B_{eq}[a]
W(1)	-0.07249(5)	-0.00407(5)	-0.14753(5)	1.27(1)
W(2)	0.13300(5)	0.08081(5)	-0.02662(5)	1.19(1)
W(3)	0.05182(5)	-0.13149(5)	-0.03839(5)	1.17(1)
Te(1)	0.01114(8)	0.20940(8)	-0.13843(8)	1.57(2)
Te(2)	0.26042(8)	-0.04729(8)	0.08069(8)	1.78(2)
Te(3)	0.11437(8)	-0.05629(9)	-0.21554(8)	1.85(2)
Te(4)	0.15327(8)	0.21867(8)	0.16201(8)	1.85(2)
Na(1)	0.5000	0.5000	0.5000	2.7(2)
N(1)	-0.1627(10)	-0.0075(10)	-0.3208(9)	2.2(3)
N(2)	0.2929(9)	0.181(1)	-0.0539(10)	2.2(3)
N(3)	0.1130(9)	-0.2887(9)	-0.0816(9)	1.7(3)
N(10)	0.665(1)	0.620(1)	0.462(1)	4.6(4)
N(20)	0.619(1)	0.415(1)	0.646(1)	4.2(4)
N(30)	0.456(1)	0.642(1)	0.635(1)	3.6(4)
C(11)	-0.267(1)	-0.051(1)	-0.353(1)	3.8(4)
C(12)	-0.327(2)	-0.053(2)	-0.458(1)	6.1(6)
C(13)	-0.276(2)	0.000(2)	-0.527(1)	5.9(6)
C(14)	-0.168(2)	0.044(2)	-0.494(1)	5.5(6)
C(15)	-0.115(1)	0.042(1)	-0.390(1)	3.2(4)
C(21)	0.374(1)	0.140(1)	-0.088(1)	2.7(4)
C(22)	0.471(1)	0.195(2)	-0.104(2)	4.7(6)
C(23)	0.487(1)	0.306(2)	-0.081(2)	4.6(5)
C(24)	0.408(1)	0.355(1)	-0.047(1)	3.4(4)
C(25)	0.313(1)	0.287(1)	-0.034(1)	2.7(4)
C(31)	0.051(1)	-0.386(1)	-0.085(1)	2.5(4)
C(32)	0.081(2)	-0.481(1)	-0.116(2)	4.0(5)
C(33)	0.181(2)	-0.483(1)	-0.137(1)	3.7(5)
C(34)	0.249(2)	-0.387(1)	-0.133(1)	3.6(5)
C(35)	0.210(1)	-0.293(1)	-0.109(1)	2.4(4)
C(101)	0.687(2)	0.470(2)	0.731(2)	5.4(6)
C(102)	0.743(2)	0.422(2)	0.806(2)	7.6(8)

C(103)	0.739(2)	0.317(2)	0.796(2)	5.7(7)
C(104)	0.673(3)	0.254(2)	0.703(2)	7.7(9)
C(105)	0.610(2)	0.310(2)	0.636(1)	5.0(6)
C(201)	0.749(2)	0.672(2)	0.535(2)	4.9(6)
C(202)	0.835(2)	0.742(2)	0.515(2)	6.0(6)
C(203)	0.835(2)	0.761(2)	0.414(2)	6.7(7)
C(204)	0.746(2)	0.709(2)	0.333(2)	5.7(7)
C(205)	0.666(2)	0.643(2)	0.362(2)	5.0(6)
C(301)	0.524(1)	0.708(2)	0.714(2)	4.8(6)
C(302)	0.504(2)	0.796(2)	0.767(2)	5.6(6)
C(303)	0.404(2)	0.824(2)	0.747(2)	5.2(6)
C(304)	0.328(2)	0.756(2)	0.671(2)	6.1(7)
C(305)	0.355(1)	0.667(2)	0.616(1)	3.8(5)
C(400)	-0.038(3)	0.462(4)	0.583(3)	11.7(9)
N(400)[b]	-0.038(3)	0.462(4)	0.583(3)	11.7(9)
C(401)[b]	-0.058(3)	0.377(3)	0.487(4)	13(1)
N(401)[b]	-0.058(3)	0.377(3)	0.487(4)	13(1)
C(402)[b]	0.015(3)	0.563(3)	0.592(3)	11.9(9)
N(402)[b]	0.015(3)	0.563(3)	0.592(3)	11.9(9)

[a]$B_{eq} = (8/3)\pi^2[U_{11}(aa^*)^2 + U_{22}(bb^*)^2 + U_{33}(cc^*)^2 + 2U_{12}aa^*bb^*\cos\gamma + 2U_{13}aa^*cc^*\cos\beta + 2U_{23}bb^*cc^*\cos\alpha]$. [b]Disordered positions.

Table 7.

Molecular Orbital Calculations

The molecular orbitals were calculated by the Extended Hückel method.[19] The H_{ij} parameters and orbital exponents for, sulfur, selenium, and tellurium were taken from the literature[20], and the parameters for W, N and H were accepted values[21]. The hypothetical complexes, $W_6Y_8(NH_3)_6$, (Y=S, Se, Te) were used as models for the EHMO calculations. Distances found from the X-ray crystal structure determinations of the $W_6Y_8(pip)_6$ complexes were averaged and used to generate the geometries of the core ($W_6Y_8N_6$) of this model complex with a O_h symmetry. The actual bond distances used in the MO calculations are listed in Table 8. The idealized hydrogen positions were calculated based on the tetrahedral symmetry around nitrogen atoms with N-H bond distance of 0.96 Å. The parameters used for the extended Hückel calculations are listed in Table 9.

Table 7. Anisotropic Thermal Parameters[a] ($Å^2$) of the Non-Hydrogen Atoms for $[Na(py)_6][W_6Te_8(py)_6]\cdot 1py$

atom	U_{11}	U_{22}	U_{33}	U_{12}	U_{13}	U_{23}
W(1)	0.0181(3)	0.0166(4)	0.0132(3)	0.0027(3)	0.0022(2)	0.0025(3)
W(2)	0.0142(3)	0.0144(3)	0.0175(3)	0.0024(2)	0.0048(2)	0.0032(3)
W(3)	0.0157(3)	0.0139(3)	0.0155(3)	0.0032(3)	0.0045(2)	0.0017(3)
Te(1)	0.0209(5)	0.0182(5)	0.0228(5)	0.0037(4)	0.0064(4)	0.0079(4)
Te(2)	0.0164(5)	0.0229(5)	0.0286(5)	0.0062(4)	0.0015(4)	0.0054(4)
Te(3)	0.0283(5)	0.0263(6)	0.0194(5)	0.0077(4)	0.0124(4)	0.0032(4)
Te(4)	0.0237(5)	0.0194(5)	0.0230(5)	-0.0003(4)	-0.0001(4)	-0.0022(3)
Na	0.038(5)	0.037(6)	0.028(5)	0.005(4)	0.009(4)	0.000(4)
N(1)	0.035(8)	0.028(8)	0.015(7)	0.006(6)	-0.008(6)	0.003(6)
N(2)	0.019(7)	0.028(8)	0.033(8)	0.002(6)	-0.001(6)	0.001(6)
N(3)	0.021(7)	0.018(7)	0.026(7)	0.005(5)	0.002(5)	0.002(6)
N(10)	0.05(1)	0.06(1)	0.05(1)	-0.028(8)	0.008(8)	0.010(9)
N(20)	0.06(1)	0.04(1)	0.05(1)	0.002(9)	0.000(9)	0.008(9)
N(30)	0.024(8)	0.05(1)	0.05(1)	0.007(7)	-0.001(7)	-0.022(8)
C(11)	0.05(1)	0.05(1)	0.03(1)	0.003(9)	-0.022(9)	-0.002(9)
C(12)	0.10(2)	0.06(2)	0.04(1)	0.02(1)	-0.05(1)	0.01(1)
C(13)	0.13(2)	0.06(2)	0.017(10)	0.00(1)	-0.02(1)	0.00(1)
C(14)	0.11(2)	0.07(2)	0.03(1)	0.01(1)	0.01(1)	0.01(1)
C(15)	0.05(1)	0.05(1)	0.014(8)	0.003(9)	0.009(8)	0.006(8)
C(21)	0.020(8)	0.025(9)	0.06(1)	-0.003(7)	0.006(8)	0.009(9)
C(22)	0.024(10)	0.08(2)	0.10(2)	0.02(1)	0.03(1)	0.05(1)
C(23)	0.014(9)	0.06(1)	0.10(2)	-0.009(9)	0.028(10)	0.03(1)
C(24)	0.04(1)	0.04(1)	0.05(1)	-0.012(8)	0.009(9)	0.014(10)
C(25)	0.033(10)	0.04(1)	0.037(10)	0.008(8)	0.019(8)	0.006(8)
C(31)	0.030(9)	0.04(1)	0.022(8)	0.002(8)	0.004(7)	-0.004(8)

C(32)	0.07(1)	0.03(1)	0.06(1)	0.01(1)	0.02(1)	0.006(10)
C(33)	0.07(1)	0.02(1)	0.05(1)	0.02(1)	0.01(1)	0.001(9)
C(34)	0.06(1)	0.04(1)	0.04(1)	0.03(1)	0.009(9)	-0.006(9)
C(35)	0.041(10)	0.022(9)	0.029(9)	0.005(7)	0.016(7)	0.001(7)
C(101)	0.05(1)	0.06(2)	0.09(2)	0.00(1)	-0.01(1)	0.04(1)
C(102)	0.05(1)	0.12(2)	0.11(2)	-0.01(2)	-0.01(1)	0.08(2)
C(103)	0.04(1)	0.11(2)	0.09(2)	0.02(1)	0.03(1)	0.06(2)
C(104)	0.21(3)	0.07(2)	0.06(2)	0.10(2)	0.09(2)	0.03(1)
C(105)	0.13(2)	0.03(1)	0.04(1)	0.02(1)	0.03(1)	-0.009(9)
C(201)	0.07(2)	0.05(1)	0.06(1)	-0.01(1)	0.01(1)	0.01(1)
C(202)	0.09(2)	0.05(1)	0.07(2)	-0.03(1)	0.01(1)	-0.01(1)
C(203)	0.08(2)	0.11(2)	0.05(1)	-0.005(1)	0.03(1)	0.00(1)
C(204)	0.11(2)	0.07(2)	0.04(1)	0.01(1)	0.05(1)	0.00(1)
C(205)	0.08(2)	0.07(2)	0.04(1)	-0.01(1)	0.01(1)	-0.01(1)
C(301)	0.03(1)	0.06(2)	0.08(2)	0.008(10)	-0.01(1)	-0.01(1)
C(302)	0.05(1)	0.07(2)	0.07(2)	-0.02(1)	0.02(1)	-0.05(1)
C(303)	0.07(2)	0.03(1)	0.09(2)	0.00(1)	0.04(1)	0.00(1)
C(304)	0.07(2)	0.09(2)	0.09(2)	0.05(2)	0.04(1)	0.01(2)
C(305)	0.04(1)	0.06(1)	0.04(1)	0.001(10)	0.004(9)	0.00(1)

[a]The coefficients U_{ij} of the anisotropic thermal parameter expression are defined as:
$\exp[-2\pi^2(a^{*2}U_{11}h^2+b^{*2}U_{22}k^2+c^{*2}U_{33}l^2+2a^*b^*U_{12}hk+2a^*c^*U_{13}hl+2b^*c^*U_{23}kl)]$

Table 8. Bond Distances in the Model Complexes for EHMO Calculations.

Formula	W-W (Å)	W-Y (Å)	W-N (Å)	N-H (Å)
$W_6S_8(NH_3)_6$	2.659	2.457	2.312	0.96
$W_6Se_8(NH_3)_6$	2.690	2.571	2.276	0.96
$W_6Te_8(NH_3)_6$	2.742	2.753	2.335	0.96

Table 9. Parameters Used in the Extended Hückel Calculations

orbital		H_{ii} (eV)	ξ_1	ξ_2	C_1	C_2
S	3s	-20.00	2.12			
	3p	-13.30	1.83			
Se	4s	-20.50	2.44			
	4p	-13.05	2.07			
Te	5s	-20.5	2.57			
	5p	-12.9	2.16			
W	6s	-8.26	2.34			
	6p	-5.17	2.31			
	5d	-10.37	4.98	2.070	0.6683	0.5422
N	2s	-26.00	1.95			
	2p	-13.40	1.95			
H	1s	-13.60	1.30			

Results and Discussion

Synthesis of $W_6Te_8(py)_6$

Substitution of sulfide for chloride in $M_6Cl_8^{4+}$ cluster units (M = Mo, W) has been extensively investigated earlier in this research group. Previous research showed that NaSH was a good sulfiding agent, as well as an oxidizing agent.[10] Xiang Zhang demonstrated the first completely sulfide-substituted hexatungsten cluster $W_6S_8L_6$ by reacting twelve moles of NaSH and six moles of $NaOBu^n$ per mole of $W_6Cl_8^{4+}$ in refluxing pyridine.[10] During sulfidation, the 24 e clusters ($M_6Cl_8^{4+}$) were oxidized to 20 e clusters (W_6S_8). Pyridine was used as the solvent since it possessed a sufficiently high boiling point to conveniently promote the reaction at reflux temperatures, and acted as good ligand for binding in the terminal positions of the W_6Y_8 cluster units, thus stabilizing the cluster complex.

However, in the telluride reactions, NaTeH was not available. Sodium telluride (Na_2Te) and sodium ditelluride (Na_2Te_2) together were chosen as the tellurium source, expecting that sodium ditelluride (Na_2Te_2) could also serve as the mild oxidizing agent, like NaSH in the sulfide system. The expected overall reaction is given by equation 1.

$$W_6Cl_{12} + 4\ Na_2Te + 4\ Na_2Te_2 \xrightarrow{\text{pyridine}} W_6Te_8(py)_6 + 12NaCl \qquad (1)$$

Therefore, the above stoichiometric reaction was conducted in refluxing pyridine. After the reaction, the faint color of the filtrate indicated that the products were all insoluble. Following a prolonged methanol extraction of the products to remove the NaCl by-product, a black amorphous material was obtained. From XPS, the derived

tungsten 4f BE (binding energies) confirmed that the material was the pure W_6Te_8 cluster compound. Furthermore, no sodium was detected by XPS. Based on XPS and IR studies, we believe that the $W_6Te_8(py)_6$ complex was obtained from this reaction in a yield of about 88%.

All attempts to grow single crystals of this compound were unsuccessful. Compared with its sulfide and selenide analogues, this $W_6Te_8(py)_6$ complex is much more insoluble in most organic solvents, and much more air and moisture sensitive. The material would burst into flames immediately after it was exposed to air.

Synthesis of $W_6Te_8(pip)_6$

The preparation of the piperidine complex, $W_6Te_8(pip)_6$, was similar to that of pyridine complex, except that the reaction was conducted in neat piperidine instead of pyridine. In contrast to the pyridine complex, the product obtained from this reaction was quite soluble. After the reaction mixture was refluxed for two days and upon filtration, a dark blue solution was obtained. Single crystals were grown from this solution. A black solid was recovered from the insoluble portion after being washed with MeOH for two days. Examination of this solid by XPS indicated that it contained at least three different kinds of tungsten, and it appeared that the cluster unit, WTe_2, and WO_3 were all present based on their W $4f_{7/2}$ binding energy (eV) values.

In comparison, this reaction was not as clean and quantitative as the reaction conducted in pyridine. However, this reaction did yield a soluble product, $W_6Te_8(pip)_6$.

Likewise, this complex is also very air and moisture sensitive.

Synthesis of $[Na(py)_6]^+[W_6Te_8(py)_6]^-$

Previous research on selenide substitutions in the $(W_6Cl_8)^{4+}$ cluster units (W_6Cl_{12}) showed that Na_2Se was a good selenium source.[12] Neutral molecular complexes, $W_6Se_8(py)_6$ and $W_6Se_8(pip)_6$, were obtained when eight moles of Na_2Se reacted with one mole of W_6Cl_{12} in refluxing pyridine and piperidine, respectively.

Thus, if eight moles of Na_2Te were reacted with one mole of W_6Cl_{12}, the neutral telluride cluster complexes, $W_6Te_8L_6$, would be expected to form. However, for the reactions conducted in pyridine, the material recovered from the filtrate was an ionic compound, $[Na(py)_6]^+[W_6Te_8(py)_6]^-$, based on single crystal X-ray diffraction, ESR, and XPS. Upon washing the insoluble residue of the reaction with MeOH for two days to remove NaCl, the neutral cluster compound, $W_6Te_8(py)_6$, was also recovered based on XPS and IR. In the case of the reaction in piperidine, single crystals of $W_6Te_8(pip)_6 \cdot 6pip$ were crystallized from the reaction filtrate, however, sodium was also detected in this filtrate by XPS.

It is evident that both the neutral, W_6Te_8, and the ionic cluster core, $W_6Te_8^-$, are formed in either piperidine or pyridine. Owing to the relatively high solubility of $W_6Te_8(pip)_6$ in piperidine, both the neutral and the ionic complexes are together in solution. However, only the neutral one crystallized. In the case of pyridine, the ionic compound, $[Na(py)_6]^+[W_6Te_8(py)_6]^-$, is soluble, while the neutral complex, $W_6Te_8(py)_6$,

remains in the insoluble residue because of its low solubility.

Mechanism of the Reactions

Ideally, if Na_2Y is used as the chalcogen source instead of NaYH, it would lead to the formation of $W_6Y_8^{4-}$ or $W_6Y_8L_6^{4-}$ as indicated by equation 2, since Na_2Y can't

$$W_6Cl_{12} + 8Na_2Y \xrightarrow{L} Na_4W_6Y_8L_6 + 12NaCl \qquad (2)$$

serve as an oxidizing agent. However, the material recovered from the filtrate contained the neutral cluster molecules, $W_6Y_8(pip)_6$ or $W_6Y_8(py)_6$ (Y=Se, Te), and the anionic cluster, $W_6Te_8L_6^-$, based on spectroscopic analyses (XPS and IR) and X-ray diffraction. What is the oxidizing agent in these reactions?

One possibility is that sodium polychalcogenides (Na_2Y_x, x>2) are present as an impurity in the reactant, Na_2Y, and thus oxidize the cluster units. However, the sodium chalcogenides (Na_2Y) were prepared by reacting the chalcogen element with a slight excess of sodium metal to prevent the formation of the polychalcogenides. The XRD patterns of these lab prepared sodium chalcogenides (Na_2Y ,Y=Se, Te) match the patterns of the corresponding pure compounds. Therefore, this possibility can be ruled out.

Another possibility is that the 24-electron $(W_6Y_8)^{4-}$ unit undergoes disproportionation to form elemental tungsten and the 20-electron neutral cluster, $W_6Y_8L_6$, as indicated in equation 3. Therefore, two out of the eight moles of Na_2Y are redundant. In order to explore this possibility, reactions with different Na_2Te/W_6Cl_{12}

$$Na_4W_6Y_8L_6 \longrightarrow (3/4)W_6Y_8L_6 + (6/4)W + 2Na_2Y \qquad (3)$$

mole ratios (Na_2Te/W_6Cl_{12} = 6, 8, 10, 12) were examined in refluxing pyridine. For the larger mole ratio (Na_2Te/W_6Cl_{12} = 8, 10, 12) reactions, about 40-50% of tungsten was converted to a soluble product, $W_6Te_8L_6^-$. The insoluble product was the neutral complex, $W_6Te_8(py)_6$. For the 1:6 (W_6Cl_{12}:Na_2Te) reactions, a relatively small amount of materials (only 5-15% of W) were soluble, while the major product was the insoluble $W_6Te_8(py)_6$, and no mixed chloride-telluride cluster complexes were detected. Different reaction times (1 day, 3 days, 6 days) were also tested for this 1:6 reaction system and it was observed that the longer the reaction time, the less amount of material was recovered from the reaction filtrates.

Although an understanding of the mechanism of this process is not completely clear at this stage, we think that the following steps (illustrated in equations 4-8) are probably involved based upon the experimental observations. The overall reaction is illustrated

$$W_6Cl_{12} + 8Na_2Te \xrightarrow{L} Na_4W_6Te_8L_x + 12NaCl \qquad (4)$$

$$13Na_4W_6Te_8 \xrightarrow{L} 12Na_3W_6Te_8L_x + 6W + 8Na_2Te \qquad (5)$$

$$14Na_3W_6Te_8L_x \xrightarrow{L} 13Na_2W_6Te_8L_x + 6W + 8Na_2Te \qquad (6)$$

$$15Na_2W_6Te_8L_x \xrightarrow{L} 14NaW_6Te_8L_6 + 6W + 8Na_2Te \qquad (7)$$

$$16NaW_6Te_8L_6 \xrightarrow{L} 15W_6Te_8L_6 + 6W + 8Na_2Te \qquad (8)$$

in equation 9. It is conceivable that the $(W_6Te_8L_6)^{4-}$ cluster units were formed as the

$$W_6Cl_{12} + 6Na_2Te \xrightarrow{L} (3/4)W_6Te_8L_6 + (6/4)W + 12NaCl \qquad (9)$$

direct product at an early stage of the substitution reaction. However, in refluxing pyridine, this $(W_6Te_8L_6)^{4-}$ unit may not be thermodynamically or kinetically stable, where

it undergoes disproportionation to give tungsten metal, Na_2Te, and a trianion salt, $(W_6Te_8L_6)^{3-}$. Further disproportionations can occur consecutively to give the dianion, monoanion, and neutral cluster complexes. The fact that the different oxidized cluster units, W_6Te_8 (20e) or $W_6Te_8^-$ (21e), were isolated in these reactions provide the evidence for this mechanism. However, only the neutral and the monoanion cluster complexes have been identified. The dianion, trianion, and even the tetra-anion cluster complexes may form and remain in the reaction mixture, but have not been identified. More likely these anions are kinetically unstable with respect to the subsequent disproportionation reactions. The last step, as shown in equation 9, probably is kinetically slow, thus the sodium salt of the monoanion cluster complex, $NaW_6Te_8(py)_6$, was obtained as a kinetically trapped product. The overall reaction suggests that only six moles of Na_2Te is sufficient for complete substitution, and the maximum yield is 75%.

For the selenide reaction systems, the same mechanism may also be applied. However, no evidence has indicated that the cluster units other than neutral complexes, $W_6Se_8L_6$, were formed. The large difference in solubility between the selenide complexes and their telluride analogues, may result in this kinetic difference. Therefore, the reduced cluster units, such as $W_6Se_8^-$ (21 e) cluster, are no longer kinetically stable and only the neutral complexes, $W_6Se_8L_6$, were obtained.

Ligand-Exchange Reactions

The complex $W_6Te_8(pip)_6$ can be readily dissolved in neat pyridine to initially form a red solution. After sitting at room temperature for one day, the solution turned light brown, and a dark brown solid precipitated out. Apparently, the substitution of pyridine for piperidine was achieved, as illustrated in equation 10. And the relatively insoluble

$$W_6Te_8(pip)_6 \xrightarrow{\text{pyridine}} W_6Te_8(py)_6 + 6pip \qquad (10)$$

complex, $W_6Te_8(py)_6$ was formed. When $W_6Te_8(py)_6$ was refluxed with excess triethylphosphine in toluene, most of the materials dissolved to formed a grape-purple solution within several hours. Single crystals of $W_6Te_8(PEt_3)_6$ were obtained from the solution. Apparently, complete substitution of triethylphosphine for pyridine was achieved, as illustrated in equation 11.

$$W_6Te_8(py)_6 + xs\ PEt_3 \xrightarrow{\text{Toluene}} W_6Te_8(PEt_3)_6 + 6py \qquad (11)$$

These results illustrated that the bonding between the hexatungsten cluster core and the organic donor ligands appear to have following order: PEt_3 > py> pip. An identical conclusion was reached in the study of the ligand exchange reactions between pyridine, piperidine, and triethylphosphine in the sulfide and selenide clusters,$M_6Y_8L_6$ (M = Mo or W, Y = S, Se)[5,10b,12].

X-ray Photoelectron Spectroscopy

As previous research has shown[10c,12], W 4f X-ray photoelectron spectra provided the most useful spectroscopic data. Like their sulfide and selenide analogues, the

telluride complexes, $W_6Te_8(pip)_6$ and $W_6Te_8(py)_6^-$, show the same tungsten binding energies at 30.8 eV (W $4f_{7/2}$) and 32.9 eV (W $4f_{5/2}$). These binding energy values are characteristic values for the tungsten chalcogenide cluster unit, W_6Y_8. For comparison, the W $4f_{7/2}$ BE for WTe_2 and WO_3 are 32.3 eV and 35.4 eV, respectively. Therefore, if WTe_2, or WO_3 occur as impurities in the product, distinct evidence for these would be found in the resolved W 4f binding energy values. The W 4f XP spectrum of $W_6Te_8(pip)_6$ could be accounted for nicely by only one major type of tungsten, and no WTe_2 was detected. Since the telluride compounds are very air sensitive, in most cases the presence of surface oxide contamination was evident. Thus, XPS is a useful technique to identify the cluster and detect any impurities in the products. However, the XPS was not able to clearly distinguish between tungsten metal and the cluster units, since the W $4f_{7/2}$ binding energy for tungsten metal[22] is nearly the same as that for cluster complexes, 31.4 and 30.8 eV, respectively. The XPS binding energies for cluster units, W_6Y_8, and related compounds are tabulated in Table 10.

Infrared Spectra

Infrared spectroscopy has proven to be a powerful tool for the characterization of the W_6Te_8 cluster complexes. Characteristic bands for the coordinated organic ligands could be identified in the mid-IR region, and a characteristic band for W-Te, could be observed in Far-IR region. The mid-IR and far-IR spectra of the $W_6Te_8(pip)_6$ complex are shown in Figure 1 and Figure 2, respectively.

Table 10. XPS Binding Energies (eV) for the W_6Y_8 Cluster Complexes and Related Compounds[a]

Compound	W $4f_{7/2}$ (eV)	W $4f_{5/2}$ (eV)	S $2p_{3/2}$ (eV)	Se $3d_{5/2}$ (eV)	Te $3d_{5/2}$ (eV)
$W_6S_8(py)_6$	30.5	32.6	160.6	–	–
$W_6Se_8(py)_6$	30.8	32.9	–	53.6	–
$W_6Te_8(py)_6$	30.8	32.9	–	–	571.9
$W_6S_8(pip)_6$	30.5	32.6	160.6	–	–
$W_6Se_8(pip)_6$	30.8	32.9	–	53.7	–
$W_6Te_8(pip)_6$	30.8	32.9	–	–	571.9
WS_2	32.7	34.8	162.4	–	–
WSe_2	32.3	34.4	–	54.6	–
W_6Cl_{12}	32.4	34.5	–	–	–
W metal	31.4	33.5	–	–	–

[a]Data has been corrected to the C 1s binding energy of 284.6 eV.

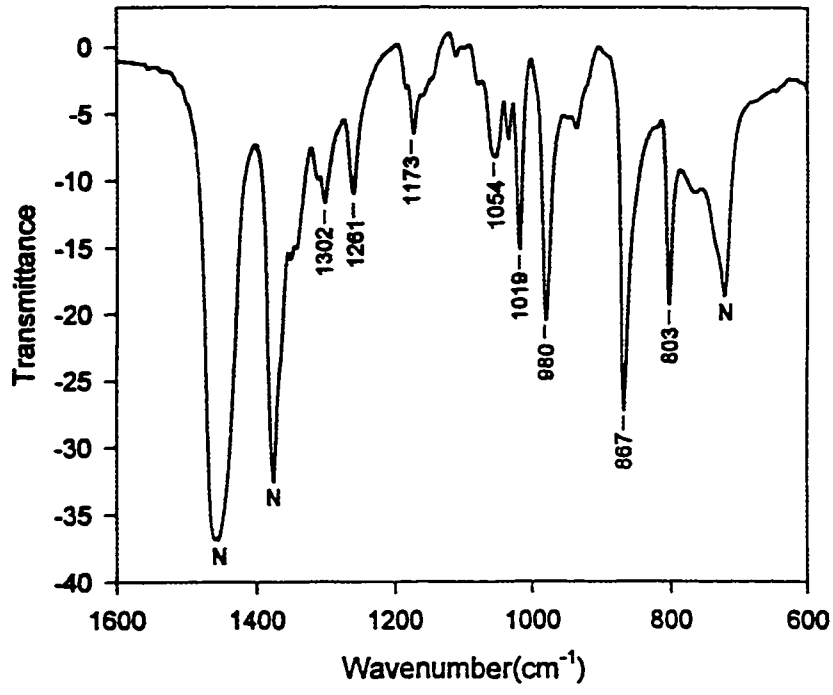

Figure 1. Mid-infrared spectrum of $W_6Te_8(pip)_6$.
The bands labeled as "N" are due to Nujol.

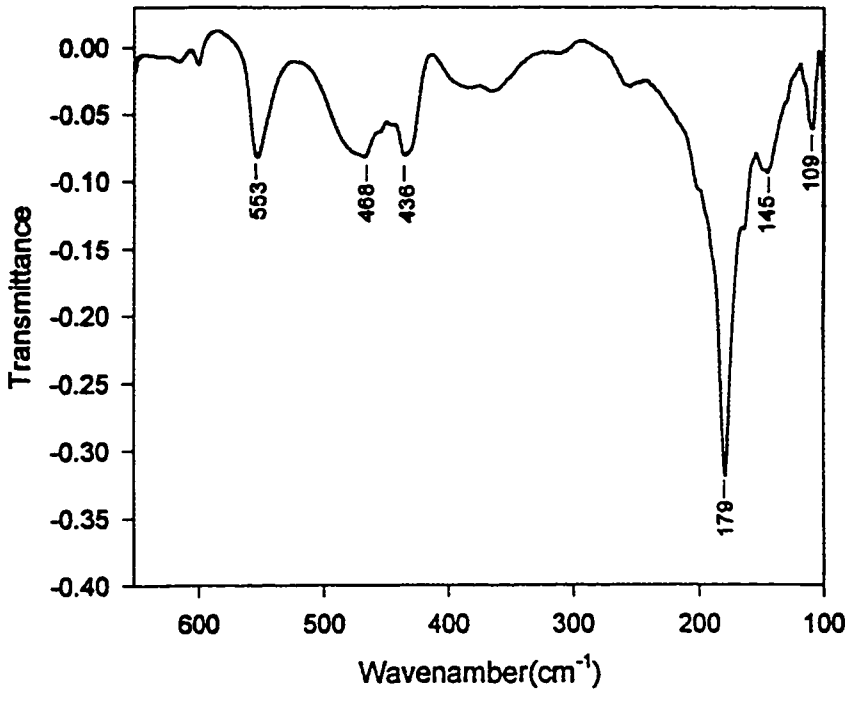

Figure 2. Far-infrared spectrum of $W_6Te_8(pip)_6$

Previous studies have resulted in the identification and assignment of these IR bands in the mid-IR region (600-3500 cm^{-1}).[10,12] In the far-IR region, one strong band at about 180 cm^{-1} can be assigned as arising from the IR-allowed T_{1u} W-Te stretching modes. The tungsten sulfide and selenide analogues, $W_6S_8(pip)_6$ and $W_6Se_8(pip)_6$, exhibit similar W-S, W-Se T_{1u} stretching bands at 376 cm^{-1}, and 243 cm^{-1}, respectively. The reduction from 376 to 240 to 180 cm^{-1} is about the change expected based upon reduced masses.

Electronic Spectra

The piperidine cluster complexes, $W_6Y_8(pip)_6$ (Y = S, Se, Te), were dissolved in neat piperidine. The sulfide cluster, $W_6S_8(pip)_6$, gave a brown yellow solution, while the selenide and telluride complexes gave purple and dark blue solutions, respectively. The solutions were transferred into sample cells equipped with stopcock by syringing. The UV-VIS data are summarized in Table 11. It is clearly evident that the absorption peak shifts to higher wavelengths when changing from sulfide to selenide to telluride.

Table 11. UV-VIS Data for $W_6Y_8(pip)_6$ Complexes (Y = S, Se, Te) in Piperidine

Complexes	$W_6S_8(pip)_6$	$W_6Se_8(pip)_6$	$W_6Te_8(pip)_6$
peak (nm)	330, 390	489	566

The assignment of these absorption bands is not completely clear. However, Saito's *DV-Xα* MO calculations on $Mo_6Y_8(PH_3)_6$ (Y = S, Se)[23] indicated that those absorptions around 400 - 500 nm might arose from ligand to metal charge transfer. According to their calculations, the absorption observed around 490 nm for the $Mo_6S_8(PEt_3)_6$ complex was assigned to a ligand-based, low energy t_{1u} to metal-based e_g (LUMO) transition. Therefore, these absorptions in tungsten chalcogenide cluster complexes can also be attributed to a similar ligand to metal charge transfer. Further EHMO calculations on $W_6Y_8(NH_3)_6$ (Y = S, Se, Te) complexes also indicated that these absorptions arose from ligand to metal charge transfer (see below).

ESR Studies

After drying overnight *in vacuo* at room temperature, the pyridine molecules associated with the sodium ion in the complex $[Na(py)_6]\,[W_6Te_8(py)_6]\cdot 1py$ were lost. The recovered black powder has a formula close to $NaW_6Te_8(py)_x$ (x = 6 - 7), based on the elemental analysis. The ESR spectrum of this powdered sample at 110K is shown in Figure 3. The very broad ESR signal indicated that the sample had an unpaired electron. Because of the low solubility of this material in organic solvents, a frozen glass spectrum was not obtained.

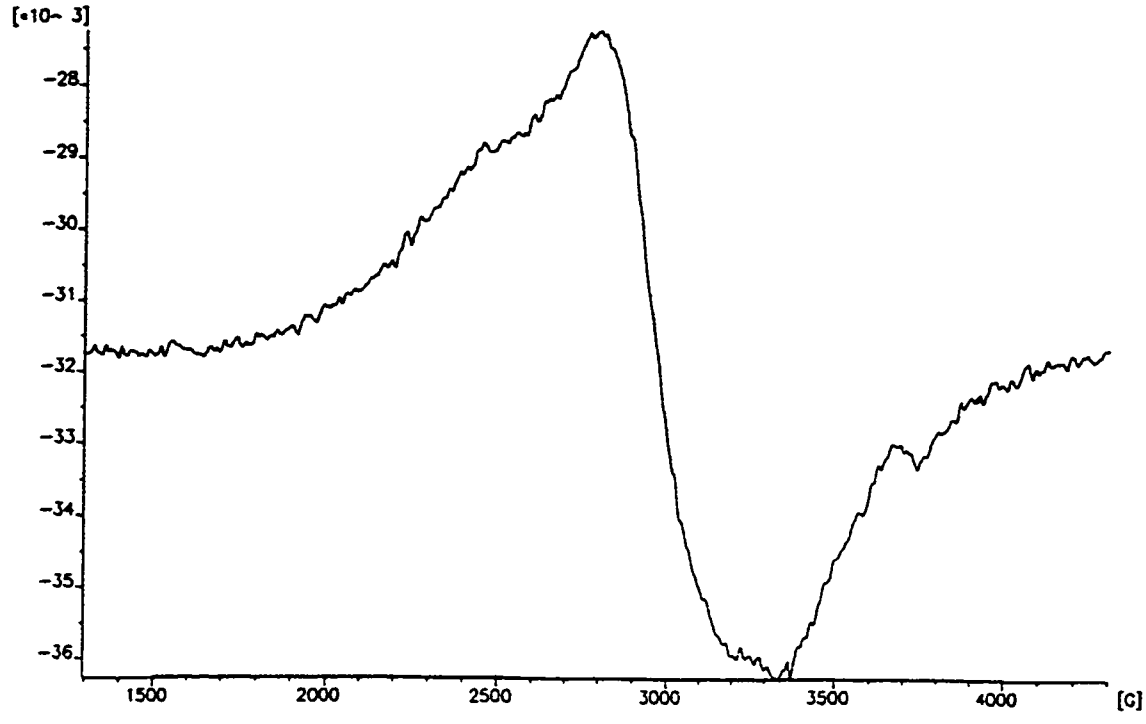

Figure 3. ESR spectrum of $NaW_6Te_8(py)_x$ at 110K.

Magnetic Properties

Single crystals of $[Na(py)_6]^+[W_6Te_8(py)_6]^-\cdot 1py$ were obtained from the filtrate of the 1:8 (W_6Cl_{12}:Na_2Te) reaction in pyridine. Therefore, the black powder recovered after drying the filtrate *in vacuo* overnight presumably is paramagnetic, and has a formula of $NaW_6Te_8(py)_6$. The magnetic susceptibility of this material was collected over the range 6-297K at 5K intervals in a field of 3 tesla. The data were corrected for diamagnetic core contributions (-1.08×10^{-3} emu/mol), based on the formula of $NaW_6Te_8(py)_6$, using values for the individual ions reported by Selwood.[24] The molar susceptibility and the

reciprocal molar susceptibility for this material are shown in Figure 4. The data can be fit by the Curie-Weiss relationship, $\chi = C/(T+\theta) + \chi_{TIP}$, from 6 to 297 K. A linear regression fitting of the observed data yielded $\chi_{TIP} = 5.70 \times 10^{-4}$ emu/mol, $C = 0.028$ emu·K/mol, and $\theta = -4.33$K. The effective magnetic moment calculated from the Weiss constant C is 0.48 μ_B, which is too low for the possibility of one unpaired electron per cluster unit (1.73 μ_B) expected from the formal electron count. Thus, the bulk material is basically diamagnetic.

This inconsistency between the magnetic data and crystal structure could result from several possibilities. First, it was assumed that all the pyridine molecules associated with the sodium cation were lost after the material was evacuated overnight. Therefore, the material was treated as having a formula of $NaW_6Te_8(py)_6$. However, it is possible that the cluster units, $(W_6Te_8)^-$, decompose during the evacuation. Secondly, this material is extremely air sensitive, which means cluster decomposition could take place during the process of preparing the sample for the magnetic measurement. Also, the bulk materials recovered from the filtrate might not be the reduced ionic cluster, $[W_6Te_8(py)_6]^-$, even though single crystals of $[Na(py)_6][W_6Te_8(py)_6]$ were obtained from the filtrate. The disproportionation reaction, as shown in equation 8, may take place slowly and therefore destroy the magnetic centers of the sample. Thus, the observed paramagnetic tail most likely arises from either an impurity or only a small amount of reduced ionic cluster unit, $(W_6Te_8)^-$.

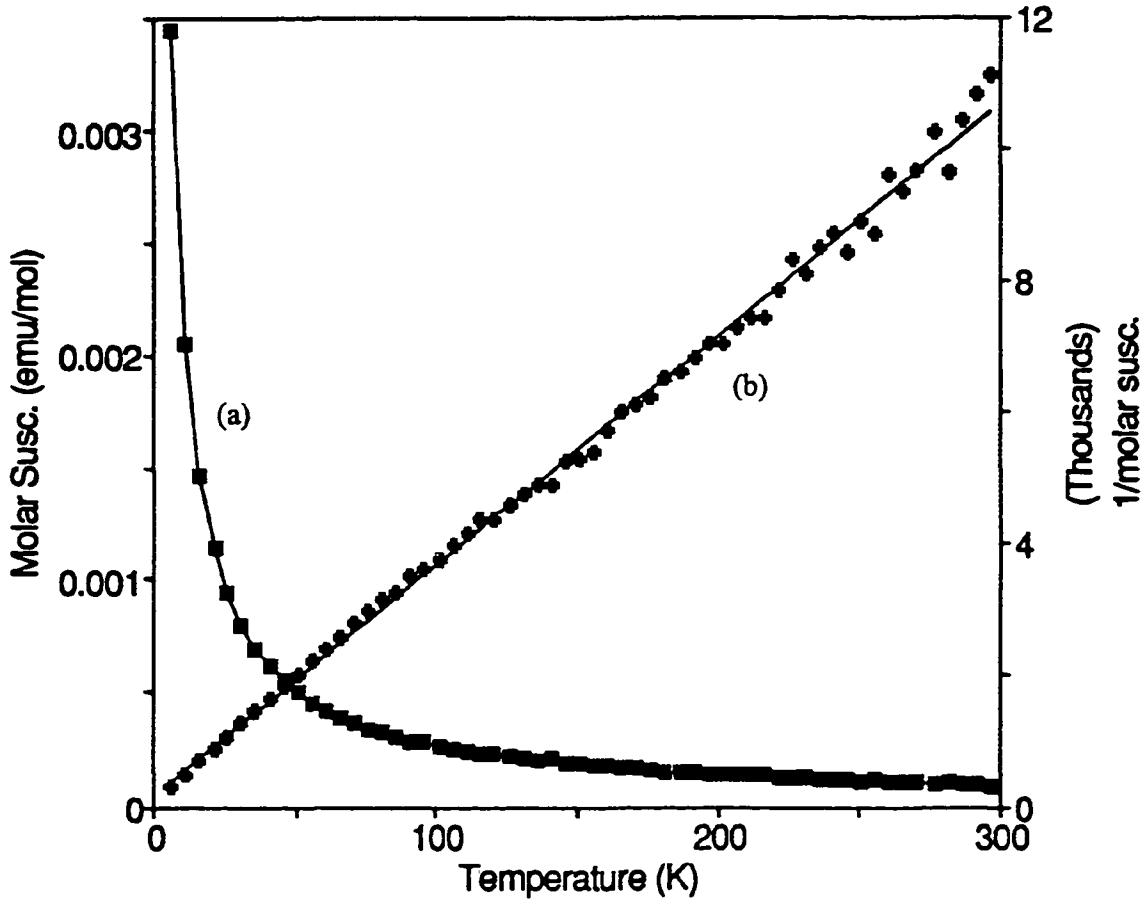

Figure 4. (a) Molar susceptibility versus temperature of $Na[W_6Te_8(py)_6]$
(b) Reciprocal Molar susceptibility versus temperature of $Na[W_6Te_8(py)_6]$. The points are experimental data points, and the straight line is the linear regression fitting.

Crystal Structures

Both of the neutral molecular complexes reported here contain the hexatungsten cluster unit $W_6Te_8L_6$. This cluster unit can be viewed as an octahedron of tungsten atoms with eight triply-bridging tellurium atoms capping the octahedral faces. Each tungsten also possesses an additional terminal coordination site located at the vertex positions of the octahedron, which are occupied by the organic donor ligands.

The $W_6Te_8(pip)_6 \cdot 6pip$ crystallizes in the trigonal space group $R\bar{3}$ with 3 molecules per unit cell. The W_6Te_8 cluster unit is centered on a $\bar{3}$ position (3a site symmetry). It is isomorphous with the $W_6Se_8(py)_6 \cdot 6py$ complex. An Ortep drawing of the cluster is shown in Figure 5. The piperidine ligand in the chair conformation coordinates to the tungsten atom such that the W-N bond occupies the equatorial position on the N atom. Selected bond distances and bond angles are listed in Table 12.

In comparison with the sulfide and selenide analogues, $W_6S_8(pip)_6$[10c] and $W_6Se_8(pip)_6$[12], the average W-W bond distance of 2.742(2) Å in the telluride cluster is much longer than that of 2.689 Å for $W_6Se_8(pip)_6$ and 2.659 Å for $W_6S_8(pip)_6$. The average W-Te distance of 2.753(2) Å is also much longer than the average W-S distance of 2.461(3) Å in $W_6S_8(pip)_6$ and average W-Se distance of 2.569(3) in $W_6Se_8(pip)_6$. The average W-N distance of 2.34(2) Å in these telluride clusters is close to the values found for the sulfide and selenide clusters. A summary of the average bond distances and bond angles in these $W_6Y_8(pip)_6$ (Y = S, Se, Te) complexes is given in Table 13. Besides the changes in W-W and W-Y bond distances, two other notable differences among these chalcogenide cluster units are the average W-Y-W and trans

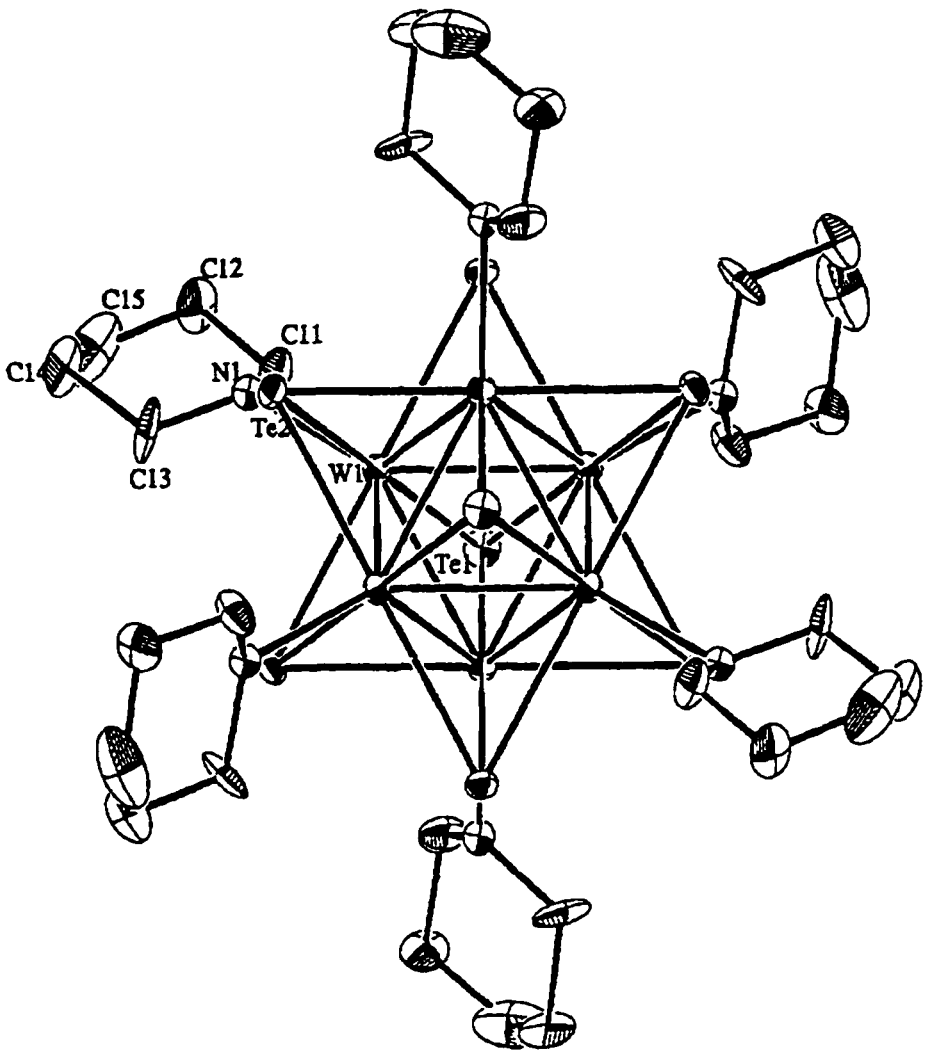

Figure 5. Molecular structure of $W_6Te_8(pip)_6$. Thermal ellipsoids are shown at 35% probability level. Hydrogen atoms have been omitted for clarity.

Table 12. Selected Bond Lengths (Å) and Angles (deg) in $W_6Te_8(pip)_6 \cdot 6pip$[a]

W(1)-W(1B)	2.744(2)	W(1)-Te(1)	2.740(2)
W(1)-W(1C)	2.740(2)	W(1)-Te(2)	2.770(2)
av. W-W	2.742(2)	W(1)-Te(2C)	2.750(2)
		W(1)-Te(2D)	2.752(2)
W(1)-N(1)	2.34(2)	av. W-Te	2.753(2)
C(11)-C(12)	1.52(3)		
C(12)-C(15)	1.47(4)	N(1)-C(11)	1.52(3)
C(13)-C(14)	1.51(3)	N(1)-C(13)	1.40(3)
C(14)-C(15)	1.51(4)		
W(1C)-W(1A)-W(1D)	60.00(3)	W(1)-W(ID)-W(IA)	90.00(4)
W(1)-W(1B)-W(1C)	59.96(4)	W(1B)-W(1)-W(1D)	90.00(4)
W(1C)-W(1)-W(1D)	60.09(4)		
av. W-W-W	60.02(4)	Te(1)-W(1)-Te(2C)	89.55(4)
		Te(1)-W(1)-Te(2D)	89.51(3)
W(1)-Te(1)-W(1B)	60.11(5)	Te(2C)-W(1)-Te(2)	90.50(5)
W(1)-Te(2)-W(1C)	59.51(4)	Te(2D)-W(1)-Te(2)	90.45(5)
W(1)-Te(2)-W(1D)	59.54(4)	av. Te-W-Te	90.00(4)
W(1)-Te(2C)-W(1B)	59.84(4)		
av. W-Te-W	59.75(4)	Te(2)-W(1)-N(1)	86.9(4)
		Te(2C)-W(1)-N(1)	90.5(4)
Te(1)-W(1)-Te(2)	180.25(5)	Te(2D)-W(1)-N(1)	88.7(4)
Te(2D)-W(1)-Te(2C)	181.28(5)	Te(1)-W(1)-N(1)	93.3(4)
av. Te-W-Te	180.76(5)	av. Te-W-N	89.9(4)

[a]Equivalent atoms generated by symmetry transformation:
A, -x,-y,-z; B, -x+y,-x,z; C, y,-x+y,-z; D, x-y,x,-z

Table 13. Summary of Selected Average Bond Distances (Å) and Bond Angles (deg) for the $W_6Y_8L_6$ (Y = S, Se, Te) Cluster Complexes

formula	W-W	W-X	W-L	X-W-X	W-X-W
$W_6S_8(pip)_6$	2.659(1)	2.461(4)	2.31(5)	173.0(2)	65.56(2)
$W_6Se_8(pip)_6$	2.689(2)	2.569(3)	2.27(3)	175.9(1)	63.13(8)
$W_6Te_8(pip)_6$	2.742(2)	2.753(2)	2.34(2)	180.76(5)	59.75(4)
$W_6Te_8(PEt_3)_6$	2.770(1)	2.744(2)	2.536(4)	179.12(4)	60.62(4)
$W_6S_8(PEt_3)_6$	2.673(1)	2.452(3)	2.513(2)	172.5(3)	66.06(7)
$[Na(py)_6][W_6Te_8(py)_6]$	2.732(1)	2.763(1)	2.30(1)	181.18(4)	59.25(3)

Y-W-Y bond angles. The average trans S-W-S, Se-W-Se, and Te-W-Te bond angles are 173.0(2), 175.9(1) and 180.76(5), respectively. Thus, the tungsten atoms reside on the outside of the cube, above the planes formed by the neighboring four chalcogen atoms in both the W_6S_8 and W_6Se_8 units, while in the W_6Te_8 unit, the tungsten atoms reside just slightly below the plane, almost coplanar with the four tellurium atoms. However, for the halide cluster compounds, $(M_6X_8)X_4$ (M = Mo, W; X = Cl, Br, I), the metal atom is sitting below the plane which is formed by four halogen atoms. Therefore, the elongation of the metal-metal bond distances in the heavier halide clusters is associated with the larger covalent radius of the heavier halogen atoms. In order to compensate for the larger radius of the heavier halogen atoms, the metal core M_6 has to expand. This effect has been termed as a "matrix effect".[25] In contrast, it is not necessary for the metal core M_6 to expand for these tungsten chalcogenide clusters. Thus, the elongation of the W-W bond distances in the selenide and telluride clusters can be attributed to both electronic and matrix effects.

The $W_6Te_8(PEt_3)_6$ crystallizes in a monoclinic space group, *C2/c*, with 4 molecules per unit cell. The W_6Te_8 cluster unit is centered on a $\bar{1}$ position (4c site symmetry). An Ortep drawing of the cluster and a packing diagram are shown in Figure 6 and Figure 7, respectively. Selected bond distances and bond angles are listed in Table 14 and Table 15, respectively. The average W-W, W-Te, and W-P bond distances are 2.770(1) Å, 2.744(2) Å, and 2.536(4) Å, respectively. Because the stronger W-P bonding resulted in increased electron density on the molecular orbitals which are slightly antibonding with respect to the W-W bonds of the cluster, the W-W distance in

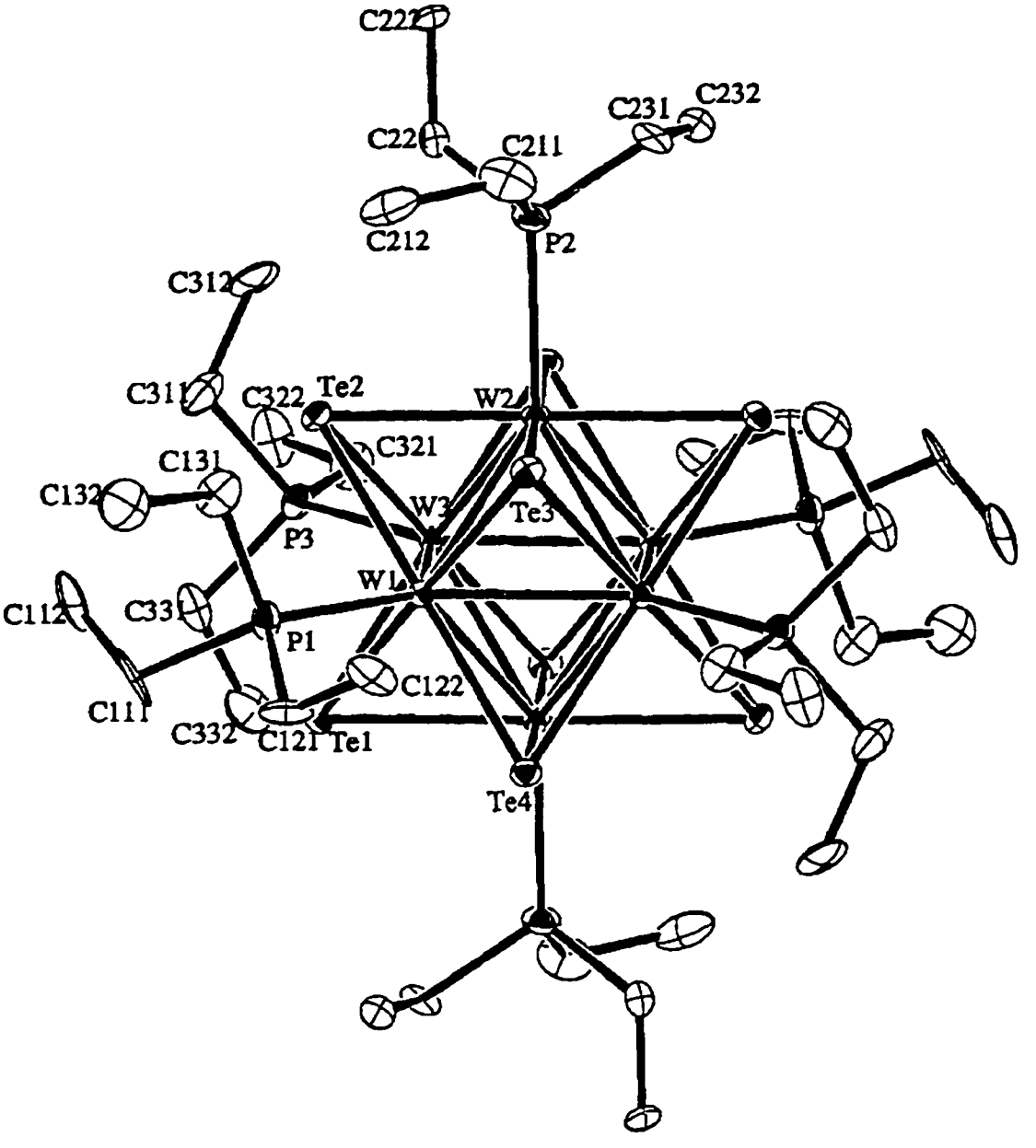

Figure 6. Molecular structure of $W_6Te_8(PEt_3)_6$. Thermal ellipsoids are shown at 35% probability level. Hydrogen atoms have been omitted for clarity.

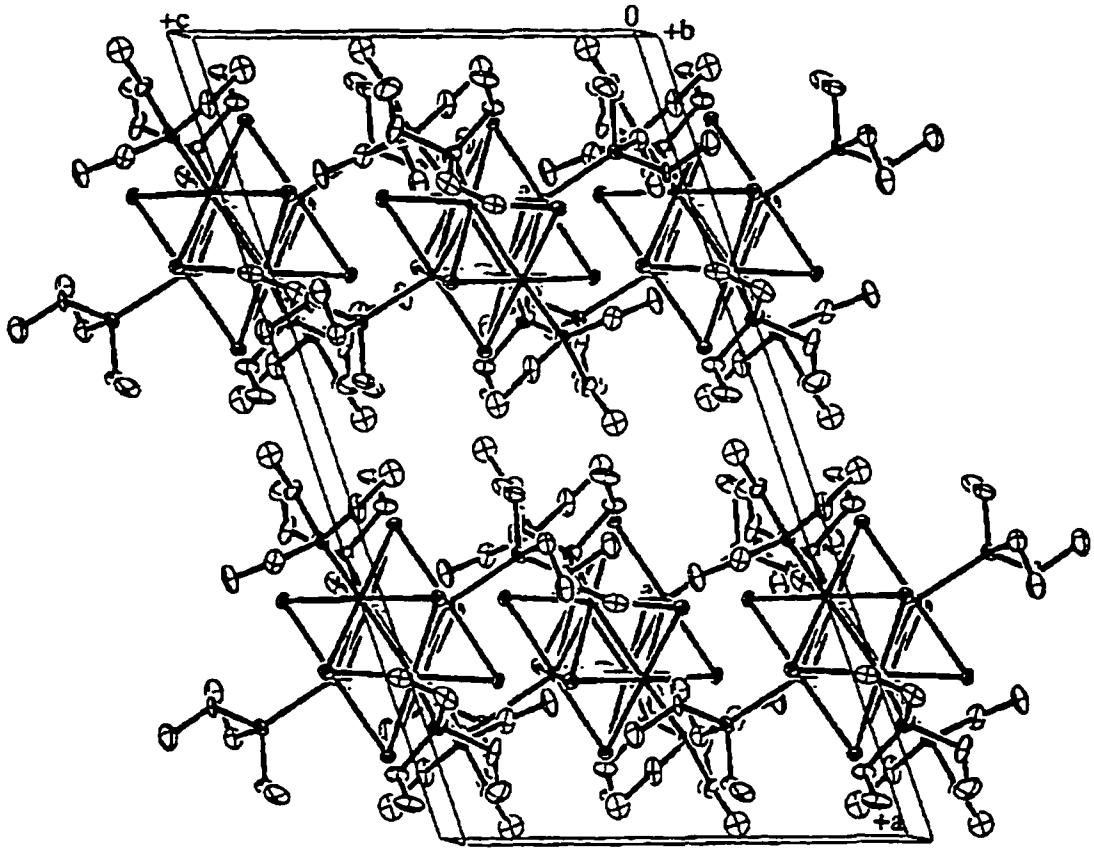

Figure 7. The unit cell packing diagram for $W_6Te_8(PEt_3)_6$ as viewed approximately along the b axis. Thermal ellipsoids are shown at 35% probability level.

Table 14. Selected Bond Distances (Å) in $W_6Te_8(PEt_3)_6$[a]

W(1) - W(2)	2.767(1)	W(1) - Te(1)	2.746(2)
W(1) - W(2A)	2.770(1)	W(1) - Te(2)	2.736(1)
W(1) - W(3)	2.770(2)	W(1) - Te(3)	2.751(2)
W(1) - W(3A)	2.775(1)	W(1) - Te(4)	2.742(1)
W(2) - W(3)	2.765(2)	W(2A) - Te(1)	2.734(1)
W(2) - W(3A)	2.771(1)	W(2) - Te(2)	2.747(1)
av. W-W	2.770(1)	W(2) - Te(3)	2.751(2)
		W(2A) - Te(4)	2.750(1)
W(1) - P(1)	2.542(5)	W(3) - Te(1)	2.748(1)
W(2) - P(2)	2.532(5)	W(3) - Te(2)	2.741(1)
W(3) - P(3)	2.535(4)	W(3A) - Te(3)	2.734(2)
av. W-P	2.536(5)	W(3A) - Te(4)	2.748(1)
		av. W-Te	2.744(2)

[a]Equivalent atoms A and B generated by symmetry transformation:

A, 1/2-X, 1/2-Y, -Z.

Table 15. Selected Bond Angles (deg) in $W_6Te_8(PEt_3)_6$[a]

W(2)-W(1)-W(2A)	89.81(3)	W(2)-W(1)-W(3)	59.91(2)
W(3)-W(1)-W(3A)	89.96(4)	W(2)-W(1)-W(3A)	59.99(2)
W(1)-W(2)-W(1A)	90.19(3)	W(2A)-W(1)-W(3)	60.02(3)
W(3)-W(2)-W(3A)	90.16(4)	W(2A)-W(1)-W(3A)	59.81(3)
W(1)-W(3)-W(1A)	90.04(4)	W(1)-W(2)-W(3)	60.09(3)
W(2)-W(3)-W(2a)	89.84(4)	W(1)-W(2)-W(3A)	60.14(2)
av. W-W-W	90.00(4)	W(1A)-W(2)-W(3)	60.18(3)
		W(1A)-W(2)-W(3A)	60.14(2)
W(1)-Te(1)-W(2A)	60.71(3)	W(1)-W(3)-W(2)	60.00(4)
W(1)-Te(1)-W(3)	60.54(4)	W(1)-W(3)-W(2A)	59.99(3)
W(2A)-Te(1)-W(3)	60.72(3)	W(1A)-W(3)-W(2)	60.00(3)
W(1)-Te(2)-W(2)	60.63(3)	W(1A)-W(3)-W(2A)	59.86(3)
W(1)-Te(2)-W(3)	60.76(4)	av. W-W-W	60.01(3)
W(2)-Te(2)-W(3)	60.50(3)		
W(1)-Te(3)-W(2)	60.39(4)	Te(1)-W(1)-Te(3)	178.54(4)
W(1)-Te(3)-W(3A)	60.79(4)	Te(2)-W((1)-Te(4)	179.53(4)
W(2)-Te(3)-W(3A)	60.68(4)	Te(1A)-W(2)-Te(2)	179.49(4)
W(1)-Te(4)-W(2A)	60.58(4)	Te(3)-W(2)-Te(4A)	178.89(4)
W(1)-Te(4)-W(3A)	60.72(3)	Te(2)-W(3)-Te(3A)	179.49(4)
W(2A)-Te(4)-W(3A)	60.37(3)	Te(1)-W(3)-Te(4A)	178.78(4)
av. W-Te-W	60.62(4)	av. Te-W-Te	179.12(4)
Te(1)-W(1)-Te(2)	90.26(5)	Te(1)-W(1)-P(1)	91.0(1)
Te(1)-W(1)-Te(4)	89.70(5)	Te(2)-W(1)-P(1)	87.6(1)
Te(3)-W(1)-Te(4)	89.49(5)	Te(3)-W(1)-P(1)	90.3(1)
Te(2)-W(1)-Te(3)	90.54(5)	Te(4)-W(1)-P(1)	92.9(1)
Te(1A)-W(2)-Te(3)	89.55(5)	Te(1A)-W(2)-P(2)	91.3(1)
Te(2)-W(2)-Te(4A)	90.37(5)	Te(2)-W(2)-P(2)	89.2(1)
Te(2)-W(2)-Te(3)	90.30(5)	Te(3)-W(2)-P(2)	92.2(1)
Te(1)-W(2A)-Te(4)	89.78(5)	Te(4A)-W(2)-P(2)	88.7(1)
Te(3)-W(3A)-Te(4)	89.71(4)	Te(1)-W(3)-P(3)	91.5(1)
Te(4A)-W(3)-Te(2)	90.53(4)	Te(2)-W(3)-P(3)	91.0(1)
Te(3A)-W(3)-Te(1)	89.64(4)	Te(3A)-W(3)-P(3)	89.4(1)
Te(1)-W(3)-Te(2)	90.12(4)	Te(4A)-W(3)-P(3)	89.5(1)
av. Te-W-Te	90.00(5)	av. Te-W-P	90.4(1)

[a]Equivalent atoms A and B generated by symmetry transformation:
A, 1/2-X, 1/2-Y, -Z.

this complex, 2.770(1) Å, is longer than that of 2.742(2) Å in $W_6Te_8(pip)_6$. The W-P bond distance of 2.536(4) Å is close to that of 2.513(2) Å in the sulfide analogue, $W_6S_8(PEt_3)_6$.[9,10b]

The $[Na(py)_6][W_6Te_8(py)_6]\cdot 1py$ crystallizes in the triclinic space group $P\bar{1}$ with one molecule per unit cell. A diagram of the unit cell of $[Na(py)_6]$ $[W_6Te_8(py)_6]\cdot 1py$ is shown in Figure 8. As illustrated, the W_6Te_8 cluster anion is centered on the origin of the unit cell (1a site symmetry), the Na^+ cation is centered on the center of the unit cell (1h site symmetry) with six pyridine molecules pseudo-octahedrally coordinated to it, and the one free pyridine solvent molecule is centered on the face center of the BC plane (1g site symmetry). Selected bond distances and bond angles are listed in Table 16 and Table 17, respectively.

A distortion of the metal octahedron can be found in the $[W_6Te_8(py)_6]^-$ unit. The main component of this distortion of the metal octahedron is a pseudo-tetragonal elongation along the W(1)-W(1A) axis: the W(1)-W(1A) distance of 3.895(1) Å is longer than the other two metal-metal distances across the center of the cluster by 0.054(1) Å and 0.041(1) Å, respectively. Also, the average W(2) - W(3) bond distance of 2.720(1) Å is noticeable shorter than the average W(1) - W(2) and W(1) - W(3) bond distance of 2.737(1) Å. This reduced complex formally has 21 electrons involved in the metal-metal bonding. The distortion may be driven by the Jahn-Teller effect resulting from the HOMO e_g^1 electron configuration and ^2E_g ground state in O_h symmetry. The average W-W and W-Te distances are 2.732(1) Å and 2.763(1) Å, respectively. In comparison, the neutral complex, $W_6Te_8(pip)_6$, has a slightly longer average W-W bond distance,

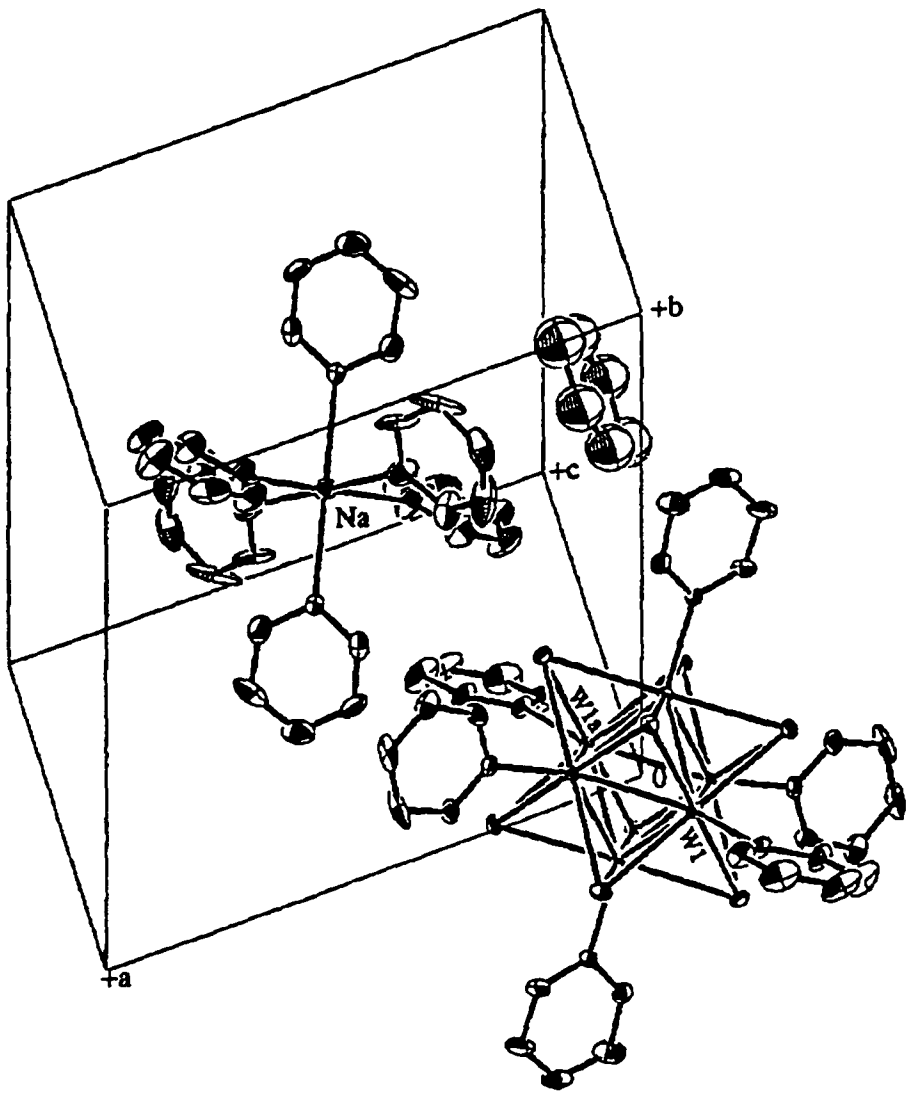

Figure 8. Unit cell of $[Na(py)_6][W_6Te_8(py)_6]\cdot py$ depicted with thermal ellipsoids at the 35% probability level.

Table 16. Selected Bond Distances (Å) in $[Na(py)_6][W_6Te_8(py)_6]\cdot 1py$[a]

W(1) - W(2)	2.742(1)	W(1) - Te(1)	2.748(1)
W(1) - W(2A)	2.729(1)	W(1) - Te(3)	2.764(1)
W(1) - W(3)	2.746(1)	W(1) - Te(2A)	2.767(1)
W(1) - W(3A)	2.733(1)	W(1) - Te(4A)	2.745(3)
W(2) - W(3)	2.723(1)	W(2) - Te(1)	2.757(1)
W(2) - W(3A)	2.718(1)	W(2) - Te(2)	2.763(1)
av. W-W	2.732(1)	W(2) - Te(3)	2.777(1)
		W(2) - Te(4)	2.776(1)
W(1) - N(1)	2.31(1)	W(3) - Te(2)	2.762(1)
W(2) - N(2)	2.30(1)	W(3) - Te(3)	2.765(1)
W(3) - N(3)	2.29(1)	W(3) - Te(1A)	2.777(1)
av. W-N	2.30(1)	W(3) - Te(4A)	2.756(1)
		av. W-Te	2.763(1)
Na(1) - N(10)	2.52(2)		
Na(1) - N(20)	2.63(2)		
Na(1) - N(30)	2.54(2)		
av. Na-N	2.56(2)		

[a]Equivalent atoms A and B generated by symmetry transformation: A, -X,-Y,-Z.

Table 17. Selected Bond Angles (deg) in $[Na(py)_6][W_6Te_8(py)_6]\cdot 1py$[a]

W(2)-W(1)-W(2A)	89.19(3)	W(2)-W(1)-W(3)	59.49(3)
W(3)-W(1)-W(3A)	89.38(3)	W(2)-W(1)-W(3A)	59.52(3)
W(1)-W(2)-W(1A)	90.81(3)	W(2A)-W(1)-W(3)	59.52(3)
W(3)-W(2)-W(3A)	90.19(3)	W(2A)-W(1)-W(3A)	59.81(3)
W(1)-W(3)-W(1A)	90.62(3)	W(1)-W(2)-W(3)	60.34(3)
W(2)-W(3)-W(2a)	89.81(3)	W(1)-W(2)-W(3A)	60.08(3)
av. W-W-W	90.00(3)	W(1A)-W(2)-W(3)	60.18(3)
		W(1A)-W(2)-W(3A)	60.56(3)
W(1)-Te(1)-W(2)	59.73(3)	W(1)-W(3)-W(2)	60.17(3)
W(1)-Te(1)-W(3A)	59.29(3)	W(1)-W(3)-W(2A)	59.93(3)
W(2)-Te(1)-W(3A)	58.81(3)	W(1A)-W(3)-W(2)	60.02(3)
W(1A)-Te(2)-W(2)	59.13(3)	W(1A)-W(3)-W(2A)	60.40(3)
W(1A)-Te(2)-W(3)	59.26(3)	av. W-W-W	60.00(3)
W(2)-Te(2)-W(3)	59.05(3)		
W(1)-Te(3)-W(2)	59.30(3)	Te(1)-W(1)-Te(4A)	181.75(4)
W(1)-Te(3)-W(3)	59.56(3)	Te(3)-W((1)-Te(2A)	180.39(3)
W(2)-Te(3)-W(3)	58.85(3)	Te(1)-W(2)-Te(2)	182.02(4)
W(1A)-Te(4)-W(2)	59.23(3)	Te(3)-W(2)-Te(4)	180.46(4)
W(1)-Te(4A)-W(3)	59.90(3)	Te(2)-W(3)-Te(4A)	181.81(4)
W(2)-Te(4)-W(3A)	58.84(3)	Te(3)-W(3)-Te(1A)	180.65(4)
av. W-Te-W	59.25(3)	av. Te-W-Te	181.18(4)
Te(2)-W(1A)-Te(4)	90.73(4)	Te(2A)-W(1)-N(1)	88.2(3)
Te(2A)-W(1)-Te(1)	90.67(4)	Te(4A)-W(1)-N(1)	89.6(3)
Te(4A)-W(1)-Te(3)	89.03(4)	Te(1)-W(1)-N(1)	89.5(3)
Te(1)-W(1)-Te(3)	89.55(4)	Te(3)-W(1)-N(1)	91.5(3)
Te(1)-W(2)-Te(3)	89.09(4)	Te(1)-W(2)-N(2)	89.3(3)
Te(1)-W(2)-Te(4)	90.95(4)	Te(2)-W(2)-N(2)	89.0(3)
Te(2)-W(2)-Te(3)	89.79(4)	Te(3)-W(2)-N(2)	91.4(3)
Te(2)-W(2)-Te(4)	90.15(4)	Te(4)-W(2)-N(2)	88.2(3)
Te(1)-W(3A)-Te(4)	90.95(4)	Te(1A)-W(3)-N(3)	89.0(3)
Te(4A)-W(3)-Te(3)	88.79(4)	Te(2)-W(3)-N(3)	89.1(3)
Te(1A)-W(3)-Te(2)	90.16(4)	Te(3)-W(3)-N(3)	90.4(3)
Te(2)-W(3)-Te(3)	90.08(4)	Te(4A)-W(3)-N(3)	89.5(3)
av. Te-W-Te	90.00(4)	av. Te-W-N	89.6(3)
N(10)-Na-N(20)	94.5(5)	N(10)-Na-N(30)	94.6(5)
N(20)-Na-N(30)	93.8(5)		

[a]Equivalent atoms A and B generated by symmetry transformation: A, -X,-Y,-Z.

2.742(2) Å, and a slightly shorter average W-Te bond distance, 2.753(2) Å. The shortening of the W-W bond distances and the elongation of the W-Te bond distances in the reduced anionic complex suggests that the HOMO e_g orbital is metal-metal bonding and metal-tellurium antibonding in nature. EHMO calculations on this tungsten telluride compound lead to a similar conclusion. In contrast, for molybdenum clusters ($[Mo_6Y_8(PEt_3)_6]^{n-}$, Y = S or Se, n = 0 or 1),[9] the reduced anionic complexes had slightly longer metal-metal bond distances than those of the neutral complexes, which indicated that the e_g MO's in these systems were slightly antibonding with respect to the metal-metal bonding. This contrasting result for the Mo_6Y_8 clusters is not accounted for in the more sophisticated calculations by the *DV-Xα* method.[23]

In the interesting and novel $[Na(py)_6]^+$ cation unit, the six pyridine molecules are pseudo-octahedrally coordinated to the Na^+ as shown in Figure 9. Doedens and Dahl concluded that in the absence of distortional forces (such as hydrogen bonding or Jahn-Teller degeneracies) a transition metal bound to six identical C_{2v} ligands would presumably exist in the T_h molecular symmetry.[26] However, the overall configuration of the $Na(py)_6^+$ cation slightly deviated from that of $Fe(py)_6^{2+}$ which has the T_h symmetry and only resulted in a C_i symmetry.

After considering the statistical errors, the Na-N bond distances are essentially identical, varying from 2.52(2) to 2.63(2) Å, and the average Na-N bond distance is 2.56(2) Å. The summation of the ionic radius for Na^+ and the van der Waals radius for N, [$r(Na)_{ion} + r(N)_{VDW} = 0.95 + 1.55 = 2.50$ Å], produces a value that is very close to the experimental value, 2.56 Å. This suggests that the pyridine molecules are very loosely

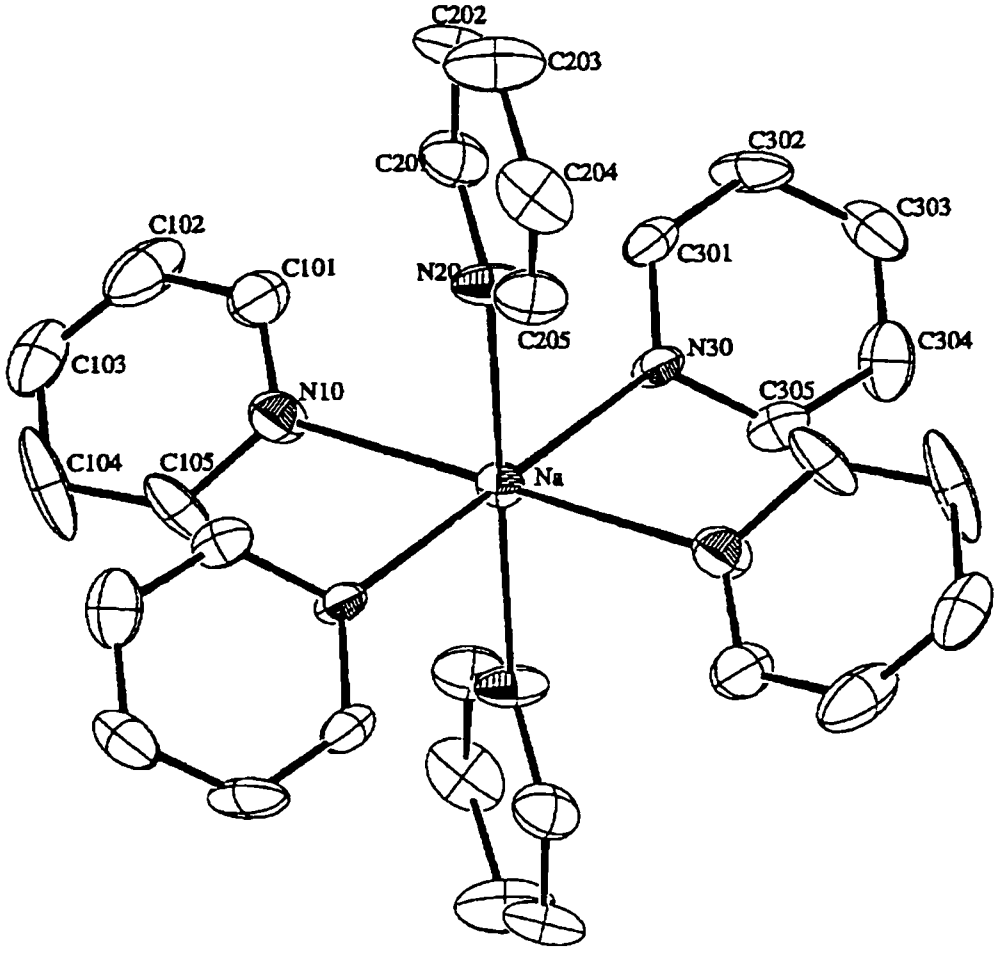

Figure 9 Ortep drawing of the cation unit, $[Na(py)_6]^+$ with thermal ellipsoids at the 35% probability level.

bonded to the sodium cation. The $[Na(NC_5H_5)_6]^+$ cation is to our knowledge the first documented example of a sodium ion octahedrally coordinated with six pyridine molecules. The average Na-N distance of 2.56(2) Å in this cation is much longer than the Na-N distances of 2.464(4) Å and 2.463(5) Å in the compounds $\{[Na(py)_4]_2[Fe_2(CO)_8]\}$[27] and $(C_5Me_5)Na(py)_3$,[28] respectively.

EHMO Calculation

For this series of molecular cluster complexes, $W_6Y_8L_6$, (Y = S, Se, Te), the absorption peak in electronic spectra shifts to higher wavelength when changing from sulfide to selenide to telluride. The crystal structures of $W_6Y_8(pip)_6$ (Y = S, Se, Te) show that W - W distances are 2.659(1) Å, 2.689(2) Å, and 2.742(2) Å, respectively. Considering the energy levels of atomic orbitals and electronegativity differences among sulfur, selenium, and tellurium, it was of interest to study the electronic structures of these series complexes by using Extended Hückel Molecular Orbital calculations.

The calculated molecular orbital energy diagrams for the metal complexes $W_6Y_8(NH_3)_6$ (Y = S, Se, Te) are shown in Figure 10. There are ten molecular orbitals (a_{1g}, t_{1u}, t_{2g}, t_{2u}) primarily involved in the metal - metal bonding interaction. The HOMO is t_{2u} and the LUMO is e_g. All three molecular complexes exhibit a very similar pattern of MO energy levels. However, the gap between HOMO and LUMO decrease slightly, as changing from sulfide and selenide to telluride, and the gap between t_{1u} (chalcogen

based) and LUMO e_g orbitals (metal based) decrease dramatically from 3.37 eV (368 nm) in sulfide cluster to 3.04 eV (408 nm) and 2.61 eV (475 nm) in selenide and telluride clusters, respectively. Considering the simplicity of EHMO calculation, these values are remarkably close to those observed in the UV-Vis spectra.

According to the calculation, the LUMO (e_g) have some metal - metal bonding character. The shorter W-W bond distances observed in the reduced anionic cluster, $[W_6Te_8]^-$, confirm that the e_g orbital is metal-metal bonding in nature.

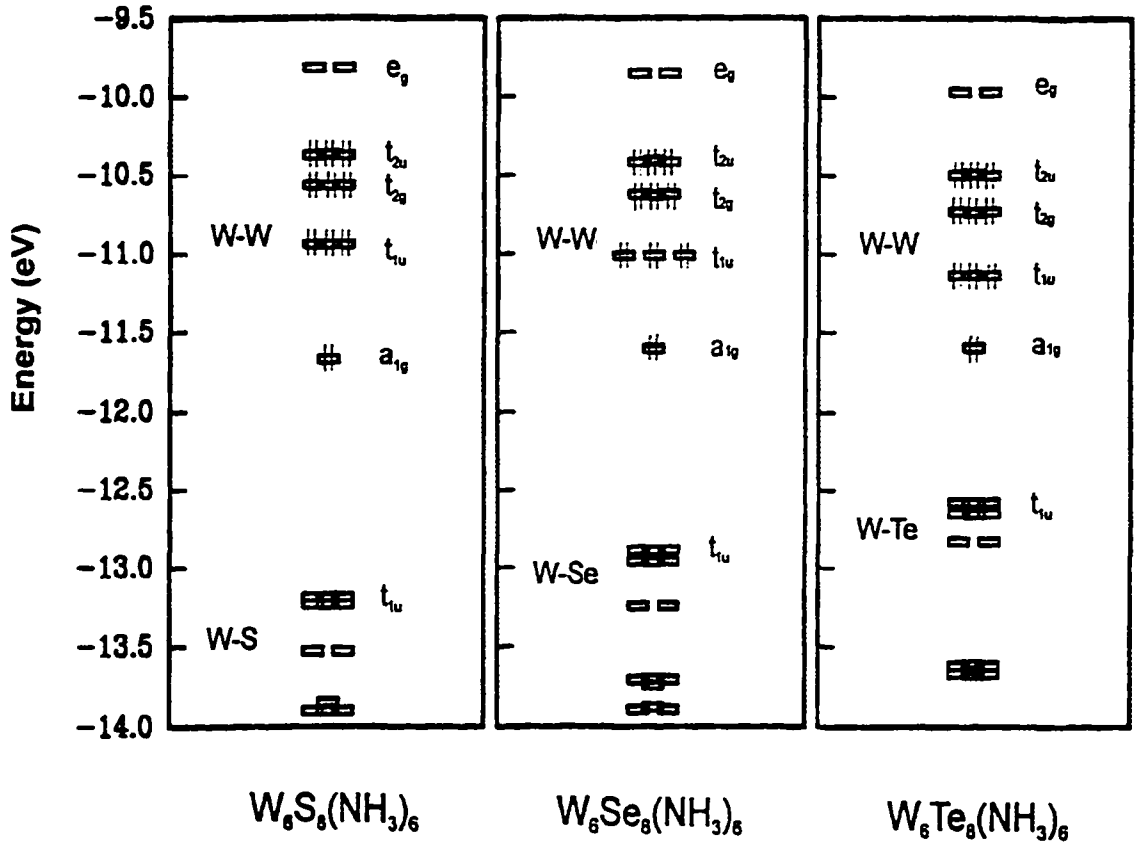

Figure. 10. Molecular orbital diagrams for $W_6Y_8(NH_3)_6$ in the HOMO-LUMO region.

Conclusion

This paper describes the preparations, characterizations, and structures of the first known molecular tungsten telluride cluster complexes, $W_6Te_8L_6$ (L = piperidine and triethylphosphine). An unexpected ionic compound $[Na(py)_6]^+[W_6Te_8(py)_6]^-$ was also discovered.

When one mole of W_6Cl_{12} reacts with four moles of Na_2Te and four moles of Na_2Te_2 in the presence of organic ligands, such as pyridine and piperidine, substitution of telluride for chloride takes place, and tungsten telluride cluster complexes, $W_6Te_8L_6$, were obtained. When one mole of W_6Cl_{12} reacts with eight moles of Na_2Te in pyridine, the ionic cluster complex, $[Na(py)_6]^+[W_6Te_8(py)_6]^-$, was surprisingly obtained. The fact that the reduced cluster units, $W_6Te_8^-$ (21e), were isolated in these reactions provided evidence for their formation by a disproportionation process. However, the mechanism of these synthetic reactions is still not completely clear. However, the presence of other oxidants, such as polychalcogenides, moisture, and solvent itself, can also result the formation of the oxidized tungsten chalcogenide cluster, W_6Te_8.

Far-infrared and X-ray photoelectron spectroscopy are two major means for characterizations of these compounds. The cluster unit, W_6Te_8, shows a characteristic far-IR band at about 180 cm^{-1}, which can be assigned as the T_{1u} W - Te stretching modes. The tungsten selenide cluster unit, W_6Se_8, exhibits a similar T_{1u} W - Se stretching band at 240 cm^{-1}. The reduction from 240 to 180 cm^{-1} is about that expected on the basis of the reduced masses. XPS was used to obtained

tungsten binding energies and gain further information about possible cluster retention or degradation. These tungsten binding energies of 30.8 eV ($4f_{7/2}$) and 32.9 eV ($4f_{5/2}$) for $W_6Te_8L_6$ compare favorably with those of sulfide (30.5, 32.6 eV) and selenide (30.8, 32.9 eV) analogues. Therefore, these tungsten binding energies of 30.8 eV ($4f_{7/2}$) and 32.9 eV ($4f_{5/2}$) are the characteristics for W_6Y_8 (Y = S, Se, Te) cluster units.

UV-Vis spectra of a series complex, $W_6Y_8(pip)_6$ in neat piperidine were obtained. As solutions color change from brown yellow to purple to dark blue, the absorption peak shift from 390 nm to 489 nm to 566 nm. EHMO calculations were performed on a series model complex, $W_6Y_8(NH_3)_6$, indicated that these absorptions were corresponding to chalcogen to tungsten metal charge transfer (t_{1u} - e_g). The energy gap between these two MOs decreased dramatically as changing from sulfide to telluride.

The first structure of tungsten telluride cluster complex, $W_6Te_8L_6$, have been determined. The W - W bond distances in these W_6Te_8 cluster units are quite longer than that of $W_6Se_8L_6$ clusters. The average W - Te bond distance is about 2.75 Å. Unlike their sulfide and selenide analogues, the W - W bond distances and W - Y bond distances are very close in W_6Te_8 cluster unit. Therefore, the tungsten atoms are almost coplanar with the four tellurium atoms in W_6Te_8 unit. While in both the W_6S_8 and W_6Se_8 units the tungsten atoms reside on the outside, above the planes formed by the neighboring four chalcogen atoms.

An interesting and unique ionic complex, $[Na(py)_6]^+[W_6Te_8(py)_6]^-$, were obtained from the 1:8 reaction in pyridine. Six pyridine molecules are pseudo-octahedrally

coordinate to a Na^+ to form an interesting $[Na(py)_6]^+$ cation unit. This is the first structure example of a sodium cation coordinated by six pyridine molecules octahedrally. The $[W_6Te_8(py)_6]^-$ unit has a distorted metal octahedron. This anionic unit formally has 21 electrons involved in the metal-metal bonding. The distortion may be driven by the Jahn-Teller effect resulting from the HOMO e_g^1 electron configuration and ^2E_g ground state in O_h symmetry.

References

(1) Chevrel, R.; Sergent, M. *Topics in Current Physics*, Fischer, Ø. and Maple, M. B., Eds.; Springer-Verlag: Heidelberg, 1982; Vol. 32, Chapter 2.

(2) Peña, O.; Sergent, M. *Prog. Solid St. Chem.* **1989**, *19*, 165.

(3) Mulhern, P. J.; Haering, R. R. Can. *J. Phys.* **1984**, *62*, 527.

(4) (a) McCarty, K. F.; Schrader, G. L. *Ind. Eng. Chem. Prod. Res. Dev.* **1984**, *23*, 519. (b) McCarty, K. F.; Anderegg, J. W.; Schrader, G. L. *J. Catal.* **1985**, *93*, 375.

(5) Hilsenbeck, S. J.; McCarley, R. E. *Inorg. Chem.* **1994**, *33*, 1822.

(6) (a) McCarley, R. E.; Laughlin, S. K.; Spink, D. A.; Hur, N. *Abstracts of papers*, 3rd Chemical Congress of North America, Toronto, Ontario, Canada, 1988; American Chemical Society: Washington, DC, 1988.
(c) Zhang, X.; Hur, N.; Spink, D. A.; Michel, J. B.; Laughlin, S. K.; McCarley, R. E. Manuscript in preparation.

(7) Saito, T.; Yamamoto, N.; Yamagata, T.; Imoto, H. *J. Am. Chem. Soc.* **1988**, *110*, 1646.

(8) Saito, T.; Yamamoto, N.; Nagase, T.; Tsuboi, T.; Kobayashi, K.; Yamagata, T.; Imoto, H.; Unoura, K. *Inorg. Chem.* **1990**, *29*, 746.

(9) Saito, T.; Yoshikawa, A.; Yamagata, T.; Imoto, H.; Unoura, K. *Inorg. Chem.* **1989**, *28*, 3588.

(10) (a) Zhang, X.; McCarley, R. E. *Inorg. Chem.* **1995**, *34*, 2678. (b) Zhang, X. Ph.D. Dissertation, Iowa State University, Ames, IA, 1991.(c) Xie, X.; McCarley, R. E. Unpublished research.

(11) Ehrlich, G. M.; Warren, C. J.; Vennos, D. A.; Ho, D. H.; Haushalter, R. C.; DiSalvo, F. J. *Inorg. Chem.* **1995**, *34*, 4454.

(12) Xie, X.; McCarley, R. E. *Inorg. Chem.* **1995**, *34*, 6124.

(13) Xie, X.; McCarley, R. E. *Inorg. Chem.* **1996**, *35*, 2713.

(14) Ehrlich, G. M.; Rauch, P. E.; DiSalvo, F. J. *Inorg. Synth.* **1995**, *30*, 1.

(15) (a) Klemm, W.; Sodomann, H.; Langmesser, P. *Z. Anorg. Allg. Chem.* **1939**, *241*, 281. (b) Fener, F. In *Handbuch der Praparativen Anorganischen Chemie;* Brauer, G., Ed.; Ferdinand Enke: Stuttgart, Germany, 1954; p. 280-281.

(16) Scheldrick, G. M. *Crystallographic Computing 3*; Oxford University Press: Oxford, U.K., 1985.

(17) *TEXSAN: Single Crystal Structure Analysis Software*, Version 1.6c; Molecular Structure Corp.: The Woodlands, TX 77381, 1985 & 1992.

(18) *DIFABS*: Walker, N. & Stuart, *Acta Cryst.* **1983**, *A39*, 158.

(19) Hoffman, R. J. *J. Chem. Phys.* **1963**, *39*, 1397.

(20) Beuze, A. L.; Loirat, H.; Zerrouki, M. C.; Lissillour, R. *J. Solid State Chem.* **1995**, *120*, 80.

(21) (a) Atomic orbital zeta parameters were taken from the following: Clementi, E.; Roetti, C. *At. Data Nucl. Data Tables* **1974**, *14,* 177. (b) H_{ii} parameters were taken from the following: Moore, C. Circular 467 U.S. Department of Commerce, National Bureau of Standards, Vol. 1-3, 1949.

(22) A sample of tungsten metal prepared in this laboratory gave W $4f_{7/2}$ BE = 31.5 eV on the spectrometer described in the experimental section. This compares with a reported value of 31.4 eV in *Handbook of X-Ray Photoelectron*

Spectroscopy, Perkin-Elmer Cooperation, Eden Prairie, Minnesota, 1992; p 173.

(23) Imoto, H.; Saito, T.; Adachi, H. *Inorg. Chem.* **1995**, *34*, 2415.

(24) Selwood, P. W. *Magnetochemistry*, 2nd ed.; Interscience Publishers: New York, New York, **1988**, P. 78.

(25) Corbett, J. D. *J. Solid State Chem.* **1981**, *37*, 335.

(26) Doedens, R. J.; Dahl, L. F. *J. Am. Chem. Soc.* **1966**, *88*, 4847.

(27) Shore, S. G.; Deng, H. *Inorg. Chem.* **1992**, *31*, 2289.

(28) Rabe, G.; Roesky, H. W.; Stalke, D.; Pauer, F.; Sheldrick, G. M. *J. Organomet. Chem.* **1991**, *403*, 11.

CHAPTER 4. SYNTHESIS, CHARACTERIZATION, AND STRUCTURE OF MIXED CHLORIDE-SELENIDE TUNGSTEN CLUSTER COMPLEXES

A paper to be submitted to Inorganic Chemistry

Xiaobing Xie and Robert E. McCarley

Abstract

The first examples of the mixed halide-chalcogenide molecular complexes for the hexatungsten cluster unit, $[W_6Se_{8-x}Cl_x(PEt_3)_6]^+$, were prepared via the reaction of W_6Cl_{12} with Na_2Se and PEt_3 in the refluxing toluene. Single crystals of the mixed chloride-selenide cluster complexes were grown from chloroform solution of the product. Two cluster complexes with differing compositions and the identical structure, $[W_6Se_{7.04}Cl_{0.96}(PEt_3)_6][Cl(CHCl_3)_6]$ and $[W_6Se_{6.39}Cl_{1.61}(PEt_3)_6][Cl(CHCl_3)_6]$, were determined: hexagonal, $R\bar{3}$, a = 18.921(4) Å, c = 21.275(4) Å, Z = 3. The bridging chlorine atoms are disordered over all the bridging ligand sites in both structures. In the unique $[Cl(CHCl_3)_6]^-$ anion unit, six chloroform solvent molecules are octahedrally coordinated to a chlorine anion via hydrogen bonding.

Introduction

The chemistry of molecular hexanuclear molybdenum-chalcogenide cluster complexes of general formulation $Mo_6Y_8L_6$ (Y=S, Se, Te) has undergone remarkable development in recent years[1-6] because of their structural relations with Chevrel phases.[7,8] The essential structural element in these complexes is a Mo_6 octahedron with eight chalcogenide atoms capping the faces and six organic donor ligands occupying the terminal positions.

This cluster unit, Mo_6Y_8, can have a variable electron population of 20-24 electrons in the metal-metal bonding orbitals.[9-11] Therefore, these cluster complexes often support multisequential electron transfer reactions. The chemically reversible addition or removal of electrons from the Se clusters can result in measurable changes in the core dimensions.

In this laboratory, research has focused on the hexamolybdenum (Mo_6) and hexatungsten (W_6) chalcogenide cluster compounds. We have developed routes for preparation of the metal cluster complexes, $M_6Y_8L_6$ (M = Mo, W), by converting M_6Cl_{12}, which contains the $(M_6Cl_8)^{4+}$ cluster unit, through substitution of chalcogenide for chloride.[12-16] The preparation and structural characterization of $W_6Y_8L_6$ molecular complexes, where L is an organic donor ligand such as pyridine,[12,13,15] piperidine,[14,15] triethylphosphine,[13,14] or tetrahydrothiophene[13] were accomplished in this laboratory. Likewise, the molybdenum sulfide cluster complexes, $Mo_6S_8L_6$, were also developed.[8]

However, examples of the molecular hexanuclear cluster complexes with mixed halide-chalcogenide bridging ligands were rare. The first molecular Mo_6X_8 cluster compound with mixed bridging ligands, $(pyH)_3[(Mo_6Cl_7S)Cl_6]$, was reported by Michel and McCarley.[17] This mixed chloride-sulfide molecular cluster was established by substituting one chlorine ligand in the $Mo_6Cl_8^{4+}$ cluster unit of molybdenum (II) chloride with a sulfur ligand. Additional substitutions have led to the discovery of molecular complexes of $Mo_6S_xCl_{8-x}L_6$, where x varies from 3 to 8.[18] The products of these preparations were not single stoichiometric clusters, but rather, mixtures of cluster products which had a range of values of x. Therefore, these complexes are usually less characterized.

No example of a mixed tungsten chloride-chalcogenide molecular complex such as $W_6Y_{8-x}Cl_xL_6$ has been reported. Considering the difficulty in differentiating sulfur and chlorine atoms by X-ray diffraction, mixed chloride-selenide cluster complexes should be a better system to be explored. The present paper describes the syntheses, characterization and structures of the first two new molecular complexes of the mixed chloride-selenide tungsten clusters, $[W_6Se_{7.04}Cl_{0.96}(PEt_3)_6][Cl(CHCl_3)_6]$ and $[W_6Se_{6.39}Cl_{1.61}(PEt_3)_6][Cl(CHCl_3)_6]$.

Experimental

Materials

The reagents and products are air and moisture sensitive. Therefore, all manipulations were performed by the use of an inert-atmosphere drybox, a high-vacuum manifold, and Schlenk techniques, unless otherwise stated. W_6Cl_{12} was prepared by literature methods.[13,19] Na_2Se and K_2Se were prepared by the reaction of corresponding alkali metal and selenium in refluxing tetrahydrofuran with catalytic amounts of naphthalene.[20]

All solvents were purified and dried prior to use. Also, the solvents were de-oxygenated by use of the freeze-thaw process: freeze to liquid nitrogen temperature, evacuate the gaseous material, and then thaw. This process was repeated three times prior to distillation of the purified solvent onto Linde 3- or 4-Å molecular sieves and stored under vacuum or a nitrogen atmosphere. Pyridine (Fisher), piperidine (Fisher), and triethylphosphine (Strem) were purified by refluxing over calcium hydride for at least 4 hours. Toluene (Fisher) and chloroform were refluxed over phosphorus pentoxide. Without heating, tetrahydrofuran (Fisher) was dried by stirring with sodium metal and a benzophenone indicator. Methanol (Mallinckrodt) was dried by refluxing over sodium methoxide. When used, the solvents were vacuum-distilled or syringed under a flowing nitrogen gas atmosphere.

Physical Measurements

Infrared spectroscopy

The samples were prepared in the drybox and were temporarily stored under nitrogen before being placed in the sample chamber of the instrument. Mid-infrared (4000-200 cm^{-1}) spectra were recorded with a Bomem MB-102 Fourier transform infrared spectrometer manufactured by Hartman and Braun. Samples were prepared as Nujol mulls and pressed between two cesium iodide plates. The sample chamber of the instrument was continuously purged with dry, compressed air and the reference spectra were collected in the empty chamber. Far-infrared (650-100 cm^{-1}) spectra were recorded separately with an IBM IR/98 Fourier transform infrared spectrometer. Thick sample mulls were placed on a polyethylene film in the drybox, and the film was mounted on a sample holder. Then the sample was transferred to the sample chamber. Data were collected for these samples while the sample chamber was under vacuum, and Nujol on the polyethylene film was used as a reference.

X-ray photoelectron spectroscopy

XP spectra were collected by James Anderegg at room temperature with a Physical Electronics Industries 5500 multitechnique surface analysis system. This system was equipped with a hemispherical analyzer, a toroidal monochromator, and multichannel detector which sampled a 2 mm^2 area. The samples were pressed on

an indium substrate and loaded into an air-sensitive sample holder in the dry-box. Then the sample holder was transferred into the chamber of the spectrometer. After the system was completely evacuated, the sample holder was opened and the sample was excited with monochromatic Mg *Kα* radiation (1253.6 eV) at the power of 300 W. The photoelectron binding energies were calibrated with C 1s = 284.6 eV.

X-ray powder diffraction

Powder X-ray diffraction (XRD) data were obtained with a Philips ADP3520 θ-2θ diffractometer using Cu *Kα* radiation. The air-sensitive samples were loaded into a specially designed, gas-tight sample holder and sealed under N_2 while in the drybox.

Magnetic Susceptibility

The magnetic properties were examined on powder samples with a Quantum SQUID magneto-susceptometer. The samples were loaded into a 3 mm inner diameter fused silica tube that had been sealed on the bottom half with a 3 mm outer diameter fused silica rod. Another fused silica rod was placed on top of the sample, thus giving an arrangement where an uniform measurement could be made. The data were subsequently corrected for the diamagnetic contribution of the quartz.

Analytical Procedures

Tungsten was determined gravimetrically as the trioxide. If ternary metal cations were not present, the samples were placed in tared crucibles and decomposed initially with dilute (3M) nitric acid. Concentrated nitric acid was then added to ensure complete oxidation and the samples evaporated to dryness. After ignition in a muffle furnace at 800°C, the resulting WO_3 solid was weighed. If ternary metal cations were present, the sample was dissolved in 0.5 M KOH with the aid of hydrogen peroxide. The solutions were then treated with equal volumes of concentrated nitric acid and hydrogen peroxide to form a peroxy-acid complex. The hydrated oxide, $WO_3 \cdot nH_2O$, was then completely precipitated by slowly decomposing this complex at 100°C and collected in tared ceramic filter crucibles. Then the materials were dried to constant weight at 800°C.

Chlorine was determined by potentiometric titration with a standardized silver nitrate solution after dissolving the sample in KOH-H_2O_2 solution and neutralization. A silver/silver chloride electrode was used as the reference, and a silver wire as the working electrode. The endpoint was determined by using the second derivative method.

Synthetic Procedures

Attempts to prepare mixed chloride-selenide cluster complexes

It has been found that $W_6Se_8L_6$ was the major product when one mole of W_6Cl_{12} reacted with eight moles, or more, of Na_2Se in amine solvents. Therefore, it is conceivable that partially substituted complexes, such as $W_6Se_{8-x}Cl_xL_6$ ($0<x<8$), can be obtained when a lesser amount of Na_2Se is used in the reaction. Thus, a series of reactions with different mole ratios of Na_2Se:W_6Cl_{12} was attempted in these amine solvents.

1:1 stoichiometry. W_6Cl_{12} (0.50 g, 0.328 mmol), and Na_2Se (0.041 g, 0.328 mmol) were weighed in the drybox and transferred into a 100-mL Schlenk reaction flask equipped with a water-cooled condenser. By distillation, 40 mL of piperidine were added to the reactants and the mixture was refluxed for 4 days. A tan solid of 0.27 g and brown-red solution were separated by filtration. The solvent was then removed from the filtrate under dynamic vacuum, and after drying overnight *in vacuo,* 0.65 g of a black powder was obtained. Found: W, 42.6; Cl, 5.2; Cl/W, 0.63.

1:2 stoichiometry. W_6Cl_{12} (0.50 g, 0.328 mmol), and Na_2Se (0.082 g, 0.656 mmol) were weighed in the drybox and transferred into a 100-mL Schlenk reaction flask equipped with a water-cooled condenser. By distillation, 40 mL of piperidine were added to the reactants and the mixture was refluxed for 4 days. A tan solid and brown-red solution were separated by filtration. The solvent was then removed from the filtrate under dynamic vacuum, and after drying overnight *in vacuo,* 0.65 g

of a black powder was obtained. Found: W, 48.0; Cl, 4.0; Cl/W, 0.43.

1:4 stoichiometry. W_6Cl_{12} (0.50 g, 0.328 mmol), and Na_2Se (0.164 g, 1.31 mmol) were weighed in the drybox and transferred into a 100-mL Schlenk reaction flask equipped with a water-cooled condenser. By distillation, 40 mL of piperidine were added to the reactants and the mixture was refluxed for 4 days. A white solid and red solution were separated by filtration. The solvent was then removed from the filtrate under dynamic vacuum, and after drying overnight *in vacuo,* 0.64 g of a black powder was obtained. Found: Cl, 4.2.

1:6 stoichiometry. W_6Cl_{12} (0.15 g, 0.098 mmol), and Na_2Se (0.074 g, 0.590 mmol) were weighed in the drybox and transferred into a 100-mL Schlenk reaction flask equipped with a water-cooled condenser. By distillation, 30 mL of piperidine were added to the reactants and the mixture was refluxed for 4 days. About 0.06 g of white solid and orange pink-red solution were separated by filtration. The solvent was then removed from the filtrate under dynamic vacuum, and after drying overnight *in vacuo,* 0.18 g of a black powder was obtained. Found: W, 46.7; Cl, 4.5; Cl/W, 0.50.

Preparation of $[W_6Se_{7.04}Cl_{0.96}(PEt_3)_6][Cl(CHCl_3)_6]$ (1)

W_6Cl_{12} (0.250 g, 0.164 mmol), and Na_2Se (0.164 g, 1.31 mmol) were weighed in the drybox and transferred into a 100-mL Schlenk reaction flask equipped with a water-cooled condenser. By vacuum distillation, 40 mL of toluene were transferred into the flask. Then 0.25 mL of triethylphosphine were added to the reactants and

the mixture was refluxed for 3 days. The color of the reaction mixture was light gray to start with, then it slowly turned light brown and then darker brown as the reaction proceeded. About 0.19 grams of tan solid and a reddish brown solution were separated by filtration. The filtrate was evaporated and dried overnight under dynamic vacuum to remove the solvent. About 0.30 g of dark brown oily material was thus recovered. This oily material was then washed with 5 mL Et_2O, and about 0.12 g of yellow brown powder was obtained. IR (Nujol, cm^{-1}): 1414 (m), 1247 (w), 1032 (s), 863 (w), 760 (s), 712 (m), 620 (ms), 404 (s), 368(w), 332 (w), ν(W-Se) 254 (m). About 0.030 g of this brown material were refluxed in 10mL $CHCl_3$ for one day. The resulting yellow brown solution was allowed to stand at -20°C for one week. Some dark brown rhombohedral crystals of $[W_6Se_{7.04}Cl_{0.96}(PEt_3)_6][Cl(CHCl_3)_6]$ **(1)** were obtained.

The insoluble product obtained by filtration of the reaction mixture was washed with methanol for 2-3 days to remove NaCl, and about 0.035 g of brown powder was recovered. XPS data for this brown powder indicated that WSe_2 was the major component.

Preparation of $[W_6Se_{6.39}Cl_{1.61}(PEt_3)_6][Cl(CHCl_3)_6]$ (2)

W_6Cl_{12} (0.50 g, 0.327 mmol), and K_2Se (0.51 g, 3.2 mmol) were weighed in the drybox and transferred into a 100-mL Schlenk reaction flask equipped with a water-cooled condenser. By vacuum distillation, 50 mL of toluene were transferred into the flask. Then 0.23 mL of triethylphosphine were added to the reactants and the

mixture was refluxed for 3 days. The color of the reaction mixture was light gray to start with, then it slowly turned light brown and then darker brown as the reaction proceeded. About 0.80 grams of tan solid and a reddish brown solution were separated by filtration. The filtrate was evaporated and dried overnight under dynamic vacuum to remove the solvent. About 0.25 g of dark orange powder was thus recovered. IR (Nujol, cm^{-1}): 1414 (w), 1255 (w), 1033 (s), 759 (s), 712 (ms), 622 (m), 404 (m), 368 (m), 334 (m), 280 (m), ν(W-Se) 254 (m). About 0.050 g of this brown material were refluxed in 10mL $CHCl_3$ for one day. The resulting yellow brown solution was allowed to stand at -20°C for one week. Some dark brown rhombohedral crystals of $[W_6Se_{6.39}Cl_{1.61}(PEt_3)_6][Cl(CHCl_3)_6]$ **(2)** were obtained.

X-ray Structure Determinations

In each case, a crystal was chosen from material still in contact with the mother solution. The crystal was encased in epoxy cement, attached to the tip of a glass fiber, and immediately inserted into the low-temperature nitrogen stream of the diffractometer for data collection. The cell constants were determined from 25 randomly located and centered reflections. The structures were solved by direct methods using SHELXS[21] and refined on F by full-matrix, least-squares techniques with the TEXSAN package.[22] Pertinent crystallographic data are listed in Table 1.

Table 1. Crystallographic Data for the Mixed Selenide-Chloride Tungsten Cluster Complexes.

compound	$[W_6Se_{7.04}Cl_{0.96}(PEt_3)_6][Cl(CHCl_3)_6]$	$[W_6Se_{6.39}Cl_{1.61}(PEt_3)_6][Cl(CHCl_3)_6]$
chemical formula	$C_{42}Cl_{19.96}H_{96}P_6Se_{7.04}W_6$	$C_{42}Cl_{20.61}H_{96}P_6Se_{6.39}W_6$
formula weight	3151.94	3125.50
space group	$R\bar{3}$ (No. 148)	$R\bar{3}$ (No. 148)
a, Å	18.921(4)	18.908(5)
c, Å	21.275(4)	21.306(5)
V, Å^3	6596.(2)	6596.(3)
Z	3	3
ρcalcd, g/cm^3	2.380	2.360
μ, cm^{-1}	114.67	112.32
radiation (Mo $K\alpha$)	0.71069Å	0.71069Å
T, °C	-70.0	-70.0
2θ range, deg	3-55	3-45
total data	3695	6061
unique data	3391	2004
data observed	1577[$I>4\sigma(I)$]	1335[$I>4\sigma(I)$]
no. parameter	123	123
data/parameter	12.8	10.85
abs. correction	DIFABS	PSI
trans. factors	0.86-1.20	0.2692-1.00
R^a	0.0347	0.0329
R_w^b	0.0321	0.0297
diff. peaks, e/Å^3	1.59, -1.27	2.73, -1.73

[a] $R = \Sigma||F_o|-|F_c||/\Sigma|F_o|$.

[b] $R_w = [\Sigma w(|F_o|-|F_c|)^2/\Sigma w|F_o|^2]^{1/2}$; $w = 1/\sigma^2(|F_o|)$.

Structure determination for $[W_6Se_{7.04}Cl_{0.96}(PEt_3)_6][Cl(CHCl_3)_6]$ (1)

A dark brown crystal, with dimensions of 0.20 x 0.20 x 0.30 mm^3, was mounted on a glass fiber, and data collection proceeded at -70°C. Data were collected with a Rigaku AFC6R diffractometer using Mo Kα radiation, over the range $3° < 2\theta < 55°$ in the quarter-sphere ($+h$, $+k$, $\pm l$), using the ω-2θ scan technique. Three standard reflections were monitored every 200 reflections and showed a 3.89% intensity decrease over the collection period. A total of 3695 reflections were collected, of which 3391 were unique (R_{int} = 0.075) and 1577 were observed with $I > 4\sigma(I)$. The linear absorption coefficient, μ, for Mo Kα radiation is 114.67 cm^{-1}. First, an empirical absorption correction using the φ scan technique was applied after the structure solution. After all of the atoms were located and refined isotropically, an absorption correction using the DIFABS program[23] was applied and resulted in the relative transmission factors ranging from 0.86 to 1.20. The data were corrected for Lorentz and polarization effects.

The trigonal space group $R\bar{3}$ was chosen on the basis of systematic absences and intensity statistics. Initial tungsten atom positions were input on the basis of the SHELXS direct methods output. Subsequently, the atomic positions for Se, Cl (from chloroform molecules), P, and C were located directly from the electron density difference maps. After locating those atoms, a large peak (19 $e^-/Å^3$) remained at the origin of the unit cell. Consideration of the chemical reactions indicated that a chlorine atom should be tried in that position. After the subsequent refinement cycles, the unweighted and weighted agreement factors dropped from 0.076 and 0.078

to 0.057 and 0.058, respectively. At this point, it was noted that isotropic thermal parameters of the two unique selenium atoms were relatively large. Therefore, two chlorine atoms were introduced at identical positions to the two selenium atoms with their total population constrained to unity. The unweighted and weighted agreement factors dropped to 0.054 and 0.052, respectively, after the subsequent refinement cycles. Then all non-hydrogen atoms were refined with anisotropic thermal parameters. Idealized hydrogen positions were calculated and placed in the refinement with C-H distances equal to 1.04 Å, but their parameters were held constant during subsequent cycles. The final cycle of full-matrix least-squares refinement was based on 1577 observed reflections and 123 variable parameters, and converged with unweighted and weighted agreement factors of: R = 0.035 and R_w = 0.032, respectively. The final formula for this complex was found to be $[W_6Se_{7.04}Cl_{0.96}(PEt_3)_6][Cl(CHCl_3)_6]$. The atomic coordinates and equivalent isotropic thermal parameters of the non-hydrogen atoms are given in Table 2, and the anisotropic thermal parameters are shown in Table 3.

Structure determination for $[W_6Se_{6.39}Cl_{1.61}(PEt_3)_6][Cl(CHCl_3)_6]$ (2)

A dark brown crystal, with dimensions of 0.30 x 0.30 x 0.40 mm^3, was mounted on a glass fiber, and data collection proceeded at -70°C. Data were collected with a Rigaku AFC6R diffractometer using Mo $K\alpha$ radiation, over the range $3° < 2\theta < 45°$ in the quarter-sphere ($+h$, $+k$, $\pm l$), using the ω-2θ scan technique. Three standard reflections were monitored every 200 reflections and showed a 3.89% intensity

Table 2. Atomic Coordinates and Equivalent Isotropic Thermal Parameters ($Å^2$) of the Non-Hydrogen Atoms for $[W_6Se_{7.04}Cl_{0.96}(PEt_3)_6]$ $[Cl(CHCl_3)_6]$

atom	x	y	z	B_{eq}[a]	pop.
W(1)	0.25912(4)	0.57806(4)	0.11490(3)	1.25(1)	
Se(1)	0.1654(1)	0.6389(1)	0.11776(8)	1.57(4)	0.867(12)
Cl(11)	0.1654	0.6389	0.11776	1.57	0.133(12)
Se(2)	0.3333	0.6667	0.0193(1)	1.63(3)	0.920(6)
Cl(12)	0.3333	0.6667	0.0193	1.63	0.080(6)
Cl(01)	0.0000	0.0000	0.0000	2.3(1)	
Cl(1)	0.1183(3)	0.2364(3)	-0.1218(2)	5.3(1)	
Cl(2)	-0.0176(4)	0.1883(4)	-0.0420(3)	7.5(2)	
Cl(3)	-0.0353(5)	0.0980(4)	-0.1551(3)	8.6(2)	
P(1)	0.1565(2)	0.4604(2)	0.0481(2)	1.68(9)	
C(01)	0.029(1)	0.153(1)	-0.0934(8)	3.3(4)	
C(11)	0.194(1)	0.399(1)	0.0133(7)	2.7(4)	
C(12)	0.261(1)	0.440(1)	-0.0342(8)	3.9(5)	
C(21)	0.121(1)	0.492(1)	-0.0208(7)	3.0(4)	
C(22)	0.060(1)	0.427(1)	-0.0626(8)	4.2(5)	
C(31)	0.067(1)	0.382(1)	0.0893(7)	3.0(4)	
C(32)	0.012(1)	0.412(1)	0.1160(7)	3.8(5)	

[a] $B_{eq} = (8/3)\pi^2[U_{11}(aa^*)^2 + U_{22}(bb^*)^2 + U_{33}(cc^*)^2 + 2U_{12}aa^*bb^*\cos\gamma + 2U_{13}aa^*cc^*\cos\beta + 2U_{23}bb^*cc^*\cos\alpha]$

Table 3. Anisotropic Thermal Parameters[a] ($Å^2$) of the Non-Hydrogen Atoms for $[W_6Se_{7.04}Cl_{0.96}(PEt_3)_6]$ $[Cl(CHCl_3)_6]$

atom	U_{11}	U_{22}	U_{33}	U_{12}	U_{13}	U_{23}
W(1)	0.0148(4)	0.0154(4)	0.0159(3)	0.0067(4)	-0.0016(3)	-0.0022(3)
Se(1)	0.0138(9)	0.024(1)	0.022(1)	0.0097(8)	-0.0044(7)	-0.0016(7)
Cl(11)	0.0138	0.024	0.022	0.0097	-0.0044	-0.0016
Se(2)	0.025(1)	0.0248	0.012(1)	0.0124	0.0000	0.0000
Cl(12)	0.0248	0.0248	0.012	0.0124	0.0000	0.0000
Cl(01)	0.032(4)	0.032	0.023(5)	0.0160	0.0000	0.0000
Cl(1)	0.075(4)	0.056(4)	0.046(3)	0.015(3)	0.005(3)	0.002(3)
Cl(2)	0.089(5)	0.068(5)	0.142(6)	0.050(4)	0.042(4)	0.014(4)
Cl(3)	0.121(6)	0.058(4)	0.103(5)	0.012(4)	-0.052(5)	0.013(4)
P	0.018(2)	0.019(2)	0.024(2)	0.007(2)	-0.004(2)	-0.005(2)
C(01)	0.04(1)	0.03(1)	0.04(1)	-0.004(9)	0.003(9)	0.010(8)
C(11)	0.03(1)	0.03(1)	0.04(1)	0.014(8)	-0.013(8)	-0.023(8)
C(12)	0.05(1)	0.07(1)	0.04(1)	0.03(1)	0.005(10)	-0.03(1)
C(21)	0.03(1)	0.05(1)	0.03(1)	0.013(9)	-0.028(8)	-0.011(8)
C(22)	0.06(1)	0.07(1)	0.05(1)	0.05(1)	-0.05(1)	-0.04(1)
C(31)	0.023(10)	0.028(10)	0.035(10)	-0.008(8)	-0.003(8)	-0.010(8)
C(32)	0.021(10)	0.06(1)	0.05(1)	0.008(10)	-0.011(8)	-0.03(1)

[a]The coefficients U_{ij} of the anisotropic thermal parameter expression are defined as:
$\exp[-2\pi^2(a^{*2}U_{11}h^2+b^{*2}U_{22}k^2+c^{*2}U_{33}l^2+2a^*b^*U_{12}hk+2a^*c^*U_{13}hl+2b^*c^*U_{23}kl)]$

decrease over the collection period. A total of 6061 reflections were collected, of which 2004 were unique (R_{int} = 0.060) and 1335 were observed with $I > 4\sigma(I)$. The linear absorption coefficient, μ, for Mo $K\alpha$ radiation is 112.32 cm^{-1}. An empirical absorption correction based on azimuthal scans of four reflections was applied and resulted in transmission factors ranging from 0.27 to 1.00. The data were corrected for Lorentz and polarization effects.

The trigonal space group $R\bar{3}$ was chosen on the basis of systematic absences and intensity statistics. Initial tungsten atom positions were input on the basis of the SHELXS direct methods output. Subsequently, the atomic positions for Se, Cl, P, and C were located directly from the electron density difference maps. The unweighted and weighted agreement factors were 0.064 and 0.061, respectively when every atom was refined with isotropic thermal parameters. At this point, it was noted that isotropic thermal parameters of the two unique selenium atoms were relatively large. Therefore, two chlorine atoms were introduced at identical positions to the two selenium atoms with their total population constrained to unity. The unweighted and weighted agreement factors dropped down to 0.060 and 0.056, respectively, after the subsequent refinement cycles. Then all non-hydrogen atoms were refined with anisotropic thermal parameters. Idealized hydrogen positions were calculated and placed in the refinement with C-H distances equal to 1.04 Å, but their parameters were held constant during subsequent cycles. The final cycle of full-matrix least-squares refinement was based on 1335 observed reflections and 123 variable parameters, and converged with unweighted and weighted agreement factors of: R =

0.033 and R_w = 0.030, respectively. The final formula for this complex was found to be $[W_6Se_{6.39}Cl_{1.61}(PEt_3)_6][Cl(CHCl_3)_6]$. The atomic coordinates and equivalent isotropic thermal parameters of the non-hydrogen atoms are given in Table 4, and the anisotropical thermal parameters are shown in Table 5.

Results and Discussion

Preparation of Mixed Chloride-Selenide Complexes

It was found that $W_6Se_8L_6$ is the major product when one mole of W_6Cl_{12} reacts with eight moles, or more, of Na_2Se in amine solvents. In order to obtain the partially substituted complexes, such as $W_6Se_{8-x}Cl_xL_6$ ($0<x<8$), a series of reactions with differing Na_2Se/W_6Cl_{12} mole ratios (Na_2Se/W_6Cl_{12} = 1, 2, 4, 6, 8) was attempted in both refluxing piperidine and pyridine. In general, the starting materials were refluxed in the corresponding solvent for 3-4 days. Then, the mixtures were filtered while still hot. In all cases, the desired products were soluble and retained in the filtrate. The solvents were then stripped away from the filtrate under dynamic vacuum, and the samples were further dried *in vacuo* for one day prior to storage in a dry-box.

For the reactions conducted in piperidine, W_6Cl_{12} readily dissolved in piperidine and a dark brown solution was formed immediately after stirring. Without adding

Table 4. Atomic Coordinates and Equivalent Isotropic Thermal Parameters ($Å^2$) of the Non-Hydrogen Atoms for $[W_6Se_{6.39}Cl_{1.61}(PEt_3)_6][Cl(CHCl_3)_6]$

atom	x	y	z	B_{eq}[a]	pop.
W(1)	0.25929(3)	0.57841(3)	0.11502(2)	1.71(1)	
Se(1)	0.16576(8)	0.63906(8)	0.11777(5)	2.24(2)	0.778(7)
Cl(11)	0.16576	0.63906	0.11777	2.24	0.222(7)
Se(2)	0.33333	0.66667	0.01946(8)	2.14(2)	0.862(11)
Cl(12)	0.33333	0.66667	0.01946	2.14	0.138(11)
Cl(01)	0.0000	0.0000	0.0000	2.78(8)	
Cl(1)	0.1183(3)	0.2364(2)	-0.1220(2)	6.0(1)	
Cl(2)	-0.0181(3)	0.1888(3)	-0.0416(2)	8.4(2)	
Cl(3)	-0.0352(3)	0.0984(3)	-0.1552(3)	9.1(1)	
P(1)	0.1572(2)	0.4605(2)	0.0480(1)	2.28(7)	
C(01)	0.0275(9)	0.1535(8)	-0.0940(6)	4.6(4)	
C(11)	0.1944(9)	0.3974(8)	0.0147(5)	4.0(4)	
C(12)	0.2613(9)	0.4393(9)	-0.0337(5)	5.2(4)	
C(21)	0.1209(8)	0.4935(8)	-0.0200(5)	3.9(4)	
C(22)	0.0584(9)	0.4242(9)	-0.0636(5)	5.3(4)	
C(31)	0.0663(7)	0.3825(8)	0.0892(5)	3.5(3)	
C(32)	0.0113(8)	0.4130(9)	0.1158(5)	5.4(4)	

[a] $B_{eq} = (8/3)\pi^2[U_{11}(aa^*)^2 + U_{22}(bb^*)^2 + U_{33}(cc^*)^2 + 2U_{12}aa^*bb^*\cos\gamma + 2U_{13}aa^*cc^*\cos\beta + 2U_{23}bb^*cc^*\cos\alpha]$

Table 5. Anisotropic Thermal Parameters[a] ($Å^2$) of the Non-Hydrogen Atoms for $[W_6Se_{6.39}Cl_{1.61}(PEt_3)_6][Cl(CHCl_3)_6]$

atom	U_{11}	U_{22}	U_{33}	U_{12}	U_{13}	U_{23}
W(1)	0.0206(3)	0.0209(3)	0.0233(2)	0.0103(3)	-0.0004(2)	-0.0012(2)
Se(1)	0.0251(8)	0.0307(8)	0.0309(7)	0.0152(7)	-0.0040(5)	-0.0017(5)
Cl(11)	0.0251	0.0307	0.0309	0.0152	-0.0040	-0.0017
Se(2)	0.0310(8)	0.0310	0.0195(9)	0.0155	0.0000	0.0000
Cl(12)	0.0310	0.0310	0.0195	0.0155	0.0000	0.0000
Cl(01)	0.035(3)	0.0349	0.036(3)	0.0175	0.0000	0.0000
Cl(1)	0.087(3)	0.063(3)	0.055(2)	0.021(3)	0.008(2)	0.008(2)
Cl(2)	0.096(4)	0.075(4)	0.165(4)	0.055(3)	0.046(3)	0.014(3)
Cl(3)	0.121(5)	0.065(3)	0.116(3)	0.015(3)	-0.055(3)	0.008(3)
P	0.025(2)	0.026(2)	0.032(2)	0.011(2)	-0.005(1)	-0.007(1)
C(01)	0.07(1)	0.026(8)	0.071(9)	0.021(8)	-0.001(8)	0.006(7)
C(11)	0.06(1)	0.052(9)	0.055(7)	0.040(9)	-0.026(7)	-0.029(7)
C(12)	0.05(1)	0.09(1)	0.058(8)	0.031(9)	0.006(7)	-0.022(8)
C(21)	0.06(1)	0.053(10)	0.056(7)	0.040(9)	-0.021(7)	-0.011(7)
C(22)	0.007(1)	0.009(1)	0.060(8)	0.05(1)	-0.035(8)	-0.030(8)
C(31)	0.032(8)	0.041(9)	0.055(7)	0.013(7)	0.001(6)	-0.015(6)
C(32)	0.028(9)	0.071(1)	0.065(8)	-0.002(8)	-0.005(7)	-0.022(8)

[a]The coefficients U_{ij} of the anisotropic thermal parameter expression are defined as:
$\exp[-2\pi^2(a^{*2}U_{11}h^2+b^{*2}U_{22}k^2+c^{*2}U_{33}l^2+2a^*b^*U_{12}hk+2a^*c^*U_{13}hl+2b^*c^*U_{23}kl)]$

sodium selenide, W_6Cl_{12} reacted with piperidine to form a brown solution and yellow green solid. Based on elemental analyses, this insoluble yellow green solid probably has a formula of $(W_6Cl_8)Cl_4 \cdot (pip)_2$. Surprisingly, the materials recovered from the filtrate of the reaction with Na_2Se only contained 5.2% of chlorine. When the Na_2Se/W_6Cl_{12} mole ratios were 1, 2, 4, or 6, the major products were soluble and all contained about 42~48% of tungsten and 4~5% of chlorine. However, when the Na_2Se/W_6Cl_{12} mole ratios were 8 or 12, the product did not have any chlorine.

The XP spectra of the products from this series of reactions are shown in Figure 1. When Na_2Se/W_6Cl_{12} mole ratios smaller than eight (Na_2Se/W_6Cl_{12} = 2, 4, 6,) were analyzed, two types of tungsten were found in the products regardless of the mole ratios used. One type was identified as that in the $W_6Se_8L_6$ cluster unit, whose W $4f_{7/2}$ binding energy is 30.8 eV. Single crystals of $W_6Se_8(pip)_6 \cdot 8pip$ could also be obtained from the filtrate of the 1:4 and 1:6 reactions. The second type, with BE ($W4f_{7/2}$) = 32.8 eV, has not yet been definitely identified, but corresponds most closely to that of W_6Cl_{12}, BE = 32.4 eV, and WSe_2, BE = 32.3 eV. However, the chlorine analysis indicated that the chlorine percentages (4~5%) in these materials were too low for considering that the second type of tungsten is pure tungsten chloride cluster, W_6Cl_{12}. The identity of this second component was not clear.

When more sodium selenide was used (higher Na_2Se/W_6Cl_{12} mole ratio), the XP spectrum showed a decreased relative intensity of the band at 32.8 eV. In other words, more cluster unit, W_6Se_8, and less of the second compound were obtained when more sodium selenide was used. When the Na_2Se/W_6Cl_{12} mole ratio was

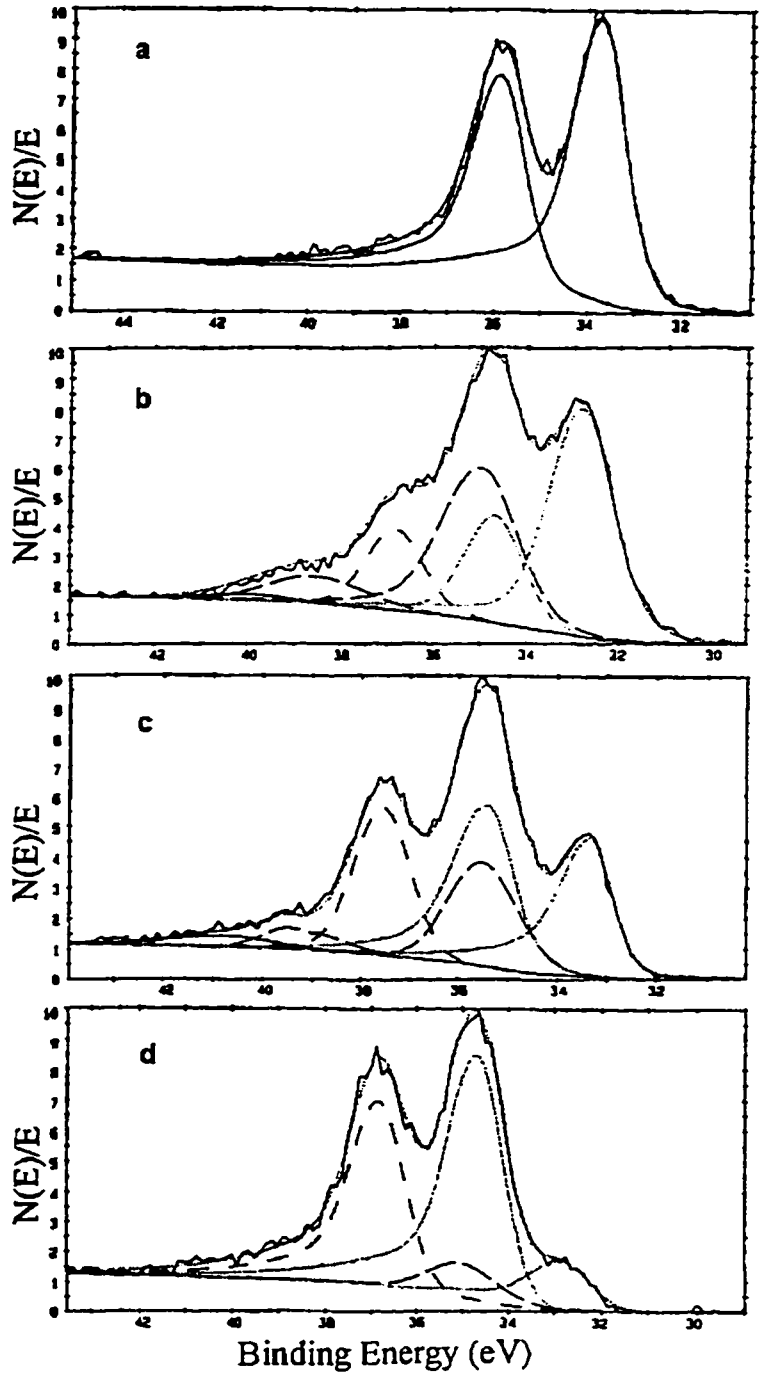

Figure 1. W 4f XP spectra of the soluble products for a series of reactions between W_6Cl_{12} and Na_2Se in various ratios: (a) 1:8, (b) 1:6, (c) 1:4, and (d) 1:2.

eight, only the cluster complex, $W_6Se_8L_6$ was isolated from the reaction filtrate. The analysis showed absence of chlorine, thus providing evidence for the lack of any mixed chloride-selenide derivative formation. Similarly, chlorine was not detected by either XPS, or by single crystal X-ray diffraction examination of crystals recovered from the reaction.

If the mixed chloride-selenide cluster complexes were the products of the 1:4 reaction as illustrated in equation 1, one would expect that only one type of tungsten would be present in the XP spectrum. The fact that the W_6Se_8 cluster

$$W_6Cl_{12} + 4Na_2Se \xrightarrow{L} W_6Cl_4Se_4\,L_6 + 8NaCl \qquad (1)$$

complex and another compound are both present in the product suggested that the mixed chloride-selenide cluster complexes were not formed as expected and thus they were probably either kinetically unstable or never formed in these amine solvents.

Synthesis of $[W_6Se_{7.04}Cl_{0.96}(PEt_3)_6][Cl(CHCl_3)_6]$

The isolation of an ionic compound, $[W_6Se_{7.04}Cl_{0.96}(PEt_3)_6][Cl(CHCl_3)_6]$, was a surprise. Originally, the neutral phosphine complex, $W_6Se_8(PEt_3)_6$, was expected to form in a manner similar to that of the piperidine and pyridine analogues. Thus, in the presence of triethylphosphine, the reaction between one mole of W_6Cl_{12} and ten moles of Na_2Se in toluene was expected to provide the neutral phosphine complex, $W_6Se_8(PEt_3)_6$. However, single crystals of the ionic complex, $[W_6Se_{7.04}Cl_{0.96}(PEt_3)_6]$

$[Cl(CHCl_3)_6]$ crystallized from the chloroform solution of the reaction products. Nevertheless, it is possible that the material recovered from the reaction filtrate was a mixture of the neutral, $W_6Se_8(PEt_3)_6$, and ionic, $[W_6Se_7Cl(PEt_3)_6]^+$, complexes. In that case, only the ionic complex was able to be crystallized from the chloroform solution.

Although it is still unclear about the mechanism of the formation of this ionic complex, the solvent toluene is believed to play an important role in isolating this mixed chloride-selenide cluster complex. In comparison, the other similar substitution reactions conducted in amine solvents, such as pyridine and piperidine, only provided the complete substitution product, $W_6Se_8L_6$. Even when a lesser amount of Na_2Se was used as a reactant, the neutral complex, $W_6Se_8L_6$, and an unidentified compound were detected. No mixed chloride-selenide cluster complexes were obtained from those reaction systems.

Synthesis of $[W_6Se_{6.39}Cl_{1.61}(PEt_3)_6][Cl(CHCl_3)_6]$

In order to reproduce the preparation of the ionic complex, $[W_6Se_7Cl(PEt_3)_6]^+$, a similar reaction on a larger scale was conducted. After three days refluxing, only about 0.25 g of brown powder was recovered from the reaction filtrate, while the majority of materials remained insoluble. Single crystals of $[W_6Se_{6.39}Cl_{1.61}(PEt_3)_6]$ $[Cl(CHCl_3)_6]$ were obtained unexpectedly instead of $[W_6Se_{7.04}Cl_{0.96}(PEt_3)_6]$ $[Cl(CHCl_3)_6]$. It seems apparent that the ionic compounds, $[W_6Se_7Cl(PEt_3)_6]^+$, and

$[W_6Se_6Cl_2\ (PEt_3)_6]^+$ cocrystallized in the lattice and resulted in an average composition of $[W_6Se_{6.39}Cl_{1.61}(PEt_3)_6]^+$. The formation of a different ionic complex from the second preparation suggested that the reaction conditions are crucial for the formation of different compounds. In the second preparation, the amount of the starting materials added were double while keeping a constant reaction time of three days. This difference could be important to the isolation of the less selenium substituted cluster cation, $[W_6Se_6Cl_2(PEt_3)_6]^+$.

Crystal Structures

The ionic complexes, $[W_6Se_{7.04}Cl_{0.96}(PEt_3)_6][Cl(CHCl_3)_6]$ **(1)** and $[W_6Se_{6.39}Cl_{1.61}(PEt_3)_6][Cl(CHCl_3)_6]$ **(2)**, both crystallize in the trigonal space group $R\bar{3}$ with 3 molecules per unit cell. These two complexes are isomorphous. The $[W_6Se_{8-x}Cl_x(PEt_3)_6]^+$ cationic cluster unit is centered on a $\bar{3}$ position (3b site symmetry), with two of the eight face capping atoms on the 3-fold axis. Chlorine and selenium atoms are randomly distributed among the eight bridging positions. Six triethylphosphine molecules coordinated to the tungsten atoms at terminal positions strongly enough to replace all terminal chlorine ions. The anionic unit, $[Cl(CHCl_3)_6]^-$, is centered on another $\bar{3}$ position (3a site symmetry), and the chlorine anion is located at the origin of the unit cell. These positions in the unit cell diagram of $[W_6Se_{8-x}Cl_x(PEt_3)_6][Cl(CHCl_3)_6]$ are shown in Figure 2.

A picture of the cationic unit $[W_6Se_{7.04}Cl_{0.96}(PEt_3)_6]^+$ is shown in Figure 3.

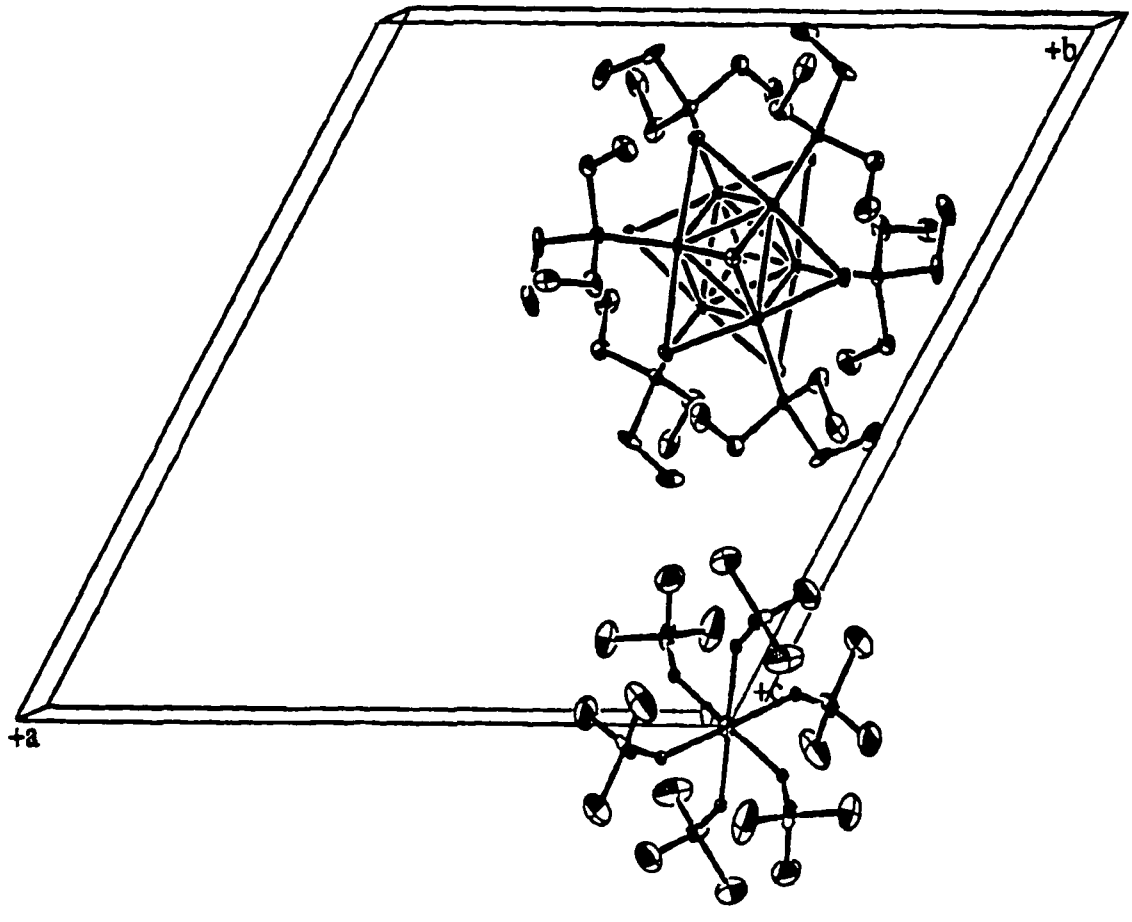

Figure 2. Unit cell of $[W_6Se_7Cl(PEt_3)_6][Cl(CHCl_3)_6]$ depicted with thermal ellipsoids at 35% probability.

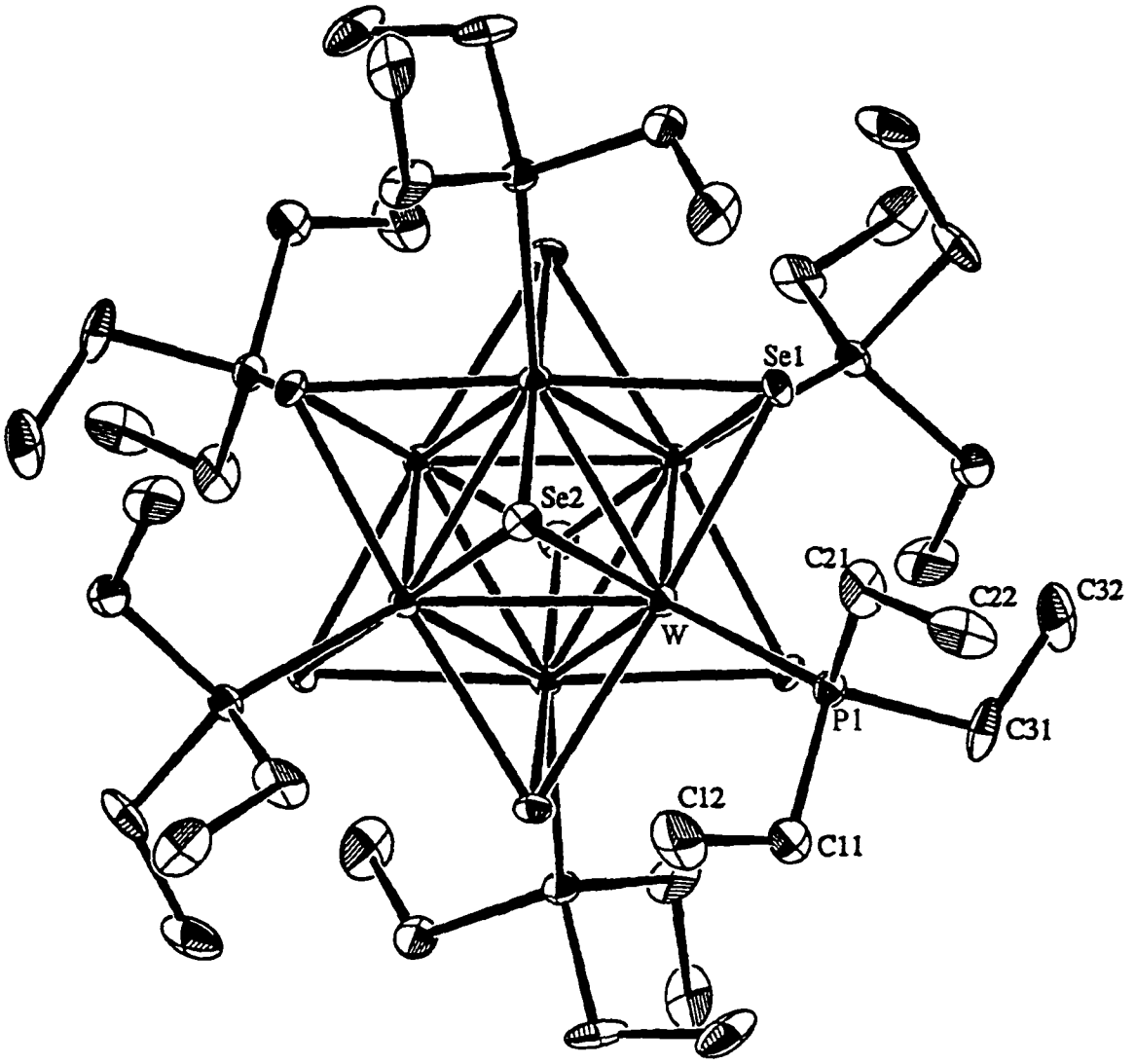

Figure 3. Molecular structure of $[W_6Se_7Cl(PEt_3)_6]^+$. Thermal ellipsoids are shown at 35% probability level. Hydrogen atoms have been omitted for clarity.

Selected bond distances and bond angles within the cluster are listed in Table 6. From this table, it can be seen that the deviations from strict octahedral symmetry are very small. The average bond distances (Å) and maximum deviation are as follows: W-W, 2.699(1) ave., 0.001; W-Se(Cl), 2.558(2) ave., 0.006; and W-P 2.535(4) ave., 0.000. This regular metal octahedron reflected that the cluster unit formally has 20 electrons involved in the metal-metal bonding and confirmed that $[W_6Se_7Cl(PEt_3)_6]^+$ is the correct formula for this complex. In comparison, $W_6Se_8(py)_6$ has similar W-W bond distances, but a slightly longer average W-Se bond distance of 2.578(2) Å than that of the mixed chloride-selenide complex. As expected, mixing a smaller chlorine atom with seven selenium atoms randomly should result in the shortening of the average W-Se bond distance.

For the second ionic compound, $[W_6Se_{6.39}Cl_{1.61}(PEt_3)_6]^+$, selected bond distances and bond angles within the cluster are listed in Table 7. The average W-W, W-Se(Cl), and W-P bond distances are 2.691(1) Å, 2.554(2) Å, and 2.537(3) Å, respectively. It is believed that this material consists of a mixture of the 21 electron cluster, $[W_6Se_6Cl_2(PEt_3)_6]^+$, and the 20 electron cluster, $[W_6Se_7Cl(PEt_3)_6]^+$. Therefore, the observed bond distances were the weighted average values of these two types of cluster units. Based on Pauling's relation,[24] d(n) = d(1)-0.6log(n), the calculated W-W bond distance difference (Δd) between a 20 e^- cluster and a 21 e^- cluster is 0.013 Å, [Δ(d) = 0.6log(21/20)=0.013 Å]. The fact that the observed average W-W bond distance of 2.691(1) Å for **(2)** is only 0.008(1) Å shorter than the average W-W distance in **(1)** further suggested that the second compound was a

Table 6. Selected Bond Lengths (Å) and Angles (deg) in $[W_6Se_{7.04}Cl_{0.96}(PEt_3)_6][Cl(CHCl_3)_6]$[a]

W(1)-W(1A)	2.698(1)	W(1)-Se(1)	2.552(2)
W(1)-W(1C)	2.699(1)	W(1)-Se(2)	2.562(2)
av. W-W	2.699(1)	W(1)-Se(1A)	2.562(2)
		W(1)-Se(1B)	2.554(2)
W(1)-P(1)	2.535(4)	av. W-Se	2.558(2)
P(1)-C(11)	1.80(2)	C(11)-C(12)	1.50(2)
P(1)-C(21)	1.84(2)	C(21)-C(22)	1.49(2)
P(1)-C(31)	1.82(2)	C(31)-C(32)	1.51(2)
Cl(01)-C(01)	3.33(2)	Cl(01)-H(01)	2.41
W(1A)-W(1)-W(1B)	60.00(3)	W(1)-W(ID)-W(IA)	90.00(2)
W(1A)-W(1)-W(1D)	59.99(2)	W(1A)-W(1B)-W(1C)	90.00(4)
W(1B)-W(1C)-W(1)	60.02(3)		
av. W-W-W	60.00(3)	Se(1)-W(1)-Se(1B)	89.98(5)
		Se(1A)-W(1)-Se(1B)	89.77(5)
W(1C)-Se(1)-W(1B)	63.66(5)	Se(1A)-W(1)-Se(2)	89.84(5)
W(1)-Se(1)-W(1B)	63.72(6)	Se(1)-W(1)-Se(2)	90.05(5)
W(1)-Se(1)-W(1C)	63.79(5)	av. Se-W-Se	89.91(6)
W(1)-Se(2)-W(1A)	63.58(6)		
av. W-Se-W	63.69(6)	Se(2)-W(1)-P(1)	93.4(1)
		Se(1A)-W(1)-P(1)	94.1(1)
Se(1A)-W(1)-Se(1)	175.37(6)	Se(1B)-W(1)-P(1)	91.1(1)
Se(1B)-W(1)-Se(2)	175.54(6)	Se(1)-W(1)-P(1)	90.5(1)
av. Se-W-Se	175.46(6)	av. Se-W-P	92.2(1)

[a]Equivalent atoms generated by symmetry transformation:

A, 1-y,1+x-y,z; B, -x+y,1-x,z; C, y-1/3,1/3-x+y,1/3-z; D, 2/3+x-y,1/3+x,1/3-z

Table 7. Selected Bond Lengths (Å) and Angles (deg) in $[W_6Se_{6.39}Cl_{1.61}(PEt_3)_6][Cl(CHCl_3)_6]$[a]

W(1)-W(1A)	2.688(1)	W(1)-Se(1)	2.545(2)
W(1)-W(1C)	2.693(1)	W(1)-Se(2)	2.560(2)
av. W-W	2.691(1)	W(1)-Se(1A)	2.556(2)
		W(1)-Se(1B)	2.554(2)
W(1)-P(1)	2.537(3)	av. W-Se	2.554(2)
P(1)-C(11)	1.81(1)	C(11)-C(12)	1.51(2)
P(1)-C(21)	1.84(1)	C(21)-C(22)	1.56(2)
P(1)-C(31)	1.83(1)	C(31)-C(32)	1.53(2)
Cl(01)-C(01)	3.35(1)	Cl(01)-H(01)	2.42
W(1A)-W(1)-W(1B)	60.00(5)	W(1)-W(ID)-W(IA)	90.00(4)
W(1A)-W(1)-W(1D)	60.06(3)	W(1A)-W(1B)-W(1C)	90.00(4)
W(1B)-W(1C)-W(1)	59.88(3)		
av. W-W-W	59.98(4)	Se(1)-W(1)-Se(1B)	90.01(4)
		Se(1A)-W(1)-Se(1B)	89.76(4)
W(1C)-Se(1)-W(1B)	63.61(5)	Se(1A)-W(1)-Se(2)	89.82(4)
W(1)-Se(1)-W(1B)	63.61(4)	Se(1)-W(1)-Se(2)	90.07(4)
W(1)-Se(1)-W(1C)	63.77(5)	av. Se-W-Se	89.92(4)
W(1)-Se(2)-W(1A)	63.34(5)		
av. W-Se-W	63.58(5)	Se(2)-W(1)-P(1)	93.03(8)
		Se(1A)-W(1)-P(1)	93.69(8)
Se(1A)-W(1)-Se(1)	175.52(4)	Se(1B)-W(1)-P(1)	91.30(8)
Se(1B)-W(1)-Se(2)	175.66(4)	Se(1)-W(1)-P(1)	90.79(8)
av. Se-W-Se	175.59(6)	av. Se-W-P	92.20(8)

[a]Equivalent atoms generated by symmetry transformation:

A, 1-y,1+x-y,z; B, -x+y,1-x,z; C, y-1/3,1/3-x+y,1/3-z; D, 2/3+x-y,1/3+x,1/3-z

mixture of 21 and 20 electron clusters.

As shown in Figure 4, the interesting and unique $[Cl(CHCl_3)_6]^-$ anion unit exhibits six chloroform solvent molecules octahedrally coordinated to a chloride anion through the hydrogen atoms of the chloroform solvent. The distance between the calculated hydrogen positions and the chloride anion for compounds **1** and **2** are 2.41 Å, and 2.42 Å, respectively. The summation of the ionic radius for Cl^- and the van der Waals radius for H, $[r(Cl)_{ion} + r(H)_{VDW} = 1.70 + 1.20 = 2.90$ Å], produces a value that is larger than the experimental value. Also the distance between the chlorine anion and carbon atoms of the chloroform is 3.34(2) Å. The summation of the ionic radius for Cl^- and the van der Waals radius for C, $[r(Cl)_{ion} + r(C)_{VDW} = 1.70 + 1.65 = 3.35$ Å], produces a value that is very close to the experimental value. These results suggest that the chloroform molecules are interacting with the chlorine anion through strong hydrogen bonding. However, because the H atoms positions are not experimentally established, the bonding interactions between chloride anion and six chloroform molecules in this anion unit are not completely clear. The $[Cl(CHCl_3)_6]^-$ cation is, to our knowledge, the first documented example of a chlorine anion octahedrally coordinated with six chlorohydrocarbon molecules.

Magnetic Properties

Considering the results from the single-crystal refinement, the second compound recovered from the toluene filtrate probably has a formula of $[W_6Se_{6.39}Cl_{1.61}(PEt_3)_6]Cl$.

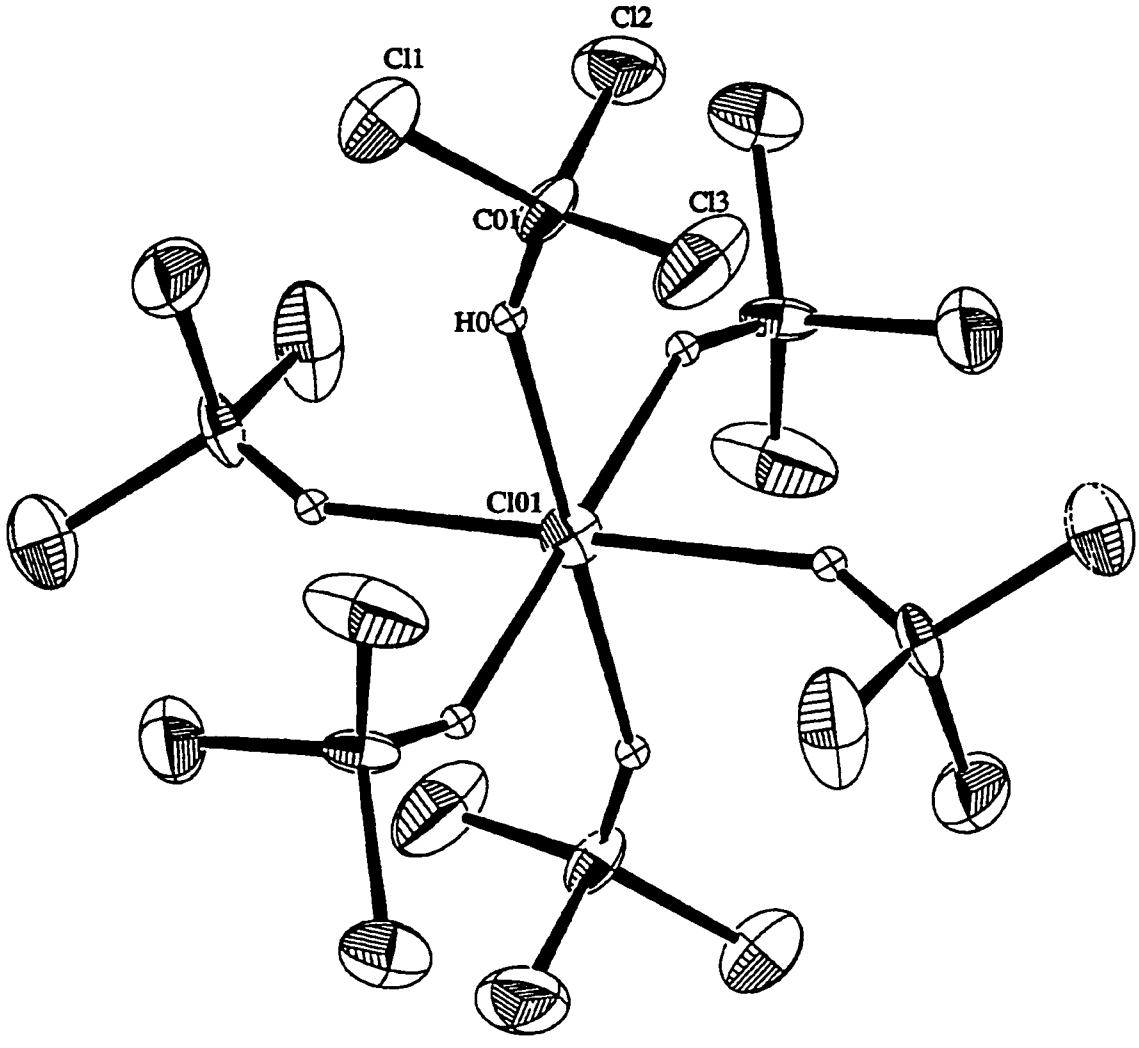

Figure 4. Ortep drawing of the anion unit, $[Cl(CHCl_3)_6]^-$ with thermal ellipsoids at the 35%probability level. H-atoms shown have been placed in calculated positions.

The magnetic susceptibility of this material was collected over the range 6-297K at 10K intervals in a field of 3 tesla. The molar susceptibility and the reciprocal molar susceptibility for this material are shown in Figure 5. The data can be fit by the Curie-Weiss relationship, $\chi = C/(T+\theta) + \chi_o$, from 6 to 297 K. A calculated value (-1.35×10^{-3} emu/mol) for χ_o was used for the diamagnetic core correction, using values for the individual ions reported by Selwood.[25] A linear regression fitting of the observed data yielded C = 0.084 emu·K/mol and θ = -2.28K. The effective magnetic moment calculated from the Weiss constant C is 0.82 μ_B.

Provided that $[W_6Se_{6.39}Cl_{1.61}(PEt_3)_6]Cl$ is the mixture of a diamagnetic component (40%), $[W_6Se_7Cl(PEt_3)_6]Cl$, and a paramagnetic component (60%), $[W_6Se_6Cl_2(PEt_3)_6]Cl$, the expected magnetic moment is 1.34 μ_B. The low measured moment could result from several possibilities. First, the materials recovered from the filtrate might not have the formula of $[W_6Se_{6.4}Cl_{1.6}(PEt_3)_6]Cl$ even though single crystals of $[W_6Se_{6.39}Cl_{1.61}(PEt_3)_6][Cl(CHCl_3)]$ were obtained from the filtrate. This material may consist of several types of cluster units. Secondly, this material is air-sensitive, and cluster decomposition could take place during the process of preparing the sample for the magnetic measurement. Yet, the observed paramagnetic moment most likely arises from a small amount of paramagnetic cluster unit, $(W_6Se_6Cl_2)^+$.

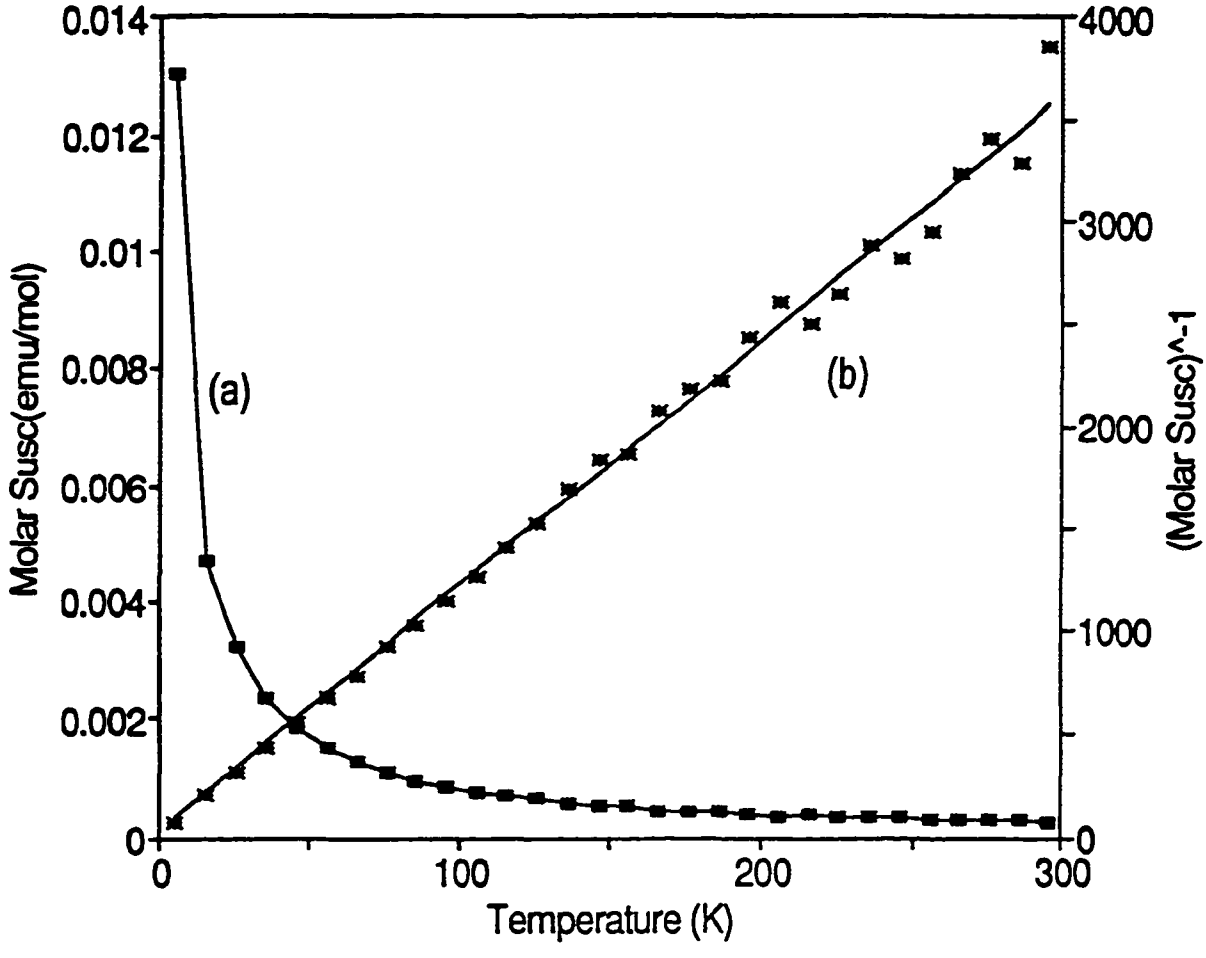

Figure 5. (a) Molar susceptibility versus temperature of $[W_6Se_{6.4}Cl_{1.6}(PEt_3)_6]Cl$
(b) Reciprocal Molar susceptibility versus temperature of $[W_6Se_{6.4}Cl_{1.6}(PEt_3)_6]Cl$. The points are experimental data points, and the straight line is the linear regression fitting.

Conclusion

This paper describes the preparation, characterization, and structures of the first mixed chloride-selenide tungsten cluster complexes with a general formula of $W_6Se_{8-x}Cl_x(PEt_3)_6$ (x=1 and 1.6).

The reactions, which were conducted between one mole of W_6Cl_{12} and *n* moles of Na_2Se (n=1,2,4,6) in an amine solvent, did not provide any mixed chloride-selenide cluster complexes besides $W_6Se_8L_6$ and an unknown compound. However, when the reactions were conducted between W_6Cl_{12} and ten moles of Na_2Se or K_2Se in toluene in the presence of triethylphosphine, mixed chloride-selenide cluster complexes, $W_6Se_{8-x}Cl_x(PEt_3)_6$, were obtained.

Single crystal structures of $[W_6Se_{7.04}Cl_{0.96}(PEt_3)_6][Cl(CHCl_3)_6]$ **(1)** and $[W_6Se_{6.39}Cl_{1.61}(PEt_3)_6][Cl(CHCl_3)_6]$ **(2)** were determined. The bridging chlorine atoms are disordered with selenium over all the bridging ligand sites in both structures. The crystallographic refinement provided fractional numbers of selenium and chlorine atoms in the formula for compound **(2)**. Thus this material may contain different kinds of cluster units which cocrystallize together to give the observed composition. The slightly shorter W-W bond distances in **(2)** than in **(1)** suggested that this material might contain a 21 e^- cluster, $[W_6Se_6Cl_2(PEt_3)_6]^+$. As expected, because of the mixing of chloride at the bridging positions, the average W-Se(Cl) bond distances of 2.554(2) Å in **(1)** were slightly shorter than that of 2.578(1) Å in $W_6Se_8(py)_6$.

In the interesting and unique $[Cl(CHCl_3)_6]^-$ anion unit, six chloroform solvent molecules are octahedrally coordinated to a chloride anion through the hydrogen atoms of the chloroform solvent. The bonding interactions between the solvents and Cl^- is probably through hydrogen bonds.

References

(1) Müller, A. *Polyhedron* **1986**, *5*, 323.

(2) Saito, T. In *Early Transition Metal Cluster with π-Donor Ligands*; Chisholm, M. H., Ed.; VCH: New York, 1995; p63.

(3) Dance, I.; Fisher, K. *Prog. Inorg. Chem.* **1994**, *41*, 637.

(4) Shibahara, T. *Adv. Inorg. Chem.* **1991**, *37*, 143.

(5) Shibahara, T. *Coord. Chem. Rev.* **1993**, *123*, 73.

(6) Roof, L. C.; Kolis, J. W. *Chem. Rev.* **1993**, *93*, 1037.

(7) Saito, T.; Yamamoto, N.; Nagase, T.; Kobayashi, K.; Yamagata, T.; Imoto, H.; Unoura, K. *Inorg. Chem.* **1990**, *29*, 764.

(8) Hilsenbeck, S. J.; Young Jr., V. G.; McCarley, R. E. *Inorg. Chem.* **1994**, *33*, 1822.

(9) K. Yvon, *in* "Current Topics in Materials Science" (E. Kaldis, Ed.), **1979**, Vol. 3, p.53. Elsevier, Amsterdam.

(10) Andersen, O. K.; Klose, W.; Nohl, H. *Phys. Rev. B: Solid State* **1978**, *B17*, 1209.

(11) Hughbanks, T.; Hoffman, R. *J. Am. Chem. Soc.* **1983**, *105*, 1150.

(12) Zhang, X.; McCarley, R. E. *Inorg. Chem.* **1995**, *34*, 2678.

(13) Zhang, X. Ph.D. Dissertation, Iowa State University, Ames, IA, 1991.

(14) Xie, X.; McCarley, R. E. Unpublished results.

(15) Xie, X.; McCarley, R. E. *Inorg. Chem.* **1995**, *34*, 6124.

(16) Xie, X.; McCarley, R. E. *Inorg. Chem.* **1996**, *35*, 2713.

(17) Michel, J. B.; McCarley, R. E. *Inorg. Chem.* **1982**, *21*, 1864.

(18) Michel, J. B.; McCarley, R. E. Ph.D Dissertation, Iowa State University, Ames, IA, 1979.

(19) Ehrlich, G. M.; Rauch, P. E.; DiSalvo, F. J. *Inorg. Synth.* **1995**, *30*, 1.

(20) Thompson, D. P.; Boudjouk, P. *J. Org. Chem.* **1988**, *53*, 2109.

(21) Scheldrick, G. M. *Crystallographic Computing 3*; Oxford University Press: Oxford, U.K., 1985.

(22) *TEXSAN: Single Crystal Structure Analysis Software*, Version 1.6c; Molecular Structure Corp.: The Woodlands, TX 77381, 1985 & 1992.

(23) *DIFABS*: Walker, N. & Stuart, *Acta Cryst.* **1983**, *A39*, 158.

(24) Pauling, L. *The Nature of the Chemical Bond*, 3rd Ed.; Cornell Univ. Press: Ithaca, New York, 1960, p 400.

(25) Selwood, P. W. *Magnetochemistry*, 2nd ed.; Interscience Publishers: New York, New York, **1988**, P. 78.

GENERAL SUMMARY

The goal of this dissertation has been to explore the chemistry of hexanuclear tungsten cluster compounds. Much less information was known in the literature for these materials as compared to the chemistry of the hexamolybdenum cluster compounds. Particularly, a rich chemistry has been found for the ternary and binary molybdenum chalcogenides or Chevrel phases, $M_xMo_6Y_8$ and Mo_6Y_8 (M = ternary metal cation; Y = S, Se, and Te). However, no such tungsten analogues have ever been synthesized. A great deal of new chemistry was developed in this work towards the establishment of the ideal tungsten analogues of the Chevrel phases.

Tungsten (II) chloride, W_6Cl_{12}, which contains the hexatungsten cluster unit $W_6Cl_8^{4+}$, was chosen as the starting material based on its structural similarity to the W_6S_8 cluster unit. Complete substitution of the chalcogenides for chloride was accomplished by refluxing a mixture of W_6Cl_{12} and NaSH, or Na_2Y in a variety of organic solvents. A large number of new compounds, which contained the cluster unit W_6Q_8 (Q = S, Se, Te, or Cl), were prepared and characterized.

The soluble and weakly-coordinated complexes $W_6S_8(pip)_6$ and $W_6S_8(BuNH_2)_6$ were prepared by reacting W_6Cl_{12} with higher stoichiometries of sodium hydrosulfide and sodium ethoxide in piperidine and butylamine, respectively. These two new complexes exhibit the weakest W-L bonding interactions and therefore can subsequently undergo ligand exchange reactions to form a variety of cluster

complexes. A Single-crystal structure determination is reported for the piperidine (pip) complex, $W_6S_8(pip)_6 \cdot 7pip$.

A new sodium ternary tungsten sulfide, $Na_{2x}(W_6S_8)S_x(MeOH)_y$, was obtained when poor coordinating ligands, such as acetonitrile, were used as the solvents in the sulfidation reaction. Formation of this sodium salt resulted from the coordination of sulfide ions in the terminal positions of the cluster units. Furthermore, the tin compound, $Sn_x(W_6S_8)S_x(MeOH)_y$. was prepared through ion-exchange reaction. Both Infrared and XP spectra supported the presence of the W_6S_8 cluster units in these ternary tungsten sulfides. However, these materials were amorphous and extremely air-sensitive, and the cluster units also slowly decomposed in methanol. These two compounds are the first examples of ternary tungsten sulfides that contain the W_6S_8 cluster unit.

Molecular complexes, $W_6Se_8(py)_6$ and $W_6Se_8(pip)_6$ were synthesized when one mole of W_6Cl_{12} reacted with eight moles of Na_2Se in pyridine and piperidine, respectively. These complexes are relatively more soluble than their sulfide analogues. Single-crystal structures of $W_6Se_8(py)_6 \cdot 6py$ and $W_6Se_8(pip)_6 \cdot 8pip$ were determined. The average W-W bond distance of 2.690(2)Å in these selenide clusters is slightly longer than that of 2.660(2)Å in the sulfide analogues. The average W-Se bond distance is about 2.57 Å in these selenide cluster units. The W_6Se_8 cluster shows a characteristic far-IR band at about 250 cm^{-1}, which can be assigned to the T_{1u} W - Se stretching modes. The observed tungsten binding energies of 30.8 eV ($4f_{7/2}$) and 32.9 eV ($4f_{5/2}$) from XPS are characteristic of the

W_6Se_8 cluster unit. These adducts are the first reported examples of molecular complexes of the W_6Se_8 cluster unit.

The molecular complexes, $W_6Te_8L_6$ (L = py and pip) were also discovered by reacting one mole of W_6Cl_{12} with four moles of Na_2Te and four moles of Na_2Te_2 in pyridine and piperidine. When one mole of W_6Cl_{12} reacts with eight moles of Na_2Te in pyridine, the ionic cluster complex, $[Na(py)_6]^+[W_6Te_8(py)_6]^-$, was surprisingly recovered from the filtrate of the reaction. The triethylphosphine adduct of W_6Te_8 was established by ligand displacement of pyridine in $W_6Te_8(py)_6$. The cluster unit, W_6Te_8, shows a characteristic far-IR band around 180-200 cm^{-1}, which can be assigned as the T_{1u} W-Te stretching modes. The tungsten binding energies of 30.8 eV ($4f_{7/2}$) and 32.9 eV ($4f_{5/2}$) for $W_6Te_8L_6$ compare favorably with those of the sulfide (30.5, 32.6 eV) and selenide (30.8, 32.9 eV) analogues. The crystal structures of $W_6Te_8(pip)_6 \cdot 6pip$, $W_6Te_8(PEt_3)_6$, and $[Na(py)_6]^+[W_6Te_8(py)_6]^- \cdot 1py$ were determined. Unfortunately, $W_6Te_8(py)_6$ was so insoluble that single crystals of it were not obtained. The W-Te bond distances are very close to the W-W bond distances of 2.74 Å in these telluride clusters. For the anionic cluster unit, both the distorted tungsten octahedral cluster and the shortening of W-W bond confirmed that it was a 21 e^- cluster unit. These compounds are the first examples of molecular complexes of the W_6Te_8 cluster unit. The unique cationic unit $[Na(py)_6]^+$ is the first documented example of a sodium ion octahedrally coordinated with six pyridine molecules.

Mixed chloride-selenide cluster complexes, $W_6Se_{8-x}Cl_x(PEt_3)_6$, were isolated when the reactions of W_6Cl_{12} and ten moles of Na_2Se or K_2Se, and triethylphosphine

were conducted in toluene. The use of toluene is important for isolating the mixed chloride-selenide cluster complexes. In comparison, similar substitution reactions were conducted in amine solvents and only provided the complete substitution product, $W_6Se_8L_6$. Structures for $[W_6Se_7Cl(PEt_3)_6]$ $[Cl(CHCl_3)_6]$ and $[W_6Se_{6.4}Cl_{1.6}(PEt_3)_6][Cl(CHCl_3)_6]$ were determined. The bridging chlorine atoms are disordered over all the bridging ligand sites in both structures. These compounds may contain several kinds of cluster units with different chlorine contents that cocrystallize to give the observed composition. In the unique $[Cl(CHCl_3)_6]^-$ anion unit, six chloroform solvent molecules are octahedrally coordinated to a chlorine anion through the hydrogen atoms of the chloroform. These complexes are the first examples of the mixed halide-chalcogenide molecular complexes for hexatungsten cluster unit.

REFERENCES

(1) K. Yvon, *in* "Current Topics in Materials Science" (E. Kaldis, Ed.), **1979**, Vol. 3, p.53. Elsevier, Amsterdam.

(2) Chevrel, R.; Sergent, M. *Topics in Current Physics*, Fischer, Ø. and Maple, M. B., Eds.; **1982**, Vol. 32, Chapter 2 Springer-Verlag: Heidelberg.

(3) McCarty, K. F.; Schrader, G. L. *Ind. Eng. Chem. Prod. Res. Dev.* **1984**, *23*, 519.

(4) McCarty, K. F.; Anderegg, J. W.; Schrader, G. L. *J. Catal.* **1985**, *93*, 375.

(5) McCarty, K. F.; Schrader, G. L. *J. Catal.* **1987**, *103*, 261.

(6) Ekman, M. E.; Anderegg, J. W.; Schrader, G. L. *J. Catal.* **1989**, *117*, 246.

(7) Kareem, S. A.; Miranda, R. *J. Molec. Catal.* **1989**, *53*, 275.

(8) Schöllhorn, R.; Kümpers, M.; Besenhard, J. O. *Mater. Res. Bull.* **1977**, *12*, 781.

(9) Mulhern, P. J.; Haering, R. R. *Can. J. Phys.* **1984**, *62*, 527.

(10) Perrin, C.; Sergent, M.; Besenhard, J. O. *Mat. Res. Dev.* **1984**, *23*, 519.

(11) Perrin, C.; Sergent, M.; Le Traon, A. *J, Solid State Chem.* **1977**, *12*, 781.

(12) Perrin, C.; Sergent, M.; *J. Chem. Res.* **1983**, 449.

(13) Perrin, C.; Potel, M.; Sergent, M.; *Acta. Crystallogr.* **1983,** *C39*, 415.

(14) Michel, J. B.; McCarley, R. E. *Inorg. Chem.* **1982**, *21*, 1864.

(15) Michel, J. B.; McCarley, R. E. *Dissertation,* Iowa State University, Ames, IA, 1979.

(16) Laughlin, S. K. *M. S. Dissertation*, Iowa State University, Ames, IA, 1986.

(17) Spink, D. A. *M.S.. Dissertation,* Iowa State University, Ames, IA, 1986.

(18) Spink, D. A. *Ph. D. Dissertation,* Iowa State University, Ames, IA, 1989.

(19) McCarley, R. E. Laughlin, S. K.; Spink, D. A.; Hur, N. *Abstracts of Papers,* 3rd, North American Chemical Congress, Toronto, Ontario, Canada; American Chemical Society: Washington D. C., **1988**, INOR 575.20.

(20) McCarley, R. E.; Zhang, X.; Spink, D. A.; Hur, N. *Abstracts of Papers,* 199th National Meeting of the American Chemical Society; Boston, MA, **1990.**

(21) Saito, T.; Yamamoto, N.; Yamagata, T.; Imoto, H. *J. Am. Chem. Soc.* **1988**, *110*, 1646.

(22) Saito, T.; Yamamoto, N.; Nagase, T.; Kobayashi, K.; Yamagata, T.; Imoto, H.; Unoura, K. *Inorg. Chem.* **1990**, *29*, 764.

(23) Zhang, X.; McCarley, R. E. *Inorg. Chem.* **1995**, *34*, 2678.

(24) Zhang, X. Ph.D. Dissertation, Iowa State University, Ames, IA, 1991.

(25) Chevrel, R.; Sergent, M. Prigent, J. *J. Solid State Chem.* **1971**, *3*, 515.

(26) Peña, O.; Sergent, M. *Prog. Solid St. Chem.* **1989**, *19*, 165.

(27) Chevrel, R.; Sergent, M.; Prigent, J. *Mater. Res. Bull.* **1974**, *9*, 1487.

(28) Schöllhorn, R.; Kümpers, Plorin, D. *Less-Common Met.* **1978**, *58*, 55.

(29) Guillevic, J.; Bars, O.; Grandjean, D. *J. Solid State Chem.* **1973**, *7*, 158.

(30) Tarascon, J. M.; Waszczak, J. V.; Hull, G. W.; DiSalvo, F. J.; Blitzer, L. D. *Solid State Comm.* **1983**, *47*, 973.

(31) Tarascon, J. M.; DiSalvo, F. J.; Murphy, D. W.; Hull, G. W.; Rietman, E. A.; Waszczak, J. V. *J. Solid State Chem.* **1984**, *54*, 204.

(32) Nohl, H.; Klose, W.; Anderson, O. K. *Topics in Current Physics*, Fischer, Ø. and Maple, M. B., Eds.; Springer-Verlag: Heidelberg, **1982**, Vol. 32, Chapter 6

(33) Hughbanks, T.; Hoffman, R. *J. Am. Chem. Soc.* **1983**, *105*, 1150.

(34) Perrin, A.; Sergent, M.; Fischer, Ø. *Mater. Res. Bull.* **1978**, *13*, 259.

(35) Schäfer, H.; von Schnering, H. G.; Tillack, J.; Kuhnen, F.; Wohrle, H.; Baumann, *H. Z. Anorg. Allg. Chem.* **1967**, *353*, 281.

(36) Perrin, A.; Sergent, M.; Le Traon, F.; Le Traon, A. *J. Solid State Chem.* **1978**, *25*, 197.

ACKNOWLEDGMENTS

I would like to express my sincere appreciation and thanks to Dr. R.E. McCarley for his guidance and instruction over the past five years. His enthusiasm, encouragement, and patience helped me through many difficult times during my years at Iowa State University. I have learned a great deal from him, about both science and humanity. Thanks, Doc.

I would also like to thank the past and present members of McCarley group, from whom I learned a lot and with whom I had a lot of fun. Special appreciation goes to Dr. Shane Hilsenbeck for his generous assistance in correcting my writing.

This research would not have been possible without the aid of the following people and their expertise:

James Anderegg for X-ray photoelectron spectroscopy data

Dr. Robert Jacobson, Dr. Victor Young, and Dr. Leonard Thomas for X-ray crystallography

Dave Scott for NMR and ESR studies

Dr. Gordon Miller for EHMO calculations

Jerome Ostenson for magnetic susceptibility measurements

I would like to thank the many friends I have gained during these years in Ames. I learned from them what friendship is really all about. I would like to thank my parents for the support and love they have shown me. They not only raised me,

but also had provided me the best environment of learning and encouraged me to work to the best of my ability. Although they are thousands of miles away at the other side of the earth, their love and encouragement have always been nearby throughout my entire period of graduate study.

Finally, my deepest appreciation goes to my lovely wife, Jianhong Wang, for her love, encouragement, patience, and support. None of my achievements would have been possible without her standing behind me. Thanks, I love you!

This work was performed at the Ames Laboratory under contract no. W-7405-eng-82 with U.S. Department of Energy. The United States government has assigned the DOE Report number IS-T 1772 to this dissertation.